MINISTRY OF SCIENCE AND HIGHER EDUCATION
OF THE RUSSIAN FEDERATION

MINISTY OF HEALTH OF THE RUSSIAN FEDERATION

STATE ATOMIC ENERGY CORPORATION ROSATOM

NATIONAL RESEARCH NUCLEAR UNIVERSITY MEPhI
(MOSCOW ENGINEERING PHYSICS INSTITUTE)

3rd International Symposium on "Physics, Engineering and Technologies for Biomedicine"

October 15-17, 2018

BOOK OF ABSTRACTS

MOSCOW

УДК 57.089
ББК 5
Р59

Physics, Engineering and Technologies for Biomedicine. The 3rd International Symposium October 15-17, 2018: Book of Abstracts. Moscow MEPhI, 2018.– 248 p.

The 3rd International Symposium on «Physics, Engineering and Technologies for Bio-Medicine» is organized following the successful 1st and 2nd Interna-tional Symposium on “Physics, Engineering and Technologies for Bio-Medicine”, held in Moscow at the occasion of the foundation of the Institute PhysBio at MEPhI (Russia).

Abstracts are published in author's edition

ISBN

3rd International Symposium on

"Physics, Engineering and Technologies for Biomedicine"

The 3rd International Symposium on «Physics, Engineering and Technologies for BioMedicine» is organized following the successful 1st and 2nd International Symposium on "Physics, Engineering and Technologies for Bio-Medicine", held in Moscow at the occasion of the foundation of the Institute PhysBio at MEPhI (Russia).

Under the auspices of the Russian Ministry of Science and Higher Education, the Ministry of Health and the State Company Rosatom, the 3rd Symposium is again organized by the Institute of Engineering Physics for Biomedicine (PhysBio) of the National Research Nuclear University MEPhI (Moscow Engineering Physics Institute) in close collaboration with non-profit partnership «Kaluga pharmaceutical cluster».

Conference topics

The Symposium aims at bringing together leading scientists and experts in nuclear medicine, biophysics, bio-photonics, and emerging fields to present their works and having invited lectures on the following topics:

- Advanced materials and methods for MRI and PET
- Bioimaging technologies and materials
- Bio-photonics for diagnosis and therapy
- Bioprinting
- Brachy-, Proton and Ion therapy methods
- Diagnosis methods, today and in the future
- Immuno-therapy
- Isotopes for medical purpose
- Medical-biological aspects of radiation effects
- Nanomaterials for biomedical applications
- Plasma and laser technologies for biomedicine
- Translational medicine

The Symposium provides a unique opportunity for fruitful scientific discussions and for establishing contacts with scientists all over the world.

Official Language
The official language of the conference is English.

Key note lecture: Marco Durante, director of the Biophysics Department at the GSI Helmholtz Center, Darmstadt, Germany.
In the framework of the Symposium, the Workshop on Nuclear Nanomedicine will be held 13 October 2018 in Moscow, Russia.
The 3rd International school for medical doctors and young scientists “Physics, Engineering and Technologies for Biomedicine” will be held 14 October 2018 in Moscow, Russia. Special lectures for medical doctors, students and young scientists will be organized from 10:00 to 17:00.

COMMITTEES

Symposium Co-Chairs

Mikhail N. Strikhanov, MEPhI, Moscow, Russia
Paras Prasad, University of Buffalo, New York, USA

Program-Committee Co-Chairs

Andrei V. Kabashin, CNRS, Aix-Marseille University, France
Oleg B. Loran, S.P. Botkin City Clinical Hospital, Department of Urology and Surgical Andrology of the Russian Medical Academy of Post-Graduate Education, Moscow, Russia

Organizing-Committee Chair

Chair: Irina N. Zavestovskaya, PhysBio of MEPhI, P.N. Lebedev Physical Institute of RAS, Moscow, Russia
Vice-chair: Andrey Postnov, MEPhI, Moscow, Russia

Scientific Secretary

Yurii A. Aleshchenko, PhysBio of MEPhI, P.N. Lebedev Physical Institute of RAS

International Program Advisory Committee

Walter Blondel, Université de Lorraine, Nancy, France
Vladimir I. Chernov, Department of Radiologic Diagnosis of the Tomsk Research Institute of Oncology, Tomsk, Russia
Sergey M. Deyev, Shemyakin-Ovchinnikov Institute of Bioorganic Chemistry, MEPhI, Moscow, Russia
Boris I. Dolgushin, Research Institute of Clinical Oncology of N.N. Blokhin Cancer Research Center, Moscow, Russia
Marco Durante, director of the Biophysics Department at the GSI Helmholtz Center, Darmstadt, Germany
Dmitry K. Fomin, Nuclear Medicine Clinic of the Russian Scientific Center of Radiology and Nuclear Medicine of the RF Ministry of Health, Head of the Society of Nuclear Medicine, Moscow, Russia
Hans H. Gutbrod, GSI Helmholtzzentrum für Schwerionenforschung, Darmstadt, Germany and MEPhI, Moscow, Russia
Roger Kamm, Massachusetts Institute of Technology, USA
Andrey D. Kaprin, Herzen Moscow Oncology Research Institute, Moscow, Russia

Anatoly V. Karalkin, Nuclear Medicine Clinic of N.I. Pirogov State Clinical Hospital No. 1, Moscow, Russia
Aleksandr A. Khasin, NRS Kurchatov Institute, Director of LLC Nuclear Medicine Development Center, Moscow, Russia
Galina E. Kodina, A.I. Burnazyan Federal Medical Biophysics Center, Department of Pharmaceutical and Radiopharmaceutical Chemistry, Moscow, Russia
Vitali I. Konov, A.M. Prokhorov General Physics Institute of RAS, PhysBio of MEPhI, Moscow, Russia
Valentina V. Kosenko, Federal Service for Surveillance in Healthcare (Roszdravnadzor)
Eduard V. Kotlyarov, FACNM, FACR, International Radiology and Nuclear Medicine, USA
Oleg N. Krokhin, P.N. Lebedev Physical Institute of RAS, MEPhI, Moscow, Russia
Yurii B. Lishmanov, Research Institute of Cardiology, Laboratory of Radionuclide Research Techniques, Tomsk, Russia
Hans-Peter Meinzer, Department Medical and Biological Informatics E130, DKFZ, Heidelberg, Germany
Oleg S. Medvedev, Department of pharmacology, Faculty of Fundamental Medicine, Lomonosov Moscow State University
John Mendelsohn, The University of Texas MD Anderson Cancer Center, USA
Igor R. Nabiev, University of Reims Champagne-Ardenne, France, LNBI, MEPhI, Moscow, Russia
Rainer Rienmuller, Radiology of Medical University of Graz, European Society of Cardiac Radiology, Austria
Sergey A. Rumiantsev, Department of Innovation development and Scientific Engineering, Ministry of Healthcare of the Russian Federation, Moscow, Russia
Nidal Salim, Center of beam therapy of The European Medical Center, Moscow, Russia
Marc Sentis, CNRS, Aix-Marseille University, France
Sergey V. Shestakov, Genetics Department, Biological Faculty of the M.V. Lomonosov Moscow State University, Moscow, Russia
Rudolf Steiner, Institut für Lasertechnologien in der Medizin (ILM), Universität Ulm, Germany
Sergey V. Suchkov, Sechenov University, MEPhI, Moscow, Russia
Gleb Sukhorukov, Queen Mary University of London, UK
Maksim V. Zabelin, Deputy Head of Federal Biomedical Agency, Moscow, Russia

Organizing Committee

Yurii A. Aleshchenko, PhysBio of MEPhI, P.N. Lebedev Physical Institute of RAS, Moscow, Russia

Yuri N. Anokhin, MEPhI, Moscow, Russia

Vladimir N. Belyaev, MEPhI, Moscow, Russia

Vladimir G. Bychenko, Research Center of Obstetrics, Gynecology and Perinatology, Ministry of Healthcare of the Russian Federation, Moscow, Russia

Philippe Delaporte, Aix -Marseille University, France

Marco Durante, Department of Biophysics at the GSI Helmholtz Center, Darmstadt, Germany

Natalia B. Epshtein, PhysBio of MEPhI, Moscow, Russia

Elena V. Gromushkina, MEPhI, Moscow, Russia

Igor A. Gulidov, Department of beam therapy of the A.F. Tsiba Radiological Medical Scientific Center, Obninsk, Russia

Hans H. Gutbrod, GSI Helmholtzzentrum für Schwerionenforschung, Darmstadt, Germany and MEPhI, Moscow, Russia

Evgeniy V. Khmelevskiy, Department of beam therapy of Herzen Moscow Oncology Research Institute, Ministry of Healthcare of the Russian Federation, Moscow, Russia

Sergey M. Klimentov, PhysBio of MEPhI, Prokhorov General Physics Institute of RAS, Moscow, Russia

Victor B. Loschenov, A.M. Prokhorov General Physics Institute of RAS, PhysBio of MEPhI, Moscow, Russia

Vladimir Lysenko, CNRS, INL, National Institute of Applied Sciences (INSA de Lyon), France

Valentin G. Nikitaev, MEPhI, Moscow, Russia

Vasyli M. Petriev, Laboratory of Experimental Nuclear Medicine, Medical Radiological Research Center, Ministry of Health, Moscow, Russia

Viktoria O. Shipunova, Shemyakin-Ovchinnikov Institute of Bioorganic Chemistry, MEPhI, Moscow, Russia

Sergey V. Shiryaev, Deparment of Radiologic Diagnosis of the N.N. Blokhin Cancer Research Center, President of the Oncological Society of Molecular Imaging, Moscow, Russia

Dmitry V. Sosin, PhysBio of MEPhI, Moscow, Russia

Victor Yu. Timoshenko, M.V. Lomonosov Moscow State University, PhysBio of MEPhI, P.N. Lebedev Physical Institute of RAS, Moscow, Russia

Igor E. Tyurin, Department of Radiodiagnostics and Medical Physics of the Russian Academy of Post-qualifying Education, Moscow, Russia

Secretary of the Local Organizing-Committee

Maria S. Grigoryeva, PhysBio of MEPhI, P.N. Lebedev Physical Institute of RAS, Moscow, Russia

Local Organizing-Committee

Yulia A. Akmalova, PhysBio of MEPhI, Moscow, Russia
Anna V. Evsovich, PhysBio of MEPhI, Moscow, Russia
Anastasia A. Fronya, MEPhI, P.N. Lebedev Physical Institute of RAS, Moscow, Russia
Nikita V. Karpov, PhysBio of MEPhI, Moscow, Russia
Anna V. Vishivanyuk, PhysBio of MEPhI, Moscow, Russia
Olesia V. Rodionova, PhysBio of MEPhI, Moscow, Russia
Daria A. Gaponova, PhysBio of MEPhI, Moscow, Russia
Alexey N. Maiorov, PhysBio of MEPhI, Moscow, Russia

CONTACTS

The Symposium webpage: http://physbio.mephi.ru/symp18/
The Symposium e-mail: PhysBioSymp@mephi.ru

Book's contents

3rd International Symposium on
"Physics, Engineering and Technologies for Biomedicine"

INVITED LECTURES

Book's contents

Book's contents

Book's contents

POSTER REPORTS

Book's contents

Book's contents

Book's contents

Book's contents

Book's contents

3rd International Symposium on "Physics, Engineering and Technologies for Biomedicine"

INVITED LECTURES

FUTURE ION BEAM RADIOBIOLOGY

Marco Durante

GSI Helmholtz Center, Germany

Biological optimization of the treatment planning is a necessary step toward a full exploitation of energetic charged particles in oncology. Most of the efforts in particle radiobiology for radiotherapy have concentrated on measurements of RBE. A large and comprehensive database of RBE measurements is available for different ions. However, *qualitative* differences between densely ionizing ions and photons have been observed and are not taken into account in the scaling factor RBE. Most cancer patients are subject to multi-modal strategies that involve, in addition to radiotherapy, drug treatments: chemotherapy, targeted therapy, or immunotherapy. The interaction radiation-drug can be substantially different when densely and sparsely ionizing radiation are compared. Considering the radiobiological differences, charged particles and X-rays should be regarded as two separate drugs in oncology.

3rd International Symposium on
"Physics, Engineering and Technologies for Biomedicine"

BIOPHOTONICS AND NANOMEDICINE FOR THERANOSTICS: TRANSLATION TO PATIENT CARE

Paras N. Prasad

Institute for Lasers, Photonics and Biophotonics
Departments of Chemistry, Physics, Electrical Engineering and Medicine
State University of New York at Buffalo, New York 14260

This talk will present our progress on Biophotonic multimodal and multispectral imaging, combined with Nanomedicine approach of image guided targeted delivery of therapy for combined diagnostics and therapy known as Theranostics. Our new strategy of Integrated Correlative Multiscale and Multimodal Pre-clinical Imaging platform (Cryo TM, linear and nonlinear optical, photoacoustic, magnetic, radiation, SPECT, PET and ultrasonic) for Cross-Species Murine to Human Network Modeling will be presented. An important in-vitro is Ramanomics using Micro Raman Spectrometry with Bimolecular Component Analysis for quantitative molecular profiling of biological structures. Using this, we measure concentrations of proteins, DNA, RNA and lipids in the single organelles of live cells and ex-vivo tissues in order to establish a new set of biomarkers to diagnose progression of diseases such as cancer.

In nanomedicine, our new approach involves integration of molecular, nano and microstructures involving microbubbles encapsulating other molecular and various nanoconstructs for multimodal image guided and targeted delivery, and real time monitoring of therapeutic action. Yet another versatile hierarchical nanostructures being developed, involves a metal-organic framework with void spaces for incorporating multiple diagnostics and therapeutic inclusions, and having multiple binding sites for introducing targeting, enhanced circulation, additional imaging and therapeutic functions. Towards translating nanomedicine, we are engaged in establishing that the nanostructures are biocompatible, cause no toxicity and can be bio-eliminated. Practical considerations are their reproducibility, scalability and long shelf life. We are advancing Nuclear medicine and Radiopharmaceuticals radiation-based diagnostics and therapy using targeted nanoformulations where we in-

volve laser ablation technique to produce them. The diseases of our focus are cancer, infections and various brain dysfunctions. In brain research, we utilize Neurophotonics, using optical and photoacoustic imaging and noninvasive actuation of optogenetic stimulation of brain activity using near IR absorbing optical nanotransformers that can provide an effective intervention/augmentation strategy to treat many cognitive disorder and diseases, ranging from Alzheimer, to traumatic brain injury, to retardation.

This talk will conclude with a discussion of existing challenges and new opportunities in translating biophotonics and nanomedicine to patient care.

1. P.N. Prasad "***Introduction to Biophotonics***", John Wiley & Sons, New York (2003)
2. P.N. Prasad "***Nanophotonics***", John Wiley & Sons, New York (2004)
3. P.N. Prasad "***Introduction to Nanomedicine and Nanobioengineering***", John Wiley & Sons, New York (2012)

3rd International Symposium on
"Physics, Engineering and Technologies for Biomedicine"

FROM PHENOTYPIC TO THERANOSTIC APPROACH IN NUCLEAR MEDICINE - NEEDS FOR NON-CONVENTIONAL RADIONUCLIDES

Mickaël Bourgeois

GIP Arronax, 1 rue Aronnax, 44800 Saint-Herblain
Nantes University Hospital – Nuclear Medicine Department – 9 quai Moncousu, 44000 Nantes
bourgeois@arronax-nantes.fr, http://www.cyclotron-nantes.fr

Keywords: Nuclear medicine, radionuclide production, nuclear imaging, radionuclide targeted therapy

Summary:

Radionuclides are used in different fields of medicine like oncology, neurology and cardiology, either for diagnostic or therapy. Only few radionuclides can be used directly (I-131 for thyroid cancer is one example for therapy, Rb-82 used for PET imaging in cardiology is another one in imaging). In most cases, these radionuclides must be coupled to a carrier molecule (a vector) to target the cells of interest. A vector can be a chemical molecule, a peptide or an antibody and its distribution time in the body is dependent on its size. Peptide can distribute within hours whereas antibodies need days. This labelled vector forms a radiopharmaceutical.

Currently, only few isotopes are used in clinical practice (Tc-99m, F-18 for imaging and I-131, Y-90 and recently Lu-177 for therapy). However, many others may be of medical interest due to their emitted radiations (alpha emitters, Auger emitters) and / or their half-lives that can be adapted to the carrier molecule transit time and to the pathology. The improvement of cellular knowledge on cancerous pathologies and the advent of targeteted therapies in the arsenal of the fight against cancer has highlighted the need for diagnostic techniques to select the patients who will be the most responsive for these new therapies. Obtaining this phenotypic information requires original vectors coupled to innovative radionuclides such copper-64, zirconium-89 or scandium-44.

Moreover, recently, the theranostic approach [1] has emerged. It combines imaging information and therapeutic use of radionuclides. This approach shows great promises especially because it may allow personalizing the treatment to each patient. The diagnosis test done prior to the treatment allows to determine patient response and to determine the needed injected dose for the therapeutic agent. After treatment, the imaging agent can be used to follow the patient response to the injected radiopharmaceutical. Finally, this approach allows a better control of the targeting and increases the benefit/toxicity ratio as useless treatments on patients with no response to the diagnosis test are avoided. For the theranostic approach, it is preferable to use pairs of radioisotopes of the same element like ((I-124/I-131, Cu-64/Cu-67,…) or to combine radionuclide of element having similar chemical properties like Ga-68 and Lu-177 for example. All these points lead to a renewal interest on radionuclide production.

After an overview of the use of radionuclides in medicine for both imaging and therapy and the presentation of the theranostic approach, I will present how these non-conventional radionuclides are produced taking the example of what is done at the Arronax facility [2] as a guide.

References:

1. 1. Srivastava S.C., JPM 2013, 47(1)31-46
2. 2. Haddad F. et al.. Eur. J. Nucl. Med. Mol. Imaging, 2008, 35:1377–1387

Acknowledgements: Our work has been, in part, supported by a grant from the French National Agency for Research called "Investissements d'Avenir", Equipex Arronax-Plus noANR-11-EQPX-0004 and Labex IRON noANR-11-LABX-18-0

3rd International Symposium on
"Physics, Engineering and Technologies for Biomedicine"

NANOPARTICLES IN CANCER MEDICINE – A PHYSICIAN'S PERSPECTIVE

Sunil Krishnan

Dept. of Radiation Oncology, MD Anderson Cancer Center, Houston, TX

An evolving body of recent literature alludes to the potential to sensitize tumors to radiation therapy using metallic nanoparticles. In preclinical studies, a technique that holds promise for eventual clinical deployment is nanoparticle-assisted radiation dose enhancement. Computational techniques offer an explanation for and predict the biophysical consequences at a nano-/meso-scopic scale. Preclinical studies in vitro and in vivo provide evidence of radiosensitization. Nonetheless, there are persisting gaps in knowledge relating to the molecular mechanism of action and optimum nanoparticle characteristics – some of these issues will be addressed. My presentation will start with familiarizing the audience with the potential applications of gold nanoparticles in radiation therapy using specific illustrative examples, explore ways to understand the underlying mechanisms of the effects observed, and provide a perspective on how to advance these concepts to the clinic.

3rd International Symposium on
"Physics, Engineering and Technologies for Biomedicine"

MULTIFUNCTIONAL NANOMATERIALS FOR THERANOSTICS

S.M. Deyev

Shemyakin & Ovchinnikov Institute of Bioorganic Chemistry, Moscow, Russia

Rapid development of nanotechnology has stimulated considerable interest in their applications in life sciences. In particular, several unique features of nanoparticles appeared very attractive for their implementation as diagnostic and therapeutic complexes. An important attribute of the nanoparticles is the ability to bind various molecules ensuring biological activity of the particles; among these molecules are toxic and/or visualizing modules, as well as targeting agents for addressed delivery.

A particular attention as new and unique therapeutic agents attract nanoparticles (NPs) that make it possible to solve old but still actual problems by principally new means and ways. A number of nanoparticle-based medications are already approved for therapeutic purposes. Important advantage of NPs is their developed surface, which can be decorated with biocompatible functional moieties, and thus form a versatile docking station. NP can serve as a nano-vehicle to host biologically significant modules, such as therapeutic, targeting and stealth modules for targeted delivery, diagnosis that guides and monitor effects of the NP-assisted therapy of pathology lesions [1-15]. These properties provide foundations for significant emerging areas in applied biomedical science including (personalised) nanomedicine and theranostics.

In the paper we review our recent results on design of immunotargeted Nano Drug Delivery Systems combinate visualizing and cytotoxic agents with important types of the nanoparticles, including luminescent upconversion NPs, as well as different toxic principles, biological pseudomonas exotoxin A and radionuclide.

Thus, recently we report [16] combined therapy using upconversion nanoparticle (UCNP) coupled to two therapeutic agents: beta-emitting radionuclide yttrium-90 (90Y) fractionally substituting yttrium in UCNP, and a fragment of the exotoxin A derived from Pseudomonas aeruginosa genetically fused with a targeting designed ankyrin repeat

protein (DARPin) specific to HER2/neu receptors. The resultant hybrid complex UCNP-R-T was tested using human breast adenocarcinoma cells SK-BR-3 overexpressing HER2/neu receptors and immunodeficient mice, bearing HER2-positive xenograft tumors. The photophysical properties of UCNPs enabled background free imaging of the UCNP-R-T distribution in cells and animals. Specific binding and uptake of UCNP complexes in SK-BR-3 cells was observed, with separate 90Y- and PE40-induced cytotoxic effects characterized by IC50 140 μg/mL (UCNP-R) and 5.2 μg/mL (UCNP-T), respectively. When two therapeutic agents were combined into UCNP-R-T, the synergetic effect increased markedly, ~2200-fold, resulting in IC50 = 0.0024 μg/mL. The combined therapy of UCNP-R-T was demonstrated in vivo.

The obtained results show promise for effective combined oncotherapy leading to prospective translation to clinical practices.

This research was supported by RFBR grant no. 17-00-00121.

1. Kostyukevich Y., Shulga A.A., Kononikhin A., Popov I., Nikolaev E., Deyev S. CID fragmentation, H/D exchange and supermetallization of Barnase-Barstar complex. // *Sci Rep.* 2017. V. 7(1). P. 6176.

2. Shipunova V.O., Zelepukin I.V., Stremovskiy O.A., Nikitin M.P., Care A., Sunna A., Zvyagin A.V., Deyev S.M. Versatile Platform for Nanoparticle Surface Bioengineering Based on SiO_2-Binding Peptide and Proteinaceous Barnase*Barstar Interface // *ACS Appl. Mater. Interfaces*. 2018. V. 10. P. 17437-17447.

3. Sokolova E., Guryev E., Yudintsev A., Vodeneev V., Deyev S., Balalaeva I. HER2-specific recombinant immunotoxin 4D5scFv-PE40 passes through retrograde trafficking route and forces cells to enter apoptosis // *Oncotarget*. 2017. V. 8(13). P. 22048-22058.

4. Semenova G., Stepanova D.S., Deyev S.M., Chernoff J. Medium throughput biochemical compound screening identifies novel agents for pharmacotherapy of neurofibromatosis type I. *Biochimie*. 2017. V. 135. P.1-5.

5. Prokofjeva M.M., Proshkina G.M., Lebedev T.D., Shulgin A.A., Spirin P.V., Prassolov V.S., Deyev S.M. Lentiviral gene delivery to plasmolipin-expressing cells using Mus caroli endogenous retrovirus envelope protein // *Biochimie.* 2017. V. 142. P. 226-233.

6. Liang L, Lu Y, Zhang R, Care A, Ortega TA, Deyev SM, Qian Y, Zvyagin AV. Deep-penetrating photodynamic therapy with KillerRed mediated by upconversion nanoparticles // *Acta Biomater.* 2017. V. 51. P. 461-470.

7. Souslova E.A., Mironova K.E., Deyev S.M. Applications of genetically encoded photosensitizer miniSOG: from correlative light electron microscopy to immunophotosensitizing *// J. Biophotonics*. 2017. V. 10(3). P. 338-352.
8. Shilova O.N., Shilov E.S., Deyev S.M. The effect of trypan blue treatment on autofluorescence of fixed cells *// Cytometry* A. 2017. V. 91(9). P. 917-925.
9. Semenova G., Stepanova D.S., Dubyk C., Handorf E., Deyev S.M., Lazar A. J., Chernoff J. Targeting Group I p21-Activated Kinases to Control Malignant Peripheral Nerve Sheath Tumor Growth and Metastasis // *Oncogene* . 2017. V. 36. P. 5421-5431.
10. Deyev S., Proshkina G., Ryabova A., Tavanti F., Menziani M.C., Eidelshtein G., Avishai G., Kotlyar A. Synthesis, Characterization, and Selective Delivery of DARPin-Gold Nanoparticle Conjugates to Cancer Cells // *Bioconjug Chem*. 2017. V.28(10). P. 2569-2574.
11. Shilova O.N., Shilov E.S., Lieber A., Deyev S.M. Disassembling a cancer puzzle: Cell junctions and plasma membrane as targets for anticancer therapy // .*J. Control. Release*. 2018. V. 286. P. 125-136.
12. Mironova K., Khochenkov D.A., Generalova A.N., Rocheva V.V., Sholina N.V., Nechaev A., Semchishen V., Deyev S.M., Zvyagin A.V., Khaydukov E. Ultraviolet phototoxicity of upconversion nanoparticles illuminated with near-infrared light *// Nanoscale*. 2017. V.9(39). P. 14921-14928.
13. Kholodenko I.V., Kalinovsky D.V., Doronin I.I., Deyev S.M., Kholodenko R.V. Neuroblastoma Origin and Therapeutic Targets for Immunotherapy // *J. Immunol. Res*. 2018. doi: 10.1155/2018/7394268
14. Vorobyeva A., Bragina O., Altai M., Mitran B., Orlova A., Shulga A., Proshkina G., Chernov V., Tolmachev V., Deyev S. Comparative Evaluation of Radioiodine and Technetium-Labeled DARPin 9_29 for Radionuclide Molecular Imaging of HER2 Expression in Malignant Tumors // *Contrast Media Mol Imaging*. 2018. V. 2018. P. 6930425. doi: 10.1155/2018/6930425.
15. Deyev S, Proshkina G, Baryshnikova O, Ryabova A, Avishai G, Katrivas L, Giannini C, Levi-Kalisman Y, Kotlyar A. Selective staining and eradication of cancer cells by protein-carrying DARPin-functionalized liposomes // *Eur J Pharm Biopharm*. 2018. V. 130. P. 296-305.
16. E. Guryev, N. Volodina, N. Shilyagina, S. Gudkov, I. Balalaeva, A. Volovetskiy, A. Lyubeshkin, A. Sen', S. Ermilov, V. Vodeneev, R. Petrov, A. Zvyagin, Zh. Alfërov, S. Deyev Radioactive (^{90}Y) upconversion nanoparticles conjugated with recombinant targeted toxin for synergistic nanotheranostics of cancer. *Proc. Nat. Acad. Sci. USA.* 2018. Sep 7. doi: 10.1073/pnas.1809258115

3rd International Symposium on
"Physics, Engineering and Technologies for Biomedicine"

BIODEGRADABLE SILICON BASED NANOPARTICLES FOR APPLICATIONS IN CANCER THERANOSTICS

V. Yu. Timoshenko

National Research Nuclear University "MEPhI", Institute Engineering Physics for Biomedicine, 115409 Moscow, Russia; Lomonosov Moscow State University, Faculty of Physics, 119991 Moscow, Russia; Lebedev Physical Institute of the Russian Academy of Sciences, 119991 Moscow, Russia

Nanoparticles (NPs) based on chemically pure silicon (Si) are biodegradable and exhibit promising physical properties for biomedical applications [1]. Si NPs are found to be able to penetrate into living cells followed with biodegradation without any cytotoxic effect. Si NPs are analyzed as marker for visualization of cancer cells and tumors can be used as sensitizer for photodynamic therapy (PDT), sonodynamic therapy (SDT) and radio-frequency-assisted hyperthermia of cancer. These properties are important in view of future applications of Si NPs in theranostics (therapy and diagnostics) of cancer [2]. Aqueous suspensions of porous Si NPs can be fabricated by high-energy milling of porous Si (PSi) films by using a planetary-type mill as well by ultrasound-assisted fragmentation of Si nanowires in water [3]. PSi films are usually formed by the standard method of electrochemical etching of crystalline silicon wafers in hydrofluoric acid solutions. Typical sizes of as-prepared porous PSi NPs are in the range from 10 to 200 nm. It was revealed that aqueous suspensions of PSi NPs with concentration up to 2 g/L were non-toxic for normal cells in darkness.

In vitro fluorescent imaging was carried out with aqueous suspensions of PSi NPs introduced to cancer and normal cells. A comparison between the fluorescent images obtained under laser excitation and white light illumination showed that PSi NPs were localized into the cell cytoplasm. *In vitro* experiments showed that photoexcited PSi NPs suppressed the proliferation of cancer cells and it was explained by oxidizing properties of singlet oxygen sensitized by PSi NPs. These results demonstrate that PSi NPs can be considered as photosensitizer for the PDT of cancer and other tumors [1,2].

PSi NPs irradiated by therapeutic ultrasound are found to induce local hyperthermia and cavitation-induced damages of cancer cells *in vitro*. *In vivo* studies confirm that PSi NPs are efficient sensitizers for SDT of malignant tumors [3]. PSi NPs with hydrophilic-hydrophobic surface properties are also prospective contrast agents for ultrasonic diagnostics of biosystems [4].

Aqueous suspensions of porous and nonporous (laser-ablated) Si NPs with concentrations below 1 mg/mL can be efficiently heated by therapeutic radiofrequency electromagnetic radiation. The heating rate was linearly dependent on NP's concentration in the range from 0.01 to 1 mg/mL. The observed effect is explained by the Joule heating due to the generation of electrical currents at the NP/water interface. Profiting from the NP-based hyperthermia, we demonstrate efficient treatment of Lewis lung carcinoma *in vivo* [2,3]. Moreover, PSi NPs with a high density of electron spin centers have been found to exhibit properties of a contrast agent for magnetic resonance imaging of cancer tumors [5].

This work was supported the Russian Science Foundation (project 16-13-10145) and by Ministry of High Education and Science of the Russian Fedration (project 16.2969.2017/4.6).

[1] V. Yu. Timoshenko, In "Handbook of Porous Silicon", Ed. L. Canham, Springer Publ., pp. 929-936 (2014).
[2] A. V. Kabashin, V. Yu. Timoshenko. Nanomedicine, 11 (17): 2247-2250 (2016).
[3] L.A. Osminkina, V.Yu. Timoshenko, Mesopor. Biomat. 3, 39-48 (2016).
[4] K. Tamarov et al., ACS Appl. Mat. & Interfaces. 9, 35234 (2017).
[5] Yu. V. Kargina, M. B. Gongalsky, A. M. Perepukhov, A. A. Gippius, A. A. Minnekhanov, E. A. Zvereva, A. V. Maximychev, V. Yu. Timoshenko. J. Appl. Phys. 123, 104302 (2018).

FLUORESCENCE LIFETIME IMAGING: TECHNOLOGY FOR MICROENVIRONMENT BIOSENSING AND ANTI-COUNTERFEITING

Junle Qu

jlqu@szu.edu.cn
Key Laboratory of Optoelectronic Devices and Systems of Ministry of Education, College of Optoelectronic Engineering, Shenzhen University, Shenzhen 518060, China

Fluorescence lifetime imaging microscopy (FLIM) has been widely applied in biomedical research. In this talk, I will first introduce the principle of FLIM, review its recent typical applications, then focus on (1) assessment of intracellular oxygen concentration in chip-based tissue culture systems; (2) temporally chameleonic ink: improved coding capacity for optical anti-counterfeiting, both based on FLIM imaging. Finally, I will present a short discussion on the current challenges for FLIM technology and its biomedical applications.

Keywords: FLIM; biomedical research; oxygen concentration; coding capacity; anti-counterfeiting; cellular imaging

3rd International Symposium on
"Physics, Engineering and Technologies for Biomedicine"

STATE-OF-THE-ART IN NANODENTISTRY: FROM NANOMATERIALS TO OPTICAL IMAGING

Anderson S. L. Gomes

Physics Department and Graduate Program in Dentistry, University Federal of Pernambuco, Recife, PE, Brazil

Nanoscience and Nanotechnology deals with science and technology at the nanoscale, whereby the materials involved should have at least one dimension less than 100nm, such that it affects some of their properties when compared to the bulk equivalent. In the healthcare area, nanoparticles of biocompatible materials have already been used for cancer treatment or for bioimaging enhancement. Nanotechnology applied to dentistry, or *nanodentistry*, has already found some developments in dental nanomaterials for caries management, restorative dentistry and orthodontic adhesives. Among the Another nanomaterial well studied in nanodentistry are silver nanoparticles, due to their bactericidal properties. In this talk, I shall review the state-of-the-art in nanodentistry, with emphasis on imaging techniques exploiting nanomaterials. As such, optical coherence tomography (OCT) has been employed with nanomaterials to enhance the acquired imaging or to exploit dielectric and metallic nanoparticles as optical clearing agents for OCT.

3rd International Symposium on
"Physics, Engineering and Technologies for Biomedicine"

OPTICAL COHERENCE TOMOGRAPHY APPLICATIONS IN BIOMEDICINE

Anderson S. L. Gomes

Physics Department and Graduate Program in Dentistry, University Federal of Pernambuco, Recife, PE, Brazil

Optical Coherence Tomography was born to see inside the eye, and it is has evolved to be "the eye seeing" throughout most parts of the human body. OCT, as it is commonly known, is one of the most fast growing optical imaging technique, which provides real time images capable of submicron resolution with penetration depths up to few millimeters. It can be used not only in hard and soft tissues, but has also been widely exploited on materials evaluation, including biomaterials.

In this talk, I shall introduce the basics aspects of the technique, which relies on optical interferometry, and then will give several examples of the state-of-the-art applications in biomedical areas, with emphasis in dermatology, ophthalmology and particularly dentistry and nanodentistry. An updated list of scientific papers in all biomedical areas can be found at http://www.octnews.org.

PERSPECTIVES OF COMPLEX STRUCTURED LIGHT WITH ORBITAL ANGULAR MOMENTUM IN OPTICAL DIAGNOSTICS

Igor Meglinski

University of Oulu, Finland; MEPhI, Russia

We investigate the applicability of using cylindrical vector beam (CVB) and Laguerre-Gaussian (LG) beams for optical biopsy. In current presentation propagation of CVB and LG beams in anisotropic turbid tissue-like scattering media is considered in comparison to conventional Gaussian beams. We demonstrate that by applying CVB and LG beams the sensitivity of the conventional polarimetry-based approach is increased at least twice in comparison with the experiments utilizing 'simple' Gaussian polarized light. The results of the study suggest that there is a high potential in application of vector light beams in tissue diagnosis.

3rd International Symposium on
"Physics, Engineering and Technologies for Biomedicine"

WISPERING GALLERY PHOTONIC MICROCAVITIES FOR BIOLOGICAL AND BIOMEDICAL APPLICATIONS

Y.P. Rakovich[1,2]

[1] *Materials Physics Center, University of the Basque Country, IKERBASQUE, Donostia-San Sebastián, Spain*
[2] *National Research Nuclear University MEPhI (Moscow Engineering Physics Institute), Moscow, Russian Federation*
Phone: (+34)94301883; e-mail address: Yury.Rakovich@gmail.com

Recent years have seen tremendous progress in the development of micro- and nanoscale optical technologies for biodetection, with research activities focused on developing highly sensitive detection schemes and a variety of biomedical and photonics applications.

Whispering gallery microresonators that confine light in a specific micro- or nano-scale volume, are extremely sensitive to their microenvironment and offer a convenient capabilities for a number of biological and biomedical applications.[1] Immensely attractive combination of optical properties makes whispering gallery mode microresonators highly efficient as biosensors, transducers and even laser surgery tools.

Label-free detection down to single molecules as well as operation in aqueous environments can be integrated cost-effectively on microchips, together with other photonic components, as well as electronic ones.[2]

In this report, the main properties of whispering-gallery mode resonators as well as operating principles of whispering-gallery-mode-bases bio-sensors and other devices are reviewed, and also different operation modes are discussed. Particular attention will be given to physics, fabrication and material science aspects of whispering gallery mode resonators, and to the most recent developments towards their application to nanoparticle analysis, biomolecular detection and biomedical applications.

[1] Y.P. Rakovich, J.F. Donegan, Photonic atoms and molecules, Laser & Photonics Reviews, vol.4, pp. 179-191, (2010).

[2] F. Vollmer, L.Yang, Label-free detection with high-Q microcavities: a review of biosensing mechanisms for integrated devices, Nanophotonics, vol.1, pp. 267-291, (2012).
[2] K.D. Heylman, K.A. Knapper, E.H.Horak, M.T. Rea, S.K. Vanga, R.H. Goldsmith, Optical Microresonators for Sensing and Transduction: A Materials Perspective, Advanced Materials, vol.29, pp. 1700037, (2017).

APOPTOTIC BODIES CONJUGATE AND REGULATE THE FUNCTIONS OF RESIDENT CARDIAC AND MESENCHYMAL STEM CELLS IN MAMMALIAN MYOCARDIUM

A.I. Tyukavin[1], G.B. Belostotskaya[2], Eu.A. Zakharov[1], S.V.Suchkov[3,4]

[1] Saint Petersburg State Chemical Pharmaceutical University (SPCPU) 14 Popova street, Saint-Petersburg, Russia
[2] Sechenov Institute of Evolutionary Physiology and Biochemistry Russian Academy of Sciences (IEPhB), 44 Toreza pr., Saint-Petersburg, Russia,
[3]I.M. Sechenov First Moscow State Medical University (Sechenov University), 15/13 Rossolimo street, Moscow, Russia
[4] National Research Nuclear University (MEPhI), 31 Kashirskoe shosse, Moscow, Russia

Key words: apoptosis, apoptotic bodies, stem cells, myocardial regeneration

Abstract. It seems that apoptotic bodies (ApBs) are prototypes of drugs that can selectively activate tissue-specific regeneration of resident cells of damaged organs, and also involve growth factors of bone marrow mesenchymal stem cells (BM MSCs). To create pharmacological agents, it is necessary to identify the nature of signaling molecules located on the surface of ApBs responsible for the homing of MSCs from blood to tissues, as well as to determine miRNA profiles in ApBs, which are the code of tissue-specificity of cells.

Introduction. One of the most promising resources of the body for restoring the myocardium after ischemic damage and optimizing the functions of the cardiac muscle during aging are resident cardiac stem cells (CSCs) and BM MSC. The mechanisms of their interaction in the whole organism remain unclear. It seems that apoptosis has a key role in myocardial regeneration and may have a linkage with functions of CSCs and MSCs in tissues after infarction and regeneration, and in the aging process as well. Apoptosis (in contrast to necrosis), simultaneously with the destruction of irreversibly damaged cells, initiates processes that stimulate the proliferation of cells. It was suggested that final products

of apoptosis, ApBs, could be an activation factors which have some tissue-specific code(s) for stem cell differentiation.

Materials and methods. ApB of cardiomyocytes (CMs) and fibroblasts (Fbs) were prepared according to the method of Hristov et al. [2004]. Influence of ApBs on cardiomyogenesis was studied on the model of neonatal cardiomyocytes colonies from CSCs of c-kit $^{+}$, Sca-1 $^{+}$, Isl-1 $^{+}$ -type by Belostotskaya, Golovanova [3]. Concentrations of RNA and mRNA were determined by UV-abs and fluorescence methods. In situ hybridization was used with sampling of the Y chromosome (ID Labs Biotechnology). Migration of BM MSC was studied in C57BL/6 mice. BM MSCs were isolated from the tubular bones of C57BL/6 mice expressing the GFP protein. Sections of tissues were examined on a confocal microscope LSM5 PASCAL. The contractile function of the myocardium after the administration of ApBs was assessed by Langendorf method.

Results and discussion.

CSCs and apoptosis. In vitro (cell culture) it was shown that ApBs of CMs, strengthened the proliferation and differentiation of CSCs inside the colonies. The contraction frequency of CM colonies during 3 weeks of cultivation increased in comparison with the control by more than 1.5 times. ApBs of Fbs did not have such effect on the CM colonies. After repeated intravenous administration of ApBs of Fbs to rats with postinfarction heart failure, the ventricular contractility increased by 30% in 3 weeks after myocardial infarction (MI) compared to the control [2]. Injections of ApBs of CMs to "old" (500 g) Wistar rats caused an increase in myocardial contractility to values characteristic of the cardiac muscle of "young" (200-300 g) animals. ApBs of Fbs caused suppression of myocardial contractility. It is shown that the cardiomyocyte ApBs activates the processes of cardiomyocyte pool renewal, and the fibroblast ApBs stimulate the development of clones, from which non-contractile structures of the myocardium, in particular the endothelium of the vessels, are formed.

Quantitative analysis showed that the concentration of RNA in CMs, before their apoptotic fragmentation, and in ApBs was 36.96 ng/μl and 14.96 ng/μl, respectively. The mRNA content in CMs and ApBs was

15.11 ng/μl and 6.42 ng/μl, respectively. With a decrease in the concentration of RNA and mRNA in ApBs, the ratio of these substances in the products of apoptosis did not change – 41.0 and 43.0%, respectively.

BM MSCs and apoptosis. BM MSCs of animals (XY), introduced into the bloodstream of rats (XX) after MI, went beyond the vessels to the perifocal zone of the infarction. For studying

of the possible migration mechanism of BM MSCs, laser dose rates were established on a fibroblast culture, this doses which ex vivo caused mainly apoptosis or necrosis of cells. In mice (C57BL/6), one of the auricles was irradiated with apoptotic or necrotic dose. The contralateral ear served as a control. After irradiation with an apoptotic dose and administration of BM MSCs with GFP through the day on a cross-sectional preparation of the ear, the whole field of vision was covered by cells with a GFP-tag. On the preparation of the cut of the control ear, only single cells with GFP were detected. With the use of a necrotic dose of the laser, the transition of BM MSCs from blood to tissue was not observed [1].

Conclusions. It seems that the functions of CSCs and BM MSCs in the areas of myocardial regeneration are matching by ApBs of cells. Signal molecules are located on the outer surface of the ApBs, which mediate the homing and directional movement of BM MSCs into the zone of myocardial regeneration. BM MSC chemotaxis provides targeted delivery of growth factors and cytokines that are necessary to maintain proliferation and directional differentiation of CSCs. ApBs have biologically active compounds that store memory of the tissue-specificity of the dead cell. It can be assumed that simultaneously with the launch of the effector cascade of apoptosis, which ends with the formation of ApBs, microRNA expression takes place, the profile of which is a "code" of tissue affiliation of cell. With endocytosis of ApBs by resident stem cells, a specific set of trigger microRNAs expresses genes that determine the direction of CSC differentiation [2]. It can be assumed that this hypothesis is valid not only for the heart but also for other organs and tissues.

Acknowledgments. The authors are grateful to the R&D department of the international innovative biotechnology company of the full cycle BIOCAD

References

1. Tyukavin A.I, Galagudza M.M, Mikhailov et al. Mechanism of targeted migration of mesenchymal stem cells. Bull Exp Biol Med. 2012;153(4):577-580.
2. Tyukavin A. I., Belostotskaya G. B., Golovanova T. A. et al. Stimulation of Proliferation and Differentiation of Rat Resident Myocardial Cells with Apoptotic Bodies of Cardiomyocytes. Bull Exp Biol Med. 2015;159(1):138-141
3. Belostotskaya G.B., Golovanova T.A. Characterization of contracting cardiomyocyte colonies in the primary culture of neonatal rat myocardial cells: A model of in vitro cardiomyogenesis. Cell Cycle. 2014; 13:910-916

Grants and Conferences:
1. Grants - AstraZeneca Research Grant (2011); RFFR (Grant № 11-04-00993a - 2011-2013)
2. The results are approved at the I and III National Congresses on Regenerative Medicine (2013, 2017, Moscow), Congress of physiologists of the CIS (2011, Yalta; 2013, 2016, Sochi), congress of physiologists of Russia (2014, 2017), Russian Finnish Symposium. (2014, Turky; 2015,2017, SPb), Russian-German Symposium. (2017 SPb) etc.

3rd International Symposium on
"Physics, Engineering and Technologies for Biomedicine"

NEUROTOXIN-RECEPTOR INTERACTIONS: MATERIALS, BIOIMAGING, DIAGNOSTICS

Victor Tsetlin[1,2], Yuri Utkin[1], Igor Kasheverov[1], Catherine Vulfius[3], Dmitri Lebedev[1], Elena Kryukova[1]

[1] Shemyakin-Ovchinnikov Institute of Bioorganic Chemistry, Russian Academy of Sciences, Moscow, Russian Federation
[2] PhysBio of MEPhI, Moscow, Russian Federation
[3]Institute of Cell Biophysics, Russian Academy of Sciences, Pushchino, Russian Federation
victortsetlin3f@gmail.com

Background: Our work on the interaction of peptide and protein neurotoxins from different venoms with the nicotinic acetylcholine receptors (nAChRs) of muscle, nervous and immune system is being conducted by combination of different approaches: proteomic and transcriptomic analysis of venoms, characterization and spatial structure determination for new biologically active compounds, preparation of their novel labeled derivatives for analysis of biological activity. This research has a fundamental importance for understanding the principles of ligand-receptor recognition and also practical values: malfunctioning of nAChRs is associated with neurodegenerative and psychiatric diseases, nicotine addiction, lung cancer – and mapping the ligand-receptor interactions opens new ways for diagnostics and drug design.

Methods: The work has been done on naturally occurring peptide and protein neurotoxins, their fluorescent and radioactive derivatives. Binding studies and analysis of functional activity were performed by radioligand analysis, patch-clamp electrophysiology and calcium imaging. We used membrane-bound muscle-type nAChR *Torpedo californica,* neuronal alpha7 nAChR, various homomeric and heteromeric nAChRs expressed in Xenopus oocytes, alpha7-like chloride channels in *L.stagnalis* molluscs models of the nAChR ligand-binding domain.

Results: For the first time the interaction of snake venom alpha-neurotoxins and alpha-conotoxins from the *Conus* molluscs has been performed on such a wide range of nAChRs and their models which al-

lowed us to clarify the selectivity of the tested toxins and their derivatives, to compare the receptor levels at normal state and in pathological models; preclinical tests on one of the snake venom peptides discovered by us demonstrated that it is a promising myorelaxant.

Supported by RFBR grant 17-00-00064

DESIGNING DRUGS: A NOVEL THERMORESPONSIVE ANTIBIOTIC

Bernhard Reuter

Zuse Institute Berlin, Germany

As shown in our group for a fentanyl derivate, it is possible to design pH-selective drugs, thereby reducing side effects by affecting only certain body regions. Inspired by this success we hypothesize that it is possible to design thermoselective respective thermoresponsive drugs as well. As a proof of concept, we designed a potentially thermoresponsive antibiotic in a process starting at the drafting table and resulting in an geometrically and energetically optimized 3D structure. After quantum-chemical calculation of the partial atomic charges and subsequent force-field parametrization, the assumed thermoresponsive features of the potential antibiotic were accessed in a molecular dynamics simulation study. Finally the results were analyzed by generalized Markov state modeling.

3rd International Symposium on
"Physics, Engineering and Technologies for Biomedicine"

NANOSCALE METAL-ORGANIC FRAMEWORKS FOR TARGETED AND CONTROLLED DRUG DELIVERY

Dr. Indrajit Roy

Department of Chemistry, University of Delhi, Delhi-110007, India.
E-mail: indrajitroy11@gmail.com

Nanoscale metal organic frameworks (NMOFs) are inorganic-organic hybrid nanoparticles that combine the benefits of active metal center/s and organic functionalities. Their extensive porosity allows the hosting of several types of drugs and other active agents. Moreover, drug molecules can also serve as part of the organic framework, which results in very high drug loading (up to 50% wt/wt). Furthermore, incorporation of optical or magnetic moieties within these nanoparticles allows for optically or magnetically guided delivery to target sites, as well as photo-activated localized therapies. Thus, NMOFs are very promising candidates for multimodal bioimaging, targeted delivery, controlled drug release, and externally activated therapy.

We have synthesized few types of NMOFs, that involve cationic centers/clusters of iron, copper and silver, along with organic ligands such as carboxylate, cyanate, gallate and alendronate. They have been incorporated with photosensitizers such as methylene blue for combined chemotherapy and photodynamic therapy. Nanosized magnetic iron clusters present in these NMOFs facilitate magnetically-targeted drug delivery. This talk will present representative examples of such research work.

A PALETTE OF FLUORESCENT NANOPARTICLES TO DEVELOP MODERN BIOMEDICAL TOOLS

V. Oleinikov[1,2], M. Tretyak[1], M. Artemyev[1,3]

[1] Shemyakin–Ovchinnikov Institute of Bioorganic Chemistry, Russian Academy of Sciences, Moscow, Russian Federation
[2] National Research Nuclear University "MEPhI", (Moscow Engineering Physics Institute), Moscow, Russian Federation
[3] Research Institute for Physical Chemical Problems of Belarusian State University, Minsk, Belarus
Presenting author e-mail address: voleinik@mail.ru

In nanomedicine, one of the most important and promising areas is the designing of fluorescent nanoparticles based nano-tools for theranostics. These are diagnostic nanoprobes for detection and visualization of inflammation area or neoplasm, micro- or nanoparticles for multiplex diagnostics by simultaneous registration of multiple disease markers. In terms of theranostic, the development of nanosystems makes it possible to take the next step in implementing the concept of the "magic bullet", formulated by Paul Ehrlich in 1908. On the basis of nanostructures, various systems are developed for the targeted delivery of medicinal agents to their targets, providing programmable, scheduled and controlled release of these agents in the injured tissue, allowing the therapeutic action of these agents to be controlled by optical or other methods.

To date, there is a fairly broad palette of fluorescent nanoparticles that have a great potential in biomedical applications. The development of nano-tools aimed at solution of specific problems requires knowledge of the properties of such nanoparticles. In this report, the capabilities and limitations of such nanoparticles in various applications are considered and compared.

Here we adduce the parameters, compare advantages and limitations, discuss potential application areas of nanosystems based on:

- fluorescent semiconductor nanocrystals (quantum dots);
- carbon graphene-like and diamond-like nanoparticles;

- polymer fluorescent nanoparticles;
- porous silicon-based nanoparticles;
- nanophosphors.

The non-linear optical properties of nanoparticles are compared, including the features of their use in deep probing of biological tissues by two-photon excitation in the IR region. Aspects of photodynamic therapy (including two-photon PDT) using fluorescent nanoparticles are considered.

To date, suspension multiplex microchip systems are becoming a routine in clinical diagnostics. The idea to use polymer microparticles, coded by fluorescent dyes, in multiplex analysis was proposed in 1984. The modern market has both tools for flow analysis of such suspensions (Luminex instruments), as well as sets of coded microspheres (xMAP technology). The replacement of organic dyes by fluorescent nanoparticles (colloidal quantum dots) gives a lot of principal advantages. The first report on the creation of a multiplex suspension system for clinical diagnosis was published in 2008. To date, much progress has been made in this direction, although there are several significant problems in the development of such systems.

In general, the development of theranostics nano-instruments based on fluorescent nanoparticles requires an understanding of the physical chemical properties of different nature nanoparticles. In this report, we tried to systemize and discuss the properties of nanoparticles from the point of view of diagnostic and therapeutic nano-tools design.

The work was supported by the Russian Foundation for Basic Research (grants 18-54-00033 and 18-04-00893).

3rd International Symposium on
"Physics, Engineering and Technologies for Biomedicine"

TRANSLATIONAL MEDICINE: MYTH OR REALITY?

Sergey Suchkov[1,2], Noel Rose[3,4], William Thilly[5], Shawn Murphy[6,7], John Mendelsohn[8], Dan Roden[9]

1National Research Nuclear University "MEPhI", (Moscow Engineering Physics Institute), Moscow, Russia
2Institute for Personalized Medicine (Science & Technology Park for Biomedicine, Sechenov University), Moscow, Russia
3School of Medicine, John Hopkins University, Baltimore, MD and
4Harvard Medical School, Boston, MA, US
5Director of MIT Center for Environmental Health Sciences and
Professor, Department of Biological Engineering, MIT, Cambridge, MA, USA
6Director, Center for Bioinformatics, Harvard Medical School and
7Partners Healthcare, Boston, MA, USA
8Director, Institute for Personalized Therapy, University of Texas
MD Anderson Cancer Center, Houston, TX, USA
9Director, Center for Personalized Medicine, Vanderbuilt University,
Nashville, TN, USA
ssuchkov57@gmail.com

As international experience shows, the development and efficacy of national economy are determined by innovative trends, acting as a necessary condition for achieving economic growth and provide an opportunity to hold a strong position in the global economy. In the area of healthcare services, the strategic indicators are becoming Biopharma, Biotech and Bioengineering being united and consolidated via philosophy and armamentarium of translational research and applications whose major goal is again becoming an upgraded model of the national healthcare system. The latter, i.e., Personalized & Precision Medicine (PPM) as being the Grand Challenge to predict and to prevent and, finally, not to treat but to cure is rooted in a big and a new science generated by Systems Biology, Translational Medicine (TM) and its applications to be focused on "bench to bedside and back" research.

The National Institutes of Health (NIH) has proposed that research moves from "bench to bedside" through a Pipeline consisting of distinct research categories and stages bridged by translation. One of the prod-

ucts of the Pipeline is the reconceptualization of the latter connecting basic research to practice via the translational bridges. So, the final Pipeline concept includes two distinct types of research, basic and human, and translation is required to connect each to the other and to practice. And, finally, translational research is the application of discoveries made in the laboratory to the development of novel drugs, vaccines, and diagnostic tools.

We define translational research as translating the findings of basic research into practice and thus meaningful health outcomes, whilst categorizing and structuring the pipeline with stages (phases) including phases of idea genera-tion, research on safety and identifying doses, utilizing proof of principle, effi-cacy effectiveness of the drug using validating and post-marketing surveillance, etc. Meanwhile, basic research encompasses not just the typical understanding of basic research as dealing with the cellular level, but also basic cognitive science. Medical practice involves assessing both cognitive status and interventions used. Meaningful health outcomes spans impacts of interest to a wide range of individuals including the patient, his or her caregivers and social support networks, payers of the health care, and policy makers.

Meanwhile, multiple levels of challenges exist in both academia and industry, spanning from scientific understanding and institutional infrastructure to busi-ness risk and feasibility. The "valley of death," the large gap between basic research and translation to novel therapeutics, underscores the need to restruc-ture education and academic research to cultivate the fertile interface between academia and industry. The Valley of Death refers to the obstacles that are keeping innovative medical research discoveries from becoming new therapies or even making it to clinical trials as applicable to the pipeline. Funding is nec-essary to bridge the gap.

Translational research facilitates the application of basic scientific discoveries in clinical and community settings to prevent and treat human diseases and has become a driver of change within academic institutions, government research centers, and the biomedical products industry. A pipeline matures into a drug portfolio requiring constant development and management. That portfolio can only become successful

when supported by the right decisions. Modern organizations often target collaboration, which makes organizational networks complex, but it also makes it feasible to build optimally structured functions with minimal cost. To remain competitive in today's pharmaceutical marketplace, many drug firms are focusing on operational improvements in the product development process, as well as on the adoption of new R&D strategies to position the company for sustained growth and success. Some companies are re-assessing R&D strategies that focus on large-market indications, and are moving toward smaller, niche pharmaceutical markets, where therapeutic need is great, competition is decreased, and return on investment may be substantial. Ultimately, new drugs and biologics may emanate from "innovation nodes" which will be disease- or therapeutic area-focused, and they will allow developers to leverage the capabilities and expertise of the participating stakeholders.

There are many reasons to be encouraged about the opportunities created by academic–industry partnerships. In particular, industry gains access to cutting-edge science and new technologies, and academics gain access to drug devel-opment expertise and an increased likelihood that their research discoveries will ultimately result in new treatments and medicines. Moreover, academic-industry partnerships represent the key to seeing the fulfillment of the ultimate objectives of translational science.

We are in a period of dynamic change in the innovation landscape. In the new environment, innovative medicines will likely result from the combined efforts of numerous stakeholders – including large and small pharmaceutical and bio-technology companies, ARCs, patient groups, CROs, and public-private-partnerships.

3rd International Symposium on
"Physics, Engineering and Technologies for Biomedicine"

CONTRAST ENHANCED RADIOTHERAPY. CURRENT STATUS AND PROSPECTS

A. Lipengolts[1,2,3], E. Grigorieva, V. Kulakov, I. Sheino

[1] N.N. Blokhin National Medical Research Center of Oncology, Moscow, Russia
[2] A.I. Burnazyan Federal Medical Biophysical Center, Moscow, Russia
[3] National Research Nuclear University MEPhI, Moscow, Russia
Presenting author e-mail address: lipengolts@mail.ru

Contrast enhanced radiotherapy (CERT) is a novel binary method of curing cancer. Like neutron capture therapy (NCT) (which is better known modality than CERT), CERT utilize preferential interaction of external radiation with a special drug delivered in a tumor and thus providing dose increase in the tumor volume. CERT is based on a physical phenomenon of photoabsorption and uses X-rays as external radiation and high-Z elements (Z>52) as dose enhancing agent (DEA). Photoabsorption probability is proportional to $\sim Z^5$, that is why high-Z element absorb external X-ray radiation more efficiently than the elements comprising biological soft tissues and thus creating increase of absorbed dose in the vicinity of high-Z element atoms. CERT feasibility and efficacy in suppressing tumor growth was shown in a number of animal studies. Most impressing first results were shown in treating spontaneous brain tumors in dogs with iodine contrast media as DEA and modified CT scanner as an irradiating X-ray facility [1]. The summit of these studies was Phase I Clinical Trial of brain tumor metastasis CERT, which showed CERT clinical feasibility and safety [2]. However, the complexity of CERT procedure didn't allow this method to move into Phase II/III clinical trials. A new impact for CERT development was provided by progress of nanoparticles synthesis, especially gold nanoparticles. Having larger Z value then iodine (79 and 53 respectively) and showing better retention in most types of tumors than iodine contrast media gold nanoparticles were widely used in all kind of CERT studies. It was gold nanoparticles to show amazing therapeutic efficacy in CERT of orthotopic transplanted brain tumors in mice [3]. However possible

long term complications of gold nanoparticles administration into human's body still limiting their introduction into medical practice and in CERT as well.

Currently three Phase I Clinical Trials of CERT are being performed and none of them uses gold as DEA. Two of the mentioned Clinical Trials are devoted to treatment of brain tumors and one – to treatment of cervical cancer. Following drugs with high-Z elements are used in these Clinical Trials: iodine contrast media drug and gadolinium nanodrug AGuIX.

Numerous results of CERT antitumor efficacy studies are currently modifying initial strategy of CERT application in curing cancer and understanding of its tumor suppressing mechanisms. At the beginning of CERT development direct radiation damage of tumor cells due to physical increase of absorbed dose in a tumor volume was supposed to be the main mechanism of tumor suppression. But later a lot of results showing contradiction between calculated actual absorbed dose in a tumor and observed antitumor effect of CERT were obtained. It's appeared that estimated absorbed dose due to DEA presence often was almost negligible, while corresponding tumor suppression was in contrast rather significant. Currently determination of real tumor suppressing mechanism is the most important task for CERT. Like any other therapy CERT requires tools for therapy results prognosis and lack of understanding of real tumor suppressing mechanisms in CERT is limiting development of these tools.

[1] A.Norman, M.Ingram, R.G. Skillen, D.B.Freshwater, K.S.Iwamoto, T. Solberg, X-ray phototherapy for canine brain masses, Radiation Oncology Investigations, vol. 5, iss. 1, Pp. 8-14 (1997)
[2] J. H. Rose, A. Norman, M. Ingram, C. Aoki, T. Solberg, A. Mesa, First radiotherapy of human metastatic brain tumors delivered by a computerized tomography scanner (CTRx), Int. J. Radiat. Oncol. Biol. Phys., vol. 45, no. 5, pp. 1127–1132 (1999)
[3] J. F. Hainfeld, H. M. Smilowitz, M. J. O'Connor, F. A. Dilmanian, and D. N. Slatkin, Gold nanoparticle imaging and radiotherapy of brain tumors in mice, Nanomedicine, vol. 8, no. 10, pp. 1601–1609 (2013)

3rd International Symposium on
"Physics, Engineering and Technologies for Biomedicine"

IMPLEMENTATION AND EARLY CLINICAL DATA FROM PARTICLE IRRADIATION

Katharina Seidensaal

Heidelberg University Hospital, Germany

Since its opening in 2009 over 4000 patients were treated at the Heidelberg Ion-Beam Therapy center (HIT) with protons and carbon ions. In 2012 the 600 tons weighting and 360°-rotating world's first carbon ion beam delivery system (gantry) began operating, allowing irradiation from any angle with submillimeter precision. Since the beginnings at GSI (Helmholtz Center for Heavy Iron Research) in the 1990's we gained experience with particle therapy for the treatment of rare and radioresistant malignant diseases as inoperable chordoma, chondrosarcoma of the base of scull as well as non-squamous cell carcinomas of the head and neck e.g. adenoidcyctic carcinoma. The physical advantages of particles allow us dose escalation in the treatment of tumors located closely to sensitive organs at risk as the brain stem, the optic nerve and optic chiasm. Treatment protocols for more common tumor entities as prostate cancer, pancreatic cancer, hepatocellular cancer and gynecologic malignancies were implemented or are currently tested in studies. We furthermore treat children and young adults, mainly suffering from neurooncologic malignancies as well as sarcomas with proton therapy in order to reduce the dose to neighboring organs at risk and thus for example decrease the risk of late side effects and secondary malignancies (e.g. craniospinal irradiation of medulloblastomas). Ongoing studies will help us to develop and improve particle therapy in future.

3rd International Symposium on
"Physics, Engineering and Technologies for Biomedicine"

BIOLOGICAL EVALUATION OF HISTIDINE AND TRYPTOPHAN LABELED WITH GALLIUM-68 AS POTENTIAL TUMOR IMAGING AGENTS

V.K. Tishchenko[1], V.M. Petriev[1,2], A.A. Mikhailovskaya[1], K.A. Kuzenkova[1], I.N. Zavestovskaya[2]

[1] Tsyb Medical Radiological Research Centre, Obninsk, Russia
[2] National Research Nuclear University MEPhI (Moscow Engineering Physics Institute), Moscow, Russia
e-mail: petriev@mrrc.obninsk.ru

Natural amino acids play important roles in many cellular processes such as protein synthesis, energy metabolism, cell signaling, carbon sources for cell growth, and neurotransmission. Radiolabeled amino acids target the increased amino acid transport in cancer cells compared with normal tissues. It is mediated by amino acid transporters overexpression in different types of tumors. Indeed, radiolabeled amino acids have the potential to overcome some of the limitations of 2-deoxy-2-[^{18}F]fluoro-D-glucose ([^{18}F]FDG) in tumor imaging.

Gallium-68 (^{68}Ga) is a promising radionuclide for PET due to its appropriate decay properties ($T_{1/2}$ = 67.7 min, β^+ = 89%, $E_{\beta max}$ = 1.9 MeV) and the availability from the ^{68}Ge/^{68}Ga-generator system. In this study we labeled two amino acids histidine and tryptophan with ^{68}Ga, investigated its biodistribution and compared them with $^{68}GaCl_3$.

The evaluation of ^{68}Ga-histidine and ^{68}Ga-tryptophan biodistribution was performed using Wistar rats with transplanted subcutaneously cholangioma RS-1. The animals were injected with 0.37 MBq of ^{68}Ga-histidine, ^{68}Ga-tryptophan, or $^{68}GaCl_3$ (n = 16 each tracer) in a volume of 0.1 ml through the tail vein. Then the animals were sacrificed at different time points, the samples of tissues and organs were isolated, weighed and counted in automatic gamma counter. Data were calculated as a percentage of the injected dose per gram of tissue (%ID/g). All the biodistribution studies were carried out in strict compliance with the national laws related to the conduct of animal experiments.

The accumulation of ^{68}Ga-histidine in tumor tissue increased approximately 6 fold from 0.11±0.04 %ID/g at 5 min post injection (p.i.) to 0.67±0.07 %ID/g at 3 h p.i. The amount of ^{68}Ga-tryptophan in tumor was also risen 2.4 fold from 0.34±0.18 %ID/g to 0.80±0.06 %ID/g at 5 min and 3 h p.i., respectively. In contrast, the uptake of $^{68}GaCl_3$ decreased throughout the study from 0.34±0.07 %ID/g to 0.13±0.04 %ID/g.

The uptake and retention of ^{68}Ga-histidine and ^{68}Ga-tryptophan in non-target organs, except kidney and femur, were higher than those of $^{68}GaCl_3$. For example, the highest blood concentration of ^{68}Ga-histidine and ^{68}Ga-tryptophan was 2.24±0.78 %ID/g and 2.99±0.51 %ID/g at 5 min p.i., respectively. Subsequently, their amounts decreased more than two times. The levels of radioactivity in other organs were less than 1 %ID/g.

On the contrary, both agents showed lower renal accumulation than $^{68}GaCl_3$. The uptake of $^{68}GaCl_3$ in kidney varied from 1.67±0.17 %ID/g to 3.57±0.89 %ID/g, whereas the uptake of ^{68}Ga-histidine and ^{68}Ga-tryptophan didn't exceed 1 %ID/g throughout the study. Also femur uptake of $^{68}GaCl_3$ was approximately 2–7 times higher than ^{68}Ga-histidine and 2–5 times higher than ^{68}Ga-tryptophan.

In conclusion, the obtained results suggest that ^{68}Ga-histidine and ^{68}Ga-tryptophan could serve as potential new PET tracers for tumor imaging.

This work was financially supported by Russian Foundation for Basic Research and the Government of Kaluga Region (project № 17-16-40007-OGN).

BIOCOMPATIBLE PHOTOMEMRISTIVE INFORMATION-SENSORY SYSTEMS BASED ON 2D CRYSTALS

G. N. Panin[1,2*], O.O. Kapitanova[3], X. Fu[1], A. S. Chan[1], T.W. Kang[1]

[1] *Nano-Information Technology Academy, Quantum-functional Semiconductor Research Center, Dongguk University, Seoul, South Korea*
[2] *Institute of Microelectronics Technology RAS, Chernogolovka, Russia*
[3] *Department of Chemistry, Moscow State University, Moscow, Russia*
[*] *g_panin@dgu.edu; panin@iptm.ru*

Von Neumann architecture of digital information processing based on CMOS technology (Fig. 1a) was developed to solve clearly defined problems with well-structured data and is inefficient for processing complex, unstructured information in real time: sound, motion and image recognition. The separation between the memory and the processor in the digital systems causes traffic issues, which limits the efficiency of power consumption and performance. High and ever-growing demands for working with big unstructured data strongly motivate the creation of new brain-like machines with neuromorphic architecture and neural networks (Fig. 1b). The unique electronic and optical properties of two-dimensional (2D) crystals, such as graphene (Fig. 1c), graphene oxide, molybdenum disulfide, etc,[1-5] demonstrate their enormous potential in creating innovative ultra-high density information-sensory systems for monitoring and processing bio-information in real time (Fig. 1d).

Memristive elements with a floating photogate, called photomemristors [2, 3] based on biocompatible graphene and 2D crystals, are investigated for use in neural networks. The photocatalytic oxidation of graphene is considered as an effective method of creating memristive elements with photoresistive switching of ultrahigh density. Particular attention is paid to the new concept of the formation of self-assembled nanoscale memristive elements for interfacing electronic neural networks and natural neurons. Biocompatible photomemristive systems exhibit multiple states that can be monitored over a wide range of radiation and can be used in neurohybrid sensory systems for recording neu-

ral signals from the visual cortex, image processing and pattern recognition as well as for selective manipulation of neurons by light.

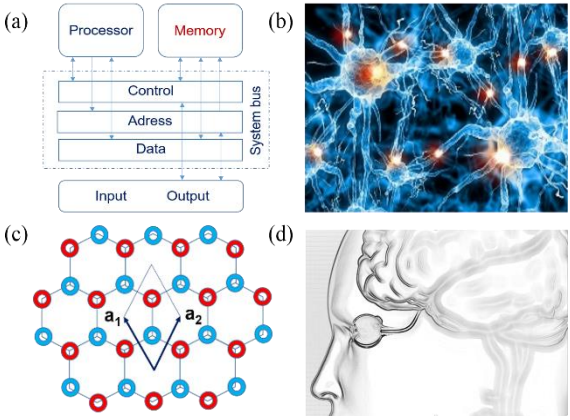

Fig. 1. (a) Von Neumann architecture of a digital computer, (b) Neural network, (c) The honeycomb lattice of graphene. (d) Retinal prostheses based on graphene.

This work was supported by Basic Science Research Program through the NRF of Korea funded by the Ministry of Education (No. 2017R1D1A1B03035102)

[1] X. Fu, P. Ilanchezhiyan, G. M. Kumar, H. D. Cho, L. Zhang, A. S. Chan, D. J. Lee, G. N. Panin and T. W. Kang, Nanoscale 9, 1820- 1826 (2017).
[2] W. Wang, G. N. Panin, X. Fu, L. Zhang, P. Ilanchezhiyan, V. O. Pelenovich, D. Fu & T. W. Kang, Scientific Reports 6, 31224 (2016).
[3] O. O. Kapitanova, G. N. Panin, H. D. Cho, A. N. Baranov and T. W. Kang, Nanotechnology 28, 204005 (2017).
[4] B. Davaji, H. D. Cho, M. Malakoutian, J.-K. Lee, G. Panin, T. W. Kang & C. H. Lee, Scientific Reports 7, 8811 (2017)
[5] E. A. Kolesov, M. S. Tivanov, O. V. Korolik, O. O. Kapitanova, H. D. Cho, T. W. Kang, G. N. Panin, Carbon 141, 190-197 (2019).

METIONINE UPTAKE BY BRAIN TUMORS OF DIFFERENT TYPES

A. A. Postnov[1,2], A. V. Agafonova[1], I. N. Pronin[2]

[1] National Research Nuclear University MEPhI, Moscow, Russia
[2] N. N. Burdenko NSCN, Moscow, Russia
Postnov.email.gmail.com

Currently one the most informative techniques for metabolic imaging of brain tumors is PET-CT with 11C-methionine as radiopharmaceutical. The goal this work was to study the details of metabolic pathway and to investigate the dynamics of the accumulation of 11C-methionine in different types of brain tumors. Also, the optimal time delay between the injection and the start of the scan had to be determined.

92 patients with the morphologically confirmed diagnosis were included in the work. The following types of brain tumors were included: pylloid astrocytoma (PA, see also in the table 1), diffuse astrocytoma (DA), anaplastic astrocytoma (AA), glioblastoma (GB), oligodendroglioma (ODG) and oligoastrocytoma (OAC). All data were acquired in list-mode. For each patient the total volume of the tumor, the mean, maximum and minimum values of the uptake ratio (T/N) and the standardized uptake value (SUV) for the tumor and the healthy tissue were determined.

The thorough study of the dynamic PET data demonstrated that PET-CT investigation with 11C-methionine can be initiated 10 min. after the administration of radiopharmaceutical to the patient. Currently, the time gap accepted by most medical centers is 20 min. or longer.

Analysis of the correlation between SUVn and SUVt showed that the accumulation of 11C-methionine in the healthy tissue is proportional to the concentration of radiopharmaceutical in the tumor for all study groups.

It was also found that the SUV of the tumor is proportional to the T/N ratio however the SUV of the healthy tissue does not correlate with the T/N ratio. This observation remains constant for all study groups.

There was no correlation found between SUV of the healthy tissue and SUV of the tumor tissue to the total tumor volume.

Table 1. Comparison of the results in each study group. Abbreviations see in the text. ODG and OAC are mixed with gr.2 and gr.3 patients together

Groups / Parameters	PA	DA	AA	GB	ODG	OAC
Total quantity	7	14	15	38	10	6
Average age	27	35	36	54	44	49
SUVt (12.5 min p.i.)	2,18±0,38	1,61±0,54	2,17±0,63	2,47±1,24	1,79±0,49	2,74±1,52
SUVt (17.5 min p.i.)	2,08±0,46	1,55±0,51	2,13±0,62	2,33±1,29	1,77±057	2,58±1,45
Student's t-test (tumor)	0,03	0004	0,007	$5,97*10^{-5}$	0,03	0,008
SUVn (12.5 min p.i)	1,01±0,21	0,94±0,21	0,90±0,24	0,85±0,24	1,08±0,19	1,11±0,51
SUVn (17.5 min p.i)	1,02±0,22	0,94±0,21	0,90±0,23	0,86±0,25	1,10±0,21	1,10±0,50
Student's t-test (healthy tissue)	0,67	0,62	0,98	0,89	0,10	0,19
T/N (12.5 min p.i)	2,19±0,36	1,68±0,33	2,41±0,72	2,93±1,23	1,64±0,18	2,58±1,26
T/N (17.5 min p.i)	2,07±0,40	1,62±0,31	2,28±0,73	2,84±1,28	1,58±0,22	2,47±1,23

DC DISCHARGE PLASMA: SURFACE MODIFICATION OF BIOMATERIALS FOR TISSUE ENGINEERING

T.S. Demina[1,2]

[1] *Enikolopov Institute of Synthetic Polymer Materials, Russian Academy of Sciences, Moscow, Russia*
[2] *Institute for Regenerative Medicine, Sechenov University, Moscow, Russia*
detans@gmail.com

Fabrication of polymeric scaffolds, i.e. biodegradable implants serving as temporary templates for cell growth and tissue formation, having well-controlled characteristics is one of key aspects of tissue engineering [1]. The scaffolds should possess a number of bulk/surface properties to meet strict requirements, which are difficult to fulfil during a fabrication process. Additional modification of scaffolds surface properties could be required to tune up the first level of cell/biomaterial interaction. Plasma treatment is one of the most effective and powerful tool to control surface properties of materials preserving their bulk characteristics. A possibility of varying plasma treatment conditions, such as discharge type, gas nature and pressure, treatment time, etc., allows to control surface chemistry, morphology and properties in a wide range [2].

In a frame of this work an effect of direct current (DC) discharge plasma treatment of various polymeric materials on their surface properties including ability to support adhesion and growth of different cell lines are discussed. Effectiveness of plasma treatment as a direct approach to modify biomaterials surface properties or as a tool to preliminary activate surface for further immobilization of different bioactive components will be presented.

A number of materials made of polymers of natural (chitosan) and synthetic (poly(L,L-lactide)) origin as well as of chitosan/gelatin/poly(L,L-lactide) graft-copolymer in a form of films or non-woven mats were treated with an air plasma at pressure of 10–20 Pa and a discharge current of 50 mA for 60 s [3,4]. As a function of treatment conditions and macromolecular features the surface

characteristics of the materials were studied in terms of surface morphology, chemical structure, surface charge and hydrophobic/hydrophilic balance using scanning electron microscopy, X-ray photoelectron spectroscopy, dynamic capacitance technique and goniometry. An ability of non-treated and plasma-treated materials to support adhesion and growth of mouse fibroblasts L929 and human mesenchymal stromal cells was evaluated as well.

A second option of plasma treatment application, i.e. surface activation method for further immobilization of bioactive components, was highlighted in terms of immobilization of protein (collagen) or polysaccharides (hyaluronic acid or chitosan) onto plasma-treated surfaces of initially hydrophobic materials made of poly(L,L-lactide) or the graft-copolymer. Here, DC discharge plasma treatment allowed to effectively control surface properties by addition of desired functionality to the scaffold. Thus, plasma treatment could be rightly considered as important tool for fabrication and modification of scaffolds for tissue engineering.

The reported study was partially funded by RFBR according to the research project № 18-32-00901.

[1] F.J. O'Brien Biomaterials and scaffolds for tissue engineering, Materials Today, vol. 14, pp. 88-95 (2011).
[2] P.K. Chu, J.Y. Chen, L.P. Wang, N. Huang, Plasma-surface modification of biomaterials, Mater. Sci. Eng., vol. 36, pp. 143-206 (2002).
[3] T. Demina, D. Zaytseva-Zotova, M. Yablokov, A. Gilman, T. Akopova, E. Markvicheva, A. Zelenetskii DC discharge plasma modification of chitosan/gelatin/PLLA films: surface properties, chemical structure and cell affinity, Surf. & Coat. Technol., vol. 207, pp. 508–516 (2012).
[4] T.S. Demina, M.G. Drozdova, M.Yu. Yablokov, A.I. Gaidar, A.B. Gilman, D.S. Zaytseva-Zotova, E.A. Markvicheva, T.A. Akopova, A.N. Zelenetskii DC discharge plasma modification of chitosan films: an effect of chitosan chemical structure, Plasma Process Polym., vol. 12, pp. 710-718 (2015).

DEVELOPMENT OF RADIOTHERAPY SYSTEM BASED ON 6 MeV C-BAND LINAC

G. Sharkov[1], T. Bondarenko[1], I. Dergacheva[1], E. Khmelevski[5], T. Krylova[1], T. Lobzhanidze[1], L. Ovchinnikova[23], S. Polikhov[1], V. Smirnov[1], V. Shvedunov[23], N. Shvedunov[23], G. Sarychev[4], A. Ableev[4]

[1] SC NIITFA, Moscow, Russia
[2] Moscow State University, Moscow, Russia
[3] LEU MGU LLC , Moscow, Russia
[4] National Research Nuclear University "MEPhI", Moscow, Russia
[5] Federal State Budgetary Institution National Medical Research Radiological Center
Presenting author e-mail address: gbsharkov@niitfa.ru

The goal of the development is to create a radiotherapy system KLT using 6 MeV electron accelerator for 3D conformal therapy in static, dynamic and rotational techniques. In the standard configuration the system is equipped with compact C-band accelerator [1], [2], [3] and cone beam CT system.

The proposed system allows to decrease dependence on import medical products, decrease the costs of medical centers for radiotherapy systems purchase and service. The serial production of KLT in Russia will allow satisfying the demand of Russian market and, hence, increasing the availability and quality of the oncological patients' treatment.

The system being developed has several advantages:

- Compactness and lightweight of C-band accelerating structure and its novel multibeam klystron allows for significant decrease of the weight and dimensions of gantry, thus bring more space and comfort to patient and medical staff.
- The usage of state-of-the art solid state modulator for accelerating system allows to create beams with fast varying duty cycle and energy. This opens the opportunity to decrease the load on MLC leaves at VMAT procedures and deliver exact dose at each angle.
- The system will be equipped with automatic adaptive therapy system using deformable registration of the images.

- The movable 6D couch allows to follow the breathing of the patient by moving the couch and hence to deliver treatment at any phase of breath.
- The accelerator allows to decrease the beam energy to 2.5 MeV, allowing to obtain MeV imaging of best in class quality.
- Standard configuration of KLT radiotherapy system will include the full functioning cone beam CT system with 3D reconstruction, allowing for 6 MeV systems precise patient positioning.

The system has classical gantry composition (see Fig. 1). The compact C-band accelerator is positioned coaxially, without bending magnets, in the radiation head. After passing the collimation jaws the beam goes through specially developed ionization chamber and the 120 multileaf collimator (MLC). The MLC has 40x40 cm field size with 0.5 cm width of internal leafs and 1 cm of outside leafs. 6D couch has state-of-the art X-ray transparent tabletop.

The gantry carries the C-band 6 MW multibeam klystron (MBK) fed through the bearing by the solid-state modulator in the stand. The MeV and kV imaging systems are placed on the arms of the gantry.

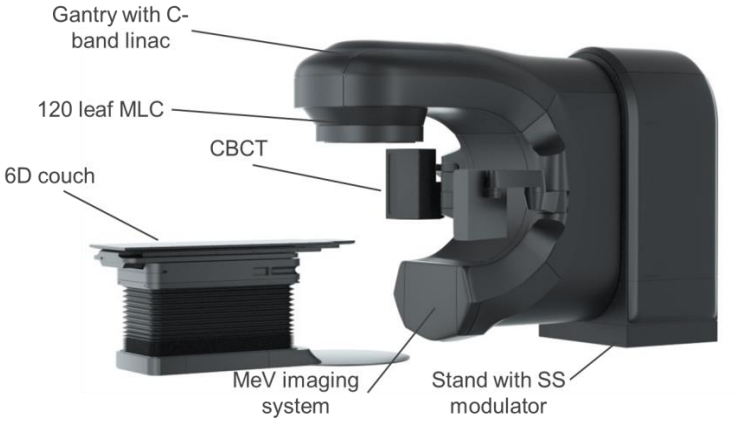

Fig.1. Preliminary layout of KLT radiotherapy system.

[1] L.Yu. Ovchinnikova, V.I. Shvedunov, "Design of C-Band Electron Linear Accelerator for a Complex of Radiation Therapy", LINAC18, MOPO59
[2] D.S. Yurov, L.Yu. Ovchinnikova, A.S. Alimov, A.N. Ermakov, V.V. Khankin, N.V. Shvedunov, V.I. Shvedunov, A.S. Simonov "Beam parameters measurement of C-band 6 MeV linear electron accelerator", LINAC18, MOPO61
[3] A.N. Ermakov, A.S. Alimov, L.Yu. Ovchinnikova, A.N. Kamanin, V.V. Khankin, N.I. Pakhomov, I.V. Shvedunov, N.V. Shvedunov, V.I. Shvedunov, A.S. Simonov, D.S. Yurov, "Linacs for Industry, Cargo Inspection and Medicine Designed by Moscow University", LINAC18, MOPO60

3D MODELING IN THE ROUTINE WORK OF THE RADIOLOGIST. EXPERIENCE OF THE BURNASYAN FEDERAL MEDICAL BIOPHYSICAL CENTER OF THE FMBA OF RUSSIA

A.N. Bashkov[1], Zh.V. Sheykh[2], S.E. Voskanyan[1], A.P. Dunaev[3], O.O Grigorieva[1], V.I. Doga[1], M.V. Popov[1], M.V. Shabalin[1], Ju.D. Udalov[1], A.S. Samojlov[1]

[1]State Research Center - Burnasyan Federal Medical Biophysical Center of Federal Medical Biological Agency, Moscow, Russia
[2]State budgetary institution of healthcare of Moscow «City clinical hospital named after S. P. Botkin of the Department of health of Moscow», Moscow, Russia
[3] State budgetary institution of healthcare of Moscow «Moscow City clinical hospital №62 of the Department of health of Moscow», Moscow, Russia
abashkov@yandex.ru. +79263499241

Objects

To analyze types of three dimensional (3D) images used in practice of radiologist depending on clinical situation. To demonstrate possibilities of new Russian sofrware «Inobitec Dicom Viewer» in providing 3D images based on segmentation tool.

Material and methods

All 3D images from database of workstation of radiologist since the year 2008 and Inobitec Dicom Viewer since the year 2017 were studied. Images were arranged depending on the fields of medicine they belong to. Number of 3D images made on workstation of radiologist with standard 3D methodics and by Inobitec Dicom Viewer in planning liver resection in patients with alveococcosis was calculated.

Results

3D images made on the workstation of radiologist were made by using following methodics: maximum intensity projection (MIP), minimum intensity projection (MinIP) and volume rendering (VR). Inobitec Dicom Viewer allowed to create 3D model based on segmentation. In general 3D images were applied in several parts of medicine: anatomy

and anomaly, neurosurgery, traumatology, cardiovascular pathology, pulmonology, abdominal surgery, oncology, education. MinIP methodic was used in pulmonology (100%). MIP methodic was applied in oncology (8%), abdominal surgery (80%) and cardiovascular pathology (12%). VR was used in all parts of medicine, mostly in neurosurgery (16%), cardiovascular pathology (13%) and abdominal surgery (67%). In education all kind of 3D images were applied.

Inobitec Dicom Viewer provided 3D model based on segmentation tool. The whole process was understandable and fast. In planning surgery for patients with alveococcosis of the liver on the workstation with standard combination of 3D methodics radiologist needed in average 5,0 3D images against 2,3 on Inobitec Dicom Viewer.

Discussion

3D images have become essential part of medicine [1]. There are a lot of literatures dedicated to applying 3D images in clinical practice. But only several authors from China in their articles shared experience of using segmentation to plan liver surgery for patients with alveococcosis of the liver [2].

Conclusion

Inobitec Dicom Viewer is cheap and reliable program which is applied successfully in our clinic. Next step in applying segmentation is 3D printing of liver for thorough planning of surgery and education.

[1] Khan U. et al. A Methodological Review of 3D Reconstruction Techniques in Tomographic Imaging. J Med Syst. Vol. 42(10), P.190, 2018.

[2] He YB et al. Application of 3D reconstruction for surgical treatment of hepatic alveolar echinococcosis. World J Gastroenterol. Vol. 21(35), P.10200-7, 2015.

POSTER REPORTS

COMBINATION OF PET TRACERS IN BRAIN TUMOR STUDIES

A.V.Agafonova[1], I.N.Pronin[2], A.A.Postnov[1,2]

[1] National Research Nuclear University MEPhI, Moscow, Russia
[2] N. N. Burdenko NSCN, Moscow, Russia
a.v.agafonova@inbox.ru

PET studies in brain oncology are essential both for the tumor staging and for the therapy planning. High procedure expenses often limit the scanning time and the number of investigations per patient. Therefor the potential benefits of the method are not always completely unfolded in clinical practice.

It is known from publications that in brain tumors the staging is not possible while using a single radiotracer. However the use of two and more radio ligands can become beneficial due to different sensitivity of tumors to those tracers at different tumor stages.

We included 11C-methionine and 18F-FDG acquisitions for each patient combined with T1, T2, T2 flair and DWI MRI. Moreover we performed dynamic scans in list-mode in order to cover all time points for tracer distribution in the tumor and healthy tissue starting acquisition process simultaneously with the tracer injection. These methods allow collecting more data without sacrificing of the clinically important quantifications.

Five patients with glioblastoma were enrolled in the study. The preliminary results obtained indicate that both radiopharmaceuticals (18F-FDG and 11C-methionine) accumulate in the tumor differently therefor the data obtained are complementary. Figure 1 demonstrates the the combined use of two radiopharmaceuticals in one patient. Combination of PET scans assists in grading the malignancy of two tumors demonstrated which was not possible with either of a single scan.

As a conclusion we can stress that the use of multitracer approach can be helpful in clinical practice due to more accurate malignancy staging.

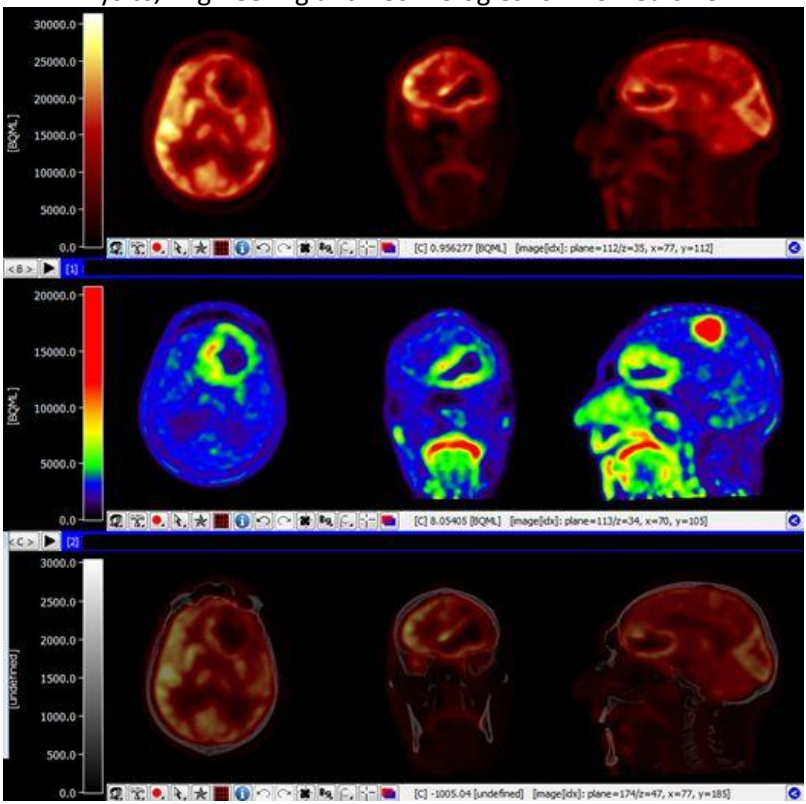

Figure 1. Brain tumors of grade 3 and grade4 imaged in one patient with FDG (upper panel, combined with CT – lower panel), Methionine (middle panel)

INFLUENCE OF NANOPARTICLES OF POROUS SILICON AND GOLD ON FREE-RADICAL HOMEOSTASIS OF THE SKIN OF RATS

Lomteva N.A.[1], Kondratenko E.I.[1], Timoshenko V.Yu.[2,3], Alykova A.F.[2], Kasimova S.K.[1], Alykova O.M.[1], Zavestovskaya I.N.[2]

[1] Astrakhan State University, Tatischev Str. 20a , 414056 Astrakhan, Russia
[2]National Research Nuclear University MEPhI, Institute of Engineering Physics for Biomedicine, Kashirskoe sh. 31, 115409 Moscow, Russia
[3]Lomonosov Moscow State University, Faculty of Physics, Leninskie Gory 1, Bdg.2, 119991 Moscow, Russia

The progressive development of nanotechnology in recent years is accompanied by a practical lack of knowledge about the impact of nanoparticles on human health, the results of early studies have shown that in the form of nanoparticles different materials acquire new, previously not inherent properties and biological effects [1,2]. The use of nanoparticles in biology and medicine increases, so they increase the sensitivity and specificity of diagnostic tools, as well as accelerate progress associated with new physical, chemical and biological effects inherent in nanomaterials. Investigation of the most common patterns of biological and toxic effects of nanoparticles is the most important fundamental issues of toxicology of nanoparticles, which, along with their biocompatibility requires careful study [1].

The aim of this work was to study the impact of exchange rate application to the skin of female rats of a suspension of nanoparticles of porous silicon and gold on the level of free radical oxidation and catalase activity in the homogenate of the skin.

Aqueous suspensions of porous silicon nanoparticles with dimensions of about 100 nm were obtained by mechanical grinding of mesoporous silicon films in water [3]. Suspensions of gold nanoparticles with average sizes of 30-50 nm were obtained by laser ablation of gold targets in deionized water [4]The experiment used 20 females of white rats with an average weight of 210 g. The age of the animals was 6 months. Female rats were divided into three groups: 1) group I – control – ani-

mals, on the skin of which the physiological solution was applied; 2) group II – animals, on the skin of which nanosilicon particles were applied in aqueous suspension; 3) group III - animals, on the skin of which nanogold particles were applied in aqueous suspension. The suspension of silicon and gold nanoparticles in the saline solution at a concentration of 0.2 mg / ml was applied once a day as a thin layer to the shaved area of the skin of animals (interscapular area) and left to dry Applications were applied for 10 days (daily, once) [5].

All animals were kept in standard vivarium conditions with free access to water and food. Animal killing by decapitation was performed after preliminary anesthesia with diethyl ether. All experiments took into account the requirements of the Directive of the European Parliament and of the Council of the European Union on the protection of anioals used for scientific purposes (2010/63/EU), Order of the Ministry of health of the Russian Federation No. 199n of 01.04.2016. "On approval of the rules of laboratory practice" and the Protocol of the Ethical Committee of the Astrakhan state medical University OF the Ministry of health of Russia № 8 dated November 24, 2015.

Skin samples were taken from the interscapular region after decapitation of animals, and then skin homogenate was prepared, in which the level of free radical oxidation and catalase activity were determined.

The level of free radical oxidation was determined by the rate of spontaneous lipid peroxidation (spLPO) and the initial content of malonic dialdehyde (MDA) in the skin homogenate by the method of Ref.[6]. Catalase activity in skin homogenate was determined by the method from Ref.[7]. The data obtained were statistically processed using Student's test.

The level of free radical oxidation in the skin changed as follows (Table 1). The level of initial MDA content in the experimental groups increased slightly compared to the same indicator in the control, while the rate of spLPO significantly increased in the groups of animals, which were applied applications of nanostructured materials.

Table 1

Effect of porous silicon and gold nanoparticles on the level of free radical oxidation and catalase activity

The studied parameters	**Experimental groups**		
	Control	**Nanoparticles of silicon**	**Nanoparticles of gold**
Initial content of MDA in the skin tissue (nmol MDA / 500 mg tissue)	2,92±0,362	4,30±0,760	3,32±0,108
The rate of spontaneous LPO (nmol MDA at 500 mg tissue for 1 hour incubation)	8,70±0,880	12,97±1,821 *	21,40±5,742 *
Catalase activity(mcat/l)	89,9±10,00	77,7±8,00	78,0±14,94

*P < 0.05 vs. experimental groups

Thus when applying nanosilicon this date increased to 1.49 times, whereas particles nanogold increase the speed spLPO 2.46 times compared to control animals ($p \leq 0.05$). The level of catalase activity practically did not change in comparison with the same index in control female rats (table.1).

Thus, the studied nanoparticles of silicon and gold did not change the initial MDA content and catalase activity in the skin tissue, but contributed to the activation of the rate of spontaneous LPO. The obtained data do not allow to fully characterize the influence of the materials under study on biological systems and require further research in this direction.

[1] Durnev A.D. Toxicology of nanoparticles // Bull. experiment. Biol. and medicine. 2008. V. 145, No. 1. P. 78-80.
[2] Durnev A.D. Investigation of Genotoxicity and Reproductive Toxicity of Silicon Nanocrystals / A.D. Durnev, A.S. Solomin and others // Bull. experiment. Biol. and medicine. 2010. P. 149, No. 4. P. 429-433.
[3] Osminkina L.A., Timoshenko V.Yu. Porous silicon as a sensitizer for biomedical applications // Mesoporous Biomaterials. -2016. -V.3. - P. 39-48.

[4] Kabashin A.V., Meunier M. Synthesis of colloidal nanoparticles during femtosecond laser ablation of gold in water. // Journal of Applied Physics - 2003. -V.94 (12). – P.7941-7943.
[5] Kasimova S.K. Influence of sulphide-silt curative mud on free-radical skin homeostasis / S.K. Kasimova, E.I. Kondratenko, A.V. Stepanov // Natural sciences. - 2012. - №4. - P. 73-77.
[6] Korolyuk, M.A. Method for determination of catalase activity. Korolyuk, L.I. Ivanova, I.G. Mayorov et al., Lab. Business, 1988. - №1. - P. 16-18.
[7] Stalnaya M.D. Method for the determination of malonic dialdehyde with thiobarbituric acid / M.D. Stalnaya, T.T. Garishvili // Modern methods in biochemistry. - M .: Medicine, 1977. - P. 66-68.

3rd International Symposium on
"Physics, Engineering and Technologies for Biomedicine"

PREPARATION NANOPARTICLES AND FILMS SI AND STUDY OF THEIR PROPERTIES BY SPM AND TEM

S. Antonenko[1], I. Derzhavin[1,2], M. **Klimentov[1], O. Uvarov[2], A. Fronya[1]**

[1] MEPhI, Moscow, Russia
[2] Prokhorov General Physics Institute of RAS, Moscow, Russia
SVAntonenko@MEPHI.RU, +7 (495) 788-5699 IP. 96-73

This present work is devoted to a search the preparation of the films and nanoparticles Si and study of their properties with the aid of scanning probe microscopy and transmission electron microscopy. The preparing samples can be used for theranostics for the purpose of the detection and treatment of cancer.

Previously submitted PLD/MBE-2000 is a deposition tool and Coherent/Lambda Physik COMPex PRO 110 excimer laser were used for the preparation of the thin films and nanoparticles Si [1]. When this was engaged the entire spectrum of possibilities of laser operates at repetition rates 1 – 105 Hz at 150 – 250 mJ per pulse (248-nm, KrF) for an average power output of 3 – 23 Watts. To increase the thickness of the films and the increase in the number of nanoparticles of working frequency and laser power up to the maximum. For the same purpose was developed and integrated into the installation of long focus lens. Range of working pressure of helium from $5 \cdot 10^{-3}$ to 5 Torr.

"Nanoeducator" – scanning probe microscope used in the mode atomic force microscopy to study prepared samples of Si. For the examination of samples was also used TEM Zeiss Libra 200 with a voltage of 200 kV. For example, two samples of Si films deposited by laser ablation on substrates were studied: monocrystalline Si and water-soluble single crystal (NaCl). Sample on Si was thinned down by mechanical from the substrate to the thickness of optical clarity, glued to the mechanical strength of the supporting ring 3 mm diameter and thinned down by ion prior to the formation perforations in the center of the sample. Sample (salt) in water to remove the watermark, then freely floating were featured on the film supports the electron microscopic grid with

cell size 200 μm. In Figure 1 presented an image of crystalline particles (left) and elektronnogramma (right), indicating the presence of such particles in the material. As an additional study to refine the elemental and chemical composition of film study method of x-ray spectral analysis of EDS (elemental composition and percentage) and electronic spectroscopy EELS losses. These data also suggest the presence of both amorphous and crystalline nanoparticles Si.

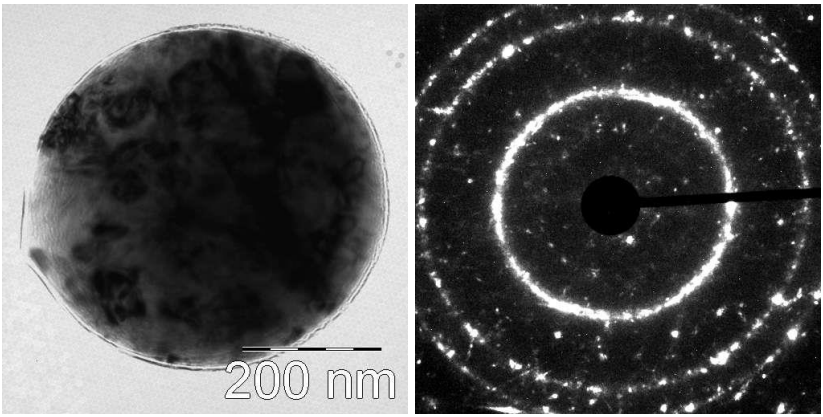

Fig.1.

[1]. S. Antonenko, S. Derzhavin, S. Klimentov Preparation of silicon nanoparticles and films by pulsed laser deposition The 2nd International Symposium "Physics, Engineering and Technologies for Biomedicine", KnE Life Sciences, pages 25–27. DOI 10.18502/5

3rd International Symposium on
"Physics, Engineering and Technologies for Biomedicine"

MORPHOLOGICAL CHANGES IN THE WALLS OF THE ARTERIES OF THE ELASTIC AND MUSCULAR-ELASTIC TYPE, ASSOCIATED WICH AGE AND CONCOMITANT PATHOLOGICAL CONDITIONS

N. Averkin[1], M. Fedorova[1], V. Brosalov[1],
S. Mozerov[2], A. Stolyarov[3], E. Kharitonov[3], O. Zhurkina[3]
[1] Penza State University, Ministry of Education and Science of the Russian Federation, 440026, Penza, Russia
[2] National Research Nuclear University MEPhI (Moscow Engineering Physics Institute), 115409, Moscow, Russia
[3]The Penza bureau is juridical-medical examination, 440067, Penza, Russia
E-mail: averkin.n@list.ru

The mortality from cardiovascular diseases (CVD) remains high both in Russia and around the world. With the help of such clinical methods as "pulse wave velocity" (PWV), the key concept of early vascular aging was "vascular rigidity", which increases with the action of the well-known classical risk factors [1,2]. What is "vascular rigidity" at the morphological level - disputes continue. Until recently, it was believed that this increase in collagen and a decrease in elastin [3]. Over time, evidence has emerged that collagen does not increase significantly, but elastin fibers are destroyed [4]. In addition, more recently, the concept of "cellular stiffness" was developed, the main value was given to smooth muscle cells (SMC) located in the middle layer of the artery, media. Under the influence of aggressive factors, SMC undergo a change in the phenotype, which varies from contractile to synthetic, chondrogenic and even osteogenic, which increases the density of the vascular wall [5].

Material and methods. A histological and morphometric analysis of 33 sections of the abdominal aorta was carried out in the deceased at the age of 25 to 91 years, without cardiovascular diseases. A study was made of the thickness of the intima and media of the artery wall, the percentage of smooth muscle cells and elastic fibers of the aortic middle layer.

Results. Differences in the histological structure of the aorta in persons of different ages were revealed. Changes in the arterial wall are often met at a young age. In individuals without CVD, confirmed at autopsy, changes in the arterial wall occur quite often already in the younger group (mean age 40,2±6,6 years): the presence of atherosclerotic plaques - in 46,1%, increased thickness of intima-media, and the percentage of smooth muscle cells and elastic fibers of the media per unit area - in 31%. At the same time, the decrease in elastic fibers reached 7,2±0,3% with an average value of 12,1±1,6%. Most often, such changes were determined in individuals with an increase in glucose detected in postmortem biochemical blood analysis (mean 12,5±0,4 mmol/L).

In the older group (mean age 65,3±7,5 years), the occurrence of these changes in the aorta is significantly increased, and there is a clear dependence of the artery wall condition on age. Understanding the patterns of development of early involute changes in the arterial wall will create the basis for fundamentally new approaches to the prevention of cardiovascular diseases.

[1] Tomiyama, H., Arai, T., Koji, Y., Yambe, M., Motobe, K., Zaydun, G., et al. The age-related increase in arterial stiffness is augmented in phases according to the severity of hypertension. *Hypertens. Res., vol.* 27, pp. 465–470. doi: 10.1291/hypres.27.465, (2004)

[2] AlGhatrif, M., Strait, J. B., Morrell, C. H., Canepa, M., Wright, J., Elango, P., et al. Longitudinal trajectories of arterial stiffness and the role of blood pressure: the Baltimore longitudinal study of aging. *Hypertension, vol.* 62, pp. 934–941. doi: 10.1161/HYPERTENSIONAHA.113.01445, (2013).

[3] Koffi, I., Lacolley, P., Kirchengaast, M., Pomiès, J. P., Laurent, S., and Benetos, A. Prevention of arterial structural alterations with verapamil and trandolapril and consequences for mechanical properties in spontaneously hypertensive rats. *Eur. J. Pharmacol.vol.* 361, pp. 51–60. doi: 10.1016/S0014-2999(98)00691-8, (1998).

[4] Sehgel, N. L., Sun, Z., Hong, Z., Hunter, W. C., Hill, M. A., Vatner, D. E., et al. Augmented vascular smooth muscle cell stiffness and adhesion when hypertension is superimposed on aging. *Hypertension* vol.65, pp. 370–377. doi: 10.1161/HYPERTENSIONAHA.114.04456, (2015)

[5] Oberleithner, H.. Aldosterone makes human endothelium stiff and vulnerable. *Kidney Int.* vol. 67, pp. 1680–1682. doi: 10.1111/j.1523-1755.2005.00263.x, (2005)

THE STIMULATING EFFECT OF LOW-INTENSITY LED IRRADIATION ON THE *IN VITRO* MODEL OF PARKINSON'S DISEASE

Bikmulina P.Y.[1], Butnaru D.V.[2], Shpichka A.I.[1], Timashev P.S.[1,3,4], Kosheleva N.V.[5,6.7], Zurina I.M.[1,5,7], Semenova M.L.[6], Gorkun A.A.[1,5,7], Maximchik P.V.[8], Yusupov V.I.[3], Gogvadze V.G.[8,9], Rochev Y.A.[1,10]

[1]Institute for Regenerative Medicine, Sechenov First Moscow State Medical University, Moscow, Russia
[2]Sechenov Biomedical Science & Technology Park, Sechenov First Moscow State Medical University, Moscow, Russia
[3]Federal Research Centre 'Crystallography and Photonics', Russian Academy of Sciences, Institute of Photonic Technologies, Moscow, Troitsk, Russia
[4]Department of Polymers and Composites, N. N. Semenov Institute of Chemical Physics, Moscow, Russia
[5]FSBSI Institute of General Pathology and Pathophysiology, Moscow, Russia
[6]Faculty of Biology, MV Lomonosov Moscow State University, Moscow, Russia
[7]FSBEI FPE "Russian Medical Academy of Continuous Professional Education" of the Ministry of Healthcare of Russia, Moscow, Russia
[8]Faculty of Fundamental Medicine, MV Lomonosov Moscow State University, Moscow, Russia
[9]Division of Toxicology, Institute of Environmental Medicine, Karolinska Institutet, Stockholm, Sweden
[10]National University of Ireland, Galway (NUI Galway), Galway, Ireland
e-mail: Polina_Bikmulina@mail.ru

Low-intensity LED irradiation (LILI) is widely used for therapeutic purposes to stimulate cell metabolism, proliferative activity and viability. The main target of LILI in cells is mitochondria. Therefore, models using cellular respiration inhibitors should be applied to study the mechanisms of LILI. An *in vitro* model of Parkinson`s disease (PD) using rotenone is one such model. PD is a neurodegenerative disorder that affects 1-2% of people over 60 years. Degeneration of dopaminergic neurons, associated with mitochondrial disfunction, oxidative stress and apoptotic cell death, has a leading role in PD pathogenesis. Rotenone is a cytotoxic agent that inhibits complex I of the electron transport chain

of mitochondria and causes PD symptoms. The aim of this work was to study the effects of LILI on rotenone-induced PD model *in vitro.*

The monolayer culture of human neuroblastoma cell line Sk-N-BE(2) was used in the work. Growth culture medium consisted of DMEM/F12 and 10% FBS. Continuous LILI was performed with two modes of LED light 1) 633nm, 1200s, 22kJ/m2 and 2) 840nm, 600s, 21kJ/m2 2 hours before the culture was treated with the inhibitor. Mitochondrial activity was suppressed by overnight culture exposure to rotenone (0,01-150μM). MTT assay was used to study cell viability. Cells stained with Hoechst 33258 (Sigma, USA) and MitoTracker Green FM (ThermoFisher, USA) were monitored via live light time-lapse microscopy in CellInsight CX7 device (ThermoFisher, USA). Oxygen consumption rate (OCR) was measured by Seahorse assay.

Both LILI modes had a stimulating effect on the neuroblastoma cell line. The preliminary irradiation with 633 nm LEDs before rotenone treatment increased cell viability by 15% compared to non-irradiated culture. Irradiation at a wavelength of 840 nm had an effect at a higher concentrations of toxin (half-lethal dose - 50 μM), increasing the cell viability by 20% on average. OCR in neuroblastoma cell line increased by 15% and 20% after irradiation with 633nm and 840nm LEDs, respectively. The irradiation of cells also resulted in elevation of mitochondrial activity by 15%.

In the current study using rotenone PD model *in vitro*, it was shown that LILI of impaired cells improved their viability and metabolic activity without causing cytotoxic effects on intact cells. Further study of the irradiation effects on human cells will prove useful in increasing the efficiency of LILI as a therapeutic agent.

The study was financially supported by Russian Science Foundation (grant № 15-15-00132, cytotoxic assay), Russian Foundation for Basic Research grants (№ 17-02-01248 and № 17-02-00832, LEDs and irradiation) and by Russain academic excellence project "5-100" (cell viability assays).

CLONING AND EXPRESSION OF *TBF* GENE AS RECOMBINANT VACCINE CANDIDATE AGAINST *VIBRIO CHOLERAE*

Y.G. Bazarnova[1], T.A. Bolotnikova[2], E.B.Aronova[3]

[1] Graduate school of biotechnology and food science, Peter the Great St.Petersburg Polytechnic University (SPbPU), Saint Petersburg, Russia, 0000-0001-9275-7913.
[2]Graduate school of biotechnology and food science, Peter the Great St.Petersburg Polytechnic University (SPbPU), Saint Petersburg, Russia, bolotnikova@ro.ru, 0000-0001-8294-0423.
[3] Graduate school of biotechnology and food science, Peter the Great St.Petersburg Polytechnic University (SPbPU), Saint Petersburg, Russia, 0000-0003-4376-2972.

Abstract

Tbf gene was cloned into pET28a(+) vector. Recombinant plasmid pET28a(+)tbf and TBF producer strain E.coli BL21(DE3)pET28a(+)tbf were obtained. Tbf gene expression in E.coli BL21(DE3)pET28a(+)tbf strain was studied. Tbf expression in E.coli BL21(DE3)pET28a(+)tbf showed a higher protein band that was inducted by IPTG as such as 0,2 % lactose. The results of the study performed have both scientific and practical significance.

Keywords: recombinant vaccine candidate, *tbf* gene, *Vibrio cholerae.*

Introduction

Cholera is an acute bacterial intestinal disease, leading to rapidly progressive dehydration and demineralization of the human body [1]. The causative agents of cholera are *Vibrio cholerae* O1 and O139 toxigenic serogroups. The major virulence factor is choleragen, i.e. the exotoxin, produced by *Vibrio cholerae*, which is substantiallyresponsible for the symptomatology of cholera and rapid disease progression [2].

Nowadays, effective prevention of cholera is oral vaccination. In addition to live-attenuated and inactivated oral cholera vaccine candidates, epitope based recombinant vaccines occupy leadership positions for the

treatment of cholera. Thus, B cell and T cell immune responses are provided by high vaccine-mediated protection.

The object of the study is *tbf* gene, encoding highly immunogenic protein epitopes of the pathogenic strains of *Vibrio cholerae*, TcpA and B(rBS), along with the site, allowing the penetratation of antigen into the gastric mucosal barrier. TcpA protein is assembled into toxin-coregulated adhesion pilus (TCP), forms polymers from subunits of 20,5 kDa [3]. This protein is a factor of *Vibrio cholerae* colonization [4]. Toxin-coregulated pilus are antigens, possessing pronounced protective properties [5]. The subunit B of cholera exotoxin (rBS) is a pentamer. Each subunit of the pentamer is represented by a polypeptide chain of 103 amino acid residues [6]. The protein contains antigenic determinants able to induce neutralizing antibodies [7]. The neonatal Fc receptor (FcRn) is an Fc receptor, which forms a heterodimer through non-covalent interaction between alpha chain and beta-2-microglobulin [8]. At acidic pH FcRn binds IgG CH2 and CH3 domains [9], ensures FcRn-mediated transcytosis of IgG across epithelial cells, which leads to the pathogen elimination [10].

The propose of the study is to clone *tbf* gene and study its expression.

Materials and Methods

Tbf gene encoding recombinant protein TBF was synthesized chemically (solid-phase oligonucleotide synthesis, phosphoramidite capping) and amplified by PCR reaction (C1000 ThermalCycler (Bio-Rad, USA)).

Primer design and analysis were performed by PCR tool FastPCR v.4.0.27 (PCRTeam, Finland), selection of primers for amplifying target gene was implemented by Oligo Calculator tool [11].

Tbf gene was cloned into pET28a(+) vector (Invitrogen, USA). XhoI and NdeI restriction sites were used for insertion of the *tbf* gene.

The expression of *tbf* from each recombinant plasmids was studied in *E.coli* BL21(DE3) strain. This strain of genotype F- ompThsdSB (rB-mB-) galdcm rne131 (DE3) is lysogenic for λ-DE3.

After performed DNA restriction digest, ligation reaction of *tbf* gene and pET28a(+) vector was used to clone purified PCR products with cohesive ends. The ligation mixture was transformed into competent

cells (*E.coli* BL21(DE3)). Competent cells were preliminarily prepared, then an electroporation method for cells transformation was applicated (electroporator Eporator (Eppendorf, Germany)). After transformation the cells were incubated with SOC medium for 40 min at 37 °C, kanamycin was a selective agent for the transformation of the cells. *PET28a(+)tbf* recombinant plasmids were purified from transformed *E.coli* cells and resolved by agarose-gel electrophoresis (0,8% agarose gel). The expression of *tbf* gene from each recombinant plasmids was studied in *E.coli* BL21(DE3)pET28a(+)tbf strain. IPTG was added to the cells to a final concentration of 1 mM. The culture without IPTG was used as a non-induced control. TBF producer cells of BL21(DE3)pET28a(+)tbf strain were grown in Luria-Bertani (LB) broth in presence of kanamycin. Except IPTG 0,2 % lactose (based on Studier's recipe) was also utilized as the inductor. Autoinduction medium with kanamycin was used under fermentation conditions. After induction aliquots of BL21(DE3)pET28a(+)tbf strain were selected and visualized in disc SDS-polyacrylamide gel electrophoresis.

To obtain TBF protein 3D structure, I-Tasser server tool was used. With the ProtParam program it was possible to analyze the recombinant protein.

Results

TBF recombinant protein produced exist in a stable structure, has a molecular weight of 74,3 kDa with pI of 8.82.

Tbf gene was successfully cloned into pET28a(+) vector. *E.coli* BL21(DE3) was transformed with recombinant plasmid pET28a(+)tbf, electrophoresed on 0,8% agarose gel. There was no mutation found in the amino acids sequence for B and T cell epitope. In this way, *E.coli* BL21(DE3)pET28a(+)tbf strain, which contains *Vibrio cholerae* antigens and produce TBF protein, was obtained. *Tbf* gene expression in *E.coli* BL21(DE3)pET28a(+)tbf showed a higher protein band that was inducted by IPTG as such as 0,2 % lactose. The results of SDS PAGE emphasized that TBF protein is a well-expressed protein.

Discussion

Expression vector pET28a(+), which was used during the study, contains the replication origin, T7 promoter, the lac operator, kanamycin

resistance gene, the start codon for translation cloned fragments. To ensure the lac operon, the plasmid contains a fragment encoding the lac repressor lacI.

Rne (rne131) gene mutation of *E.coli* BL21 (DE3) encodes RNase E truncated form which reduces the intracellular destruction of mRNA, leading to increase its enzyme stability. *Lon*- and *ompT*- protease gene mutations obtain non-proteolysed recombinant proteins in a large quantity.

Conclusion

This study is a start of design safe and stable recombinant vaccine candidate against *Vibrio cholerae*, which contains TcpA protein, the subunit B of cholera exotoxin (rBS) and domain, which acts like a Fc-binding ligand in gastric mucosal barrier (FcL).

The research was performed in the laboratory of genetic engineering of vaccines №6 at the State Research Institute of Highly Pure Biopreparations, St. Petersburg, Russia.

References

1. Harris, J. B. Cholera / J. B. Harris, R. C. LaRocque, F. Qadri, E. T. Ryan, S. B. Calderwood // The Lancet. – 2012. – № 9835. – P. 2466–76.
2. Finkelstein, R. A. Pathogenesis of Experimental Cholera: Biologic Ativities of Purified Procholeragen A / R. A Finkelstein, P. Atthasampunna, M. Chulasamaya, P. Charunmethee // Journal of Immunology. – 1966. – № 3. – P. 440–49.
3. Kiaie, S. Recombinant toxin-coregulated pilus A (TcpA) as a candidate subunit cholera vaccine / S. Kiaie, H. Abtahi, G. Mosayebi, M. Alikhani, I. Pakzad // Iranian Journal of Microbiology. – 2014. – №6. – P. 68–73.
4. Megli, C.J. Crystal structure of the Vibrio cholerae colonization factor TcpF and identification of a functional immunogenic site / C.J. Megli, A.S. Yuen, S. Kolappan, M.R. Richardson, M.N. Dharmasena // Mol Biol. – 2011. – № 409. – P. 146–158.
5. Liljeqvist, S. Surface display of the cholera toxin B subunit on Staphylococcus xylosus and Staphylococcus carnosus / S. Liljeqvist // Applied and Environmental Microbiology. 1997. –№ 63. – P. 2481–2488.

6. Sanchez, J. Recombinant cholera toxin B subunit and gene fusion proteins for oral vaccination / J. Sanchez, S. Johansson, B. Löwenadler, A. Svennerholm, J. Holmgren // Research in Microbiology. – 1990. – № 141. – P. 971–979.
7. Praetor, A. Membrane-anchored human FcRn can oligomerize in the absence of IgG / A. Praetor, R. M. Jones, W. L. Wong, W. Hunziker // Journal of Molecular Biology. – 2002. – № 321. – P. 277–284.
8. Schroeder, H.W. Structure and function of immunoglobulins / H.W. Schroeder, L. Cavacini // The Journal of Allergy and Clinical Immunology. – 2010. – P. 41-52.
9. Raghavan, M. Fc receptors and their interactions with immunoglobulins / M. Raghavan, P. J. Bjorkman // Annual Review of Cell and Developmental Biology. –1996. – №12. – P. 181–220.
10.Reed, S.M. Equine internal medicine (Fourth edition) / S.M. Reed, W.M. Bayly, D.C. Sellon. – St. Louis, Missouri: Elsevier. – 2018. – P. 1566.
11. Oligo Calculator tool [Electronic resource] : A program for calculating the properties of oligonucleotides (primers). – Access mode : http://www.bio.bsu.by/molbiol/oligocalc.html, free. – Ver. from the screen.
12 I-Tasser [Electronic resource] : A tool for obtaining a 3D protein structure. – Access mode : https://zhanglab.ccmb.med.umich.edu/I-TASSER/output/S390985/25fmau/, free. – Ver. from the screen.

DEVELOPMENT OF CONE-BEAM 4DCT FOR PROTON THERAPY OF MOVING TUMORS IN SITTING POSITION: FIRST EXPERIMENTAL RESULTS

M.A. Belikhin[1,2], A.A. Pryanichnikov[1,2], A.E. Shemyakov[1,2], A.I. Shestopalov[2]

[1]PhTC LPI RAS, Protvino, Russia
[2]Protom ltd., Protvino, Russia
Presenting author e-mail address: mikhailbelikhin@yandex.ru

The issue of intra-fractionally moving tumors due to respiratory process is one of the most important problems in particle therapy today. An essential part of treatment for such tumors is four-dimensional computed tomography (4DCT). Unlike a classical 3DCT, this one allows to acquire a tomogram of thorax and abdomen areas in a certain phase of respiration cycle. In this way, treatment planning and irradiation can be carried out for this phase, generally, for phase of a respiratory pause when tumor is immovable [1].

The cone-beam tomograph as part of proton therapy complex "Prometheus" [2] is used for tomography of head and neck areas. However, it is being planned that this tomograph will be improved for using in treatment of moving tumors located in thorax and abdomen areas, and work in this direction is already underway. For experiments a simple breathing simulator was created. This simulator consist of polypropylene pipes and it is dressed in a vest with water, thus its form repeats the shape of the human thorax. The front surface of simulator is moved by a servo motor, simulating the respiratory movements.

In this paper there are results of the first experiment with the breathing simulator. The purpose of this experiment is to compare tomograms in two cases: in the first case the movement of breathing simulator is not taken into account, in the second case this movement is being tracked by the external respiratory sensor simultaneously with the process of snapshots obtaining and the tomogram is reconstructed in a certain phase (in the phase of immovable state of simulator).

The obtained axial projections for both cases are shown in fig. 1. In the first case there is image blur in the area of movement and in the second case there is no blur, because only the snapshots corresponding to the same breathing phase were used. The significant difference between densities of the breathing simulator structure, x-ray scattering and small number of snapshots are main causes of the multiple artifacts in obtained tomograms therefore the next stages of researches and developments will be primarily aimed at solving these problems. In the future it will allow to use this cone-beam tomograph in clinical practice of moving tumors treatment in sitting position.

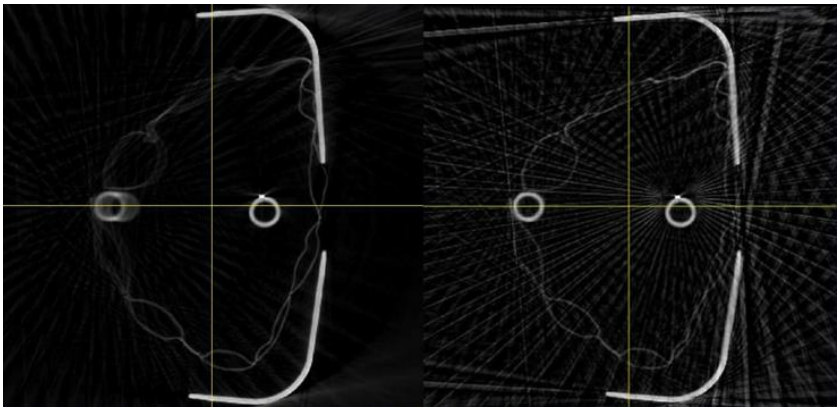

Fig. 1. Axial projections: 3DCT (left) and 4DCT (right)

[1] T. Kubiak, Particle therapy of moving targets – the strategies for tumour motion monitoring and moving targets irradiation, Br J Radiol 2016; 89: 20150275.
[2] Balakin V.E. et al., Clinical Application of New Immobilization System in Seated Position for Proton Therapy, KnE Energy & Physics | The 2nd Interna-tional Symposium "Physics, Engineering and Technologies for Biomedicine", pp. 45–51, 2018.

IN VIVO ANALYSIS OF QUANTUM DOTS FLUORESCENCE SIGNAL INTENSITY AFTER SUBCUTANEOUS INJECTION

Svetlana Bozrova[1], Maria Baryshnikova[1,2], Zinaida Sokolova[1,2], Amir Tukhvatullin[3], Denis Logunov[3], Igor Nabiev[1,4], Alyona Sukhanova[1,4]

[1] Laboratory of Nano-Bioengineering, National Research Nuclear University MEPhI (Moscow Engineering Physics Institute), Moscow, Russia
[2] N.N. Blokhin National Medical Research Center of Oncology, Ministry of Health of the Russian Federation, Moscow, Russia
[3] N.F. Gamaleya Federal National Research Center for Epidemiology and Microbiology, Moscow, Russia
[4] Laboratoire de Recherche en Nanosciences, EA4682-LRN, Université de Reims Champagne-Ardenne, Reims, France
Presenting author e-mail address: svetaboz@yandex.ru

Quantum dots (QDs) are semiconductor nanocrystals possessing unique optical properties. They are 2-10 nm in size [1] and are characterized by a wide excitation spectrum, narrow and symmetrical fluorescence spectrum, high photostability, and bright luminescence [2]. QDs are promising tools for *in vitro* and *in vivo* fluorescent imaging, and have a high potential as specific labels to be used in medical diagnosis [3].

This study was aimed at analyzing the QD fluorescence signal intensity *in vivo* after subcutaneous injection to experimental animals. The ultimate goal is to develop a mouse model of human xenograft tumors where diagnostic nanoprobes based on conjugates of QDs and specific vector molecule could be used to detect tumor cells.

To obtain biocompatible QDs, we transferred inorganic nanocrystals from an organic to an aqueous phase by means of successive two steps ligand exchange reaction on their surface. Characterization of the resultant water-soluble QDs included the estimation of their spectral properties and the measurement of the hydrodynamic diameter, electric charge, and dynamic stability of QDs under physiological conditions. Careful characterization of QD preparations is exceptionally important for the

development of protocols of QD *in vivo* imaging, because it allows the minimization of the intra- and inter-assay variations of the results.

IVIS Lumina LT Series III *in vivo* imaging system was used to perform comparative analysis of fluorescence signal intensity of QDs samples injected subcutaneously with varying doses to BalbC/nude immunodeficient mice.

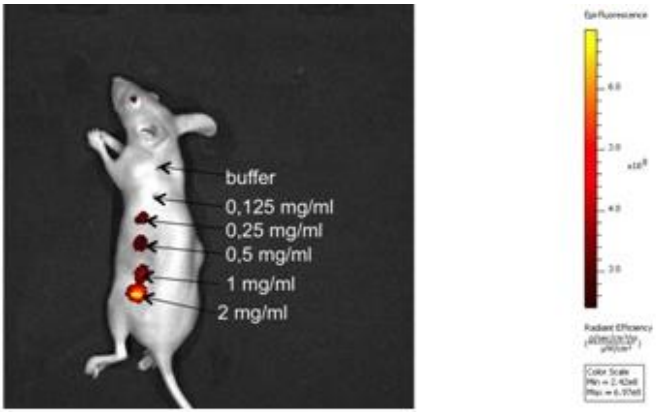

Fig. 1. Analysis of the fluorescence signal intensity after *in vivo* subcutaneous injections of different concentrations of quantum dots (EX 570, EM 575/650).

Our study has demonstrated that the concentration limit for the detection of the fluorescence signal after a single subcutaneous injection of QDs is 0.125 mg/ml (Fig. 1). The results of this study will be used for experimental analysis of the diagnostic potential of QD-based nanoprobes with the use of xenografts of the SK-BR-3 breast cancer transplanted to BalbC/nude immunodeficient mice.

This work was funded by Russian Science Foundation, contract number 17-15-01533**.** We thank Dr. Pavel Samokhvalov for providing QDs as synthetized.

[1] I.L. Medintz, H.T. Uyeda, E.R. Goldman, H. Mattoussi, Quantum dot bioconjugates for imaging, labelling and sensing, **Nature materials**, 4(6), 435–446, (2005).
[2] A. Sukhanova, K. Even-Desrumeaux, A. Kisserli, T. Tabary, B. Reveil, J.M. Millot, P. Chames, D. Baty, M. Artemyev, V. Oleinikov, M. Pluot, J.H. Cohen, I. Nabiev, Oriented conjugates of single-domain antibodies and quantum dots: Toward a new generation of ultrasmall diagnostic nanoprobes. Nanomedicine: NBM, 8(4), 516–525, (2012).
[3] R. Bilan, I. Nabiev, A. Sukhanova, Quantum dot-based nanotools for bioimaging, diagnostics, and drug delivery, ChemBioChem, 22, 2103–2114, (2016).

COLD CATHODES BASED ON CARBON NANOTUBES FOR THE X-RAY TUBE USED IN RADIATION THERAPY AND DIAGNOSTICS

A. Bratsuk[1,2], A. Simonov[1,2]

[1]FSUE «SRI SIA «LUCH», Podolsk, Russia
[2]NRNU «MEPhI», Moscow, Russia
E-mail address: avbratsuk@mail.ru

The aim of the work is to create field emission cathodes based on carbon nanotubes (CNTs) for an X-ray tube used for medical diagnostic and therapeutic purposes. Cathodes from nickel, cobalt, covar (these materials are catalysts for CNT synthesis [1]) are made in the form of a disk with a diameter of 5 mm, a thickness of 500 μm. On the cathode surface CVD method synthesized carbon nanotubes, whose diameter ranges from 30 to 70 nm.

The output dose characteristics of cathodes were determined using an X-ray experimental cell that contains a tungsten anode. X-ray emission in the cell is perpendicular to the direction of electron flow. The distance between the cathode and the anode was 10 mm. The dose of x-ray radiation was fixed at a distance of 10 mm from the cell body. Vacuum in the cell was not worse $(1,5\text{-}2,0)\cdot 10^{-6}$ Torr. The magnitude of the applied voltage is limited by electric sparking in the volume of the experimental cell.

The highest dose rate of X-rays (3.33 Gy/h) was detected during operation of the cathode from the covar at a voltage of 32 kV. The emission current was 0.33 mA. Nickel and cobalt cathodes showed the following maximum dose characteristics: 0.83 Gy/h at 28 kV, 0.2 mA and 1.89 Gy/h at 31 kV, 0.29 mA, respectively.

Such powers of radiation doses will be sufficient to accumulate a total dose of 30 to 60 Gy for radiation therapy of certain diseases (malignant or non-tumorous). So, for example, a cathode from a covar with a maximum dose rate of 3.33 Gy/h will allow to collect 30-60 Gy for 14-27 forty-minute sessions.

It is worth noting that the work of field emission cathodes based on CNTs is not accompanied by significant heating: this makes it possible to bring the X-ray source directly to the tumor and to conduct contact therapy.

In addition, X-ray sources with cold cathodes can be used for diagnostic purposes. So with the help of the experimental cell X-ray images were obtained. For example, in Figure 1 there is a snapshot of the acceptable quality of a chicken wing with a bone fracture.

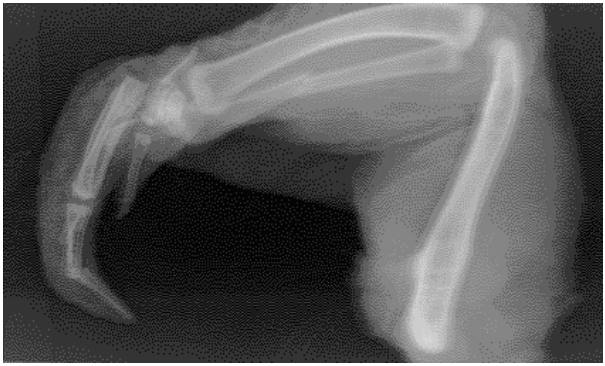

Fig.1. X-ray picture of a chicken wing obtained with the help of a cathode based on CNTs from kovar

Thus, investigations of the output doses of X-ray radiation in the operation of cathodes based on carbon nanotubes in dependence on the electric voltage and current were carried out

The dose rates obtained at room temperature (≈ 3.5 Gy/h) are acceptable for single fractions when contacting certain oncological (for example, skin cancer) and non-tumor (for example, nervous system) diseases.

[1] A. Eletsky, Carbon nanotubes and their emission properties, UFN, V.172, № 4, pp. 401-438, 2002.

CALCULATION OF THE BINDING ENERGY OF IMPLANT COATING COMPONENTS WITH A SUBSTRATE BY QUANTUM CHEMISTRY METHODS

I. Dashevskiy[1], A. Balueva[2], P. Todebush[2]

[1] Ishlinsky Institute for Problems in Mechanics RAS, Moscow, Russia
[2] University of North Georgia, Gainesville, Georgia, USA
dash@ipmnet.ru

To shorten the period of implants fusion with bone, special bioactive coatings are surfaced upon implants [1]. The most common biocompatible material for implants is titanium, one of the typical coating materials is hydroxyapatite (HAp) $Ca_{10}(PO_4)_6(OH)_2$. Since cases of delamination at the implant-coating interface were observed in clinic [2], the actual problem is to study the adhesion strength of HAp with titanium. The characteristic of that strength is the binding energy between titanium and HAp. The purpose of this work is determination of the binding energy between the hydroxyapatite functional groups (anions) and Ti (II) titanium with the help of computational quantum chemistry methods.

In this paper, all atomistic calculations, including nuclei interactions as well as determination of electronic structure with density functional theory (DFT) [3], were done with the computational chemistry suite Gaussian 09, Revision C.01 [4] using the B3LYP hybrid exchange-correlation functional (Becke, three-parameter, Lee-Yang-Parr). The program performs geometric optimization of structures and determines such a position of all the nuclei and such an electronic density function that provide the global minimum on the potential energy surface.

The interactions were studied of Ti^{2+} with: the OH^- anion (and formation of $[TiOH]^+$); two OH^- anions and formation of $Ti(OH)_2$; the anion PO_4^{3-} and formation of $[TiPO_4]^-$; the OH^- anion and the phosphate anion PO_4^{3-} and formation of $[Ti(OH)PO_4]^{2-}$; two anions OH^- and phosphate anion PO_4^{3-} and formation of $[Ti(OH)_2PO_4]^{3-}$. For all the combinations considered, the equilibrium lengths and angles of Ti-O bonds, main energy levels and binding energies were calculated, all the products structures obtained were plotted and visualized (see Fig.1). E.g. for

$[TiOH]^+$ the charge of the Ti (II) ion decreases. It means that Ti (II) experiences an increase in the electron density due to its attraction with negatively charged OH^-. For the bond between Ti (II) and O calculated length was 1.8 Å, characteristic frequency – 970 cm^{-1}, binding energy for $[TiOH]^+$ – 1.28 atomic units. One calculation took 1 to 18 hours.

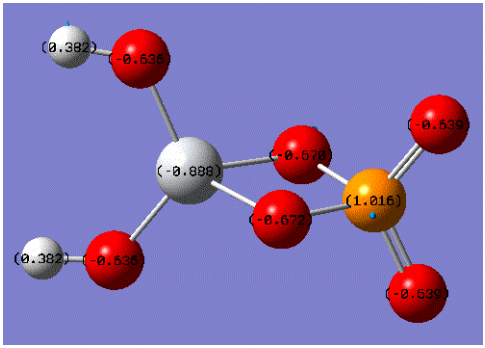

Fig.1. Stationary geometry of the interaction of Ti^{2+} with two OH^- anions and the phosphate anion PO_4^{3-} with the formation of $[Ti(OH)_2PO_4]^{3-}$

The study was carried out on the theme of the state assignment (state registration number AAAA-A17-117021310386-3) and with partial support of RFBR grants No. 17-08-01579 and No. 17-08-01312.

[1] A. Civantos, E. Martínez-Campos, V. Ramos, C. Elvira, A. Gallardo, A. Abarrategi, Titanium Coatings and Surface Modifications: Toward Clinically Useful Bioactive Implants, ACS Biomater. Sci. Eng., vol. 3 (7), pp. 1245–1261, (2017).
[2] M. Roy, A. Bandyopadhyay, S. Bose, Induction Plasma Sprayed Nano Hydroxyapatite Coatings on Titanium for Orthopaedic and Dental Implants, Surface & coatings technology, vol. 205, № 8-9, pp. 2785-2792, (2011).
[3] N. Argaman, G. Makov, Density Functional Theory -- an introduction, American Journal of Physics, vol. 68, pp. 69–79, (2000).
[4] http://www.gaussian.com/

INTERACTIVE SOFTWARE FOR IRRADIATION GUR-120 FACILITY

E.N. Denisova, A.S. Snegiryov, G.V. Kozmin, Yu.A. Kurachenko

Russian Institute of Radiology and Agroecology (RIRAE), Obninsk, Russia
ellaizaden@mail.ru

The 'GUR-120' Gamma-Facility is designed to study the effects of acute and chronic exposure with variable dose rates on agricultural products [1]. The 'GUR-120' consists of eight irradiator units (fig. 1). Ionizing radiation sources' characteristics: ^{60}Co radionuclide with total (passport) activity $4.47 \cdot 10^{15}$ Bq. The installation is in operation in RI-RAE since the mid-seventies of the last century.

Currently, the task of designing interactive software (GURSOFT) is formulated, which allows on-line mode to obtain precise values of the dose field characteristics in the irradiated object. At the GURSOFT work, it is not expected to perform radiation transport calculations with application of powerful and time-consuming software tools. All information necessary for the dose modeling in irradiated objects is formed in the databases (DB) as a result of advance preparation by precise calculations [2]. In this case, the installation operator in the interactive dialogue receives the answer "instantly" by interpolation on the databases.

The use of the GURSOFT is expected in three main modes:

- dose calculation in a given points' set in the volume of the irradiated object at a given geometry "radiation source – the irradiated object" (direct problem mode);
- estimation of the radiation source characteristics and irradiation geometry ensuring the achievement of optimal dose/dose rate in preset points (inverse problem mode);
- irradiation scenario optimization, including simulation of mechanical displacement of individual product blocks during irradiation (irradiation mode).

Software manufacturing sequence:

- program description of the irradiation object (geometry, chemical composition, package sizes, etc.));
- designing the DB;
- selection and justification of calculation methods and data libraries;

- calculations for DB;
- development of logic and algorithms of GURSOFT in three modes;
- GURSOFT programming;
- GURSOFT debugging and testing;
- GURSOFT verification based on available empirical data;
- development of technological regulations of irradiation.

The MCNP5 code [3] is used as the main software tool in conjunction with the multigroup photon data library [4]. Currently, in calculations the factors allowing to simplify the structure and content of the database under construction are established.

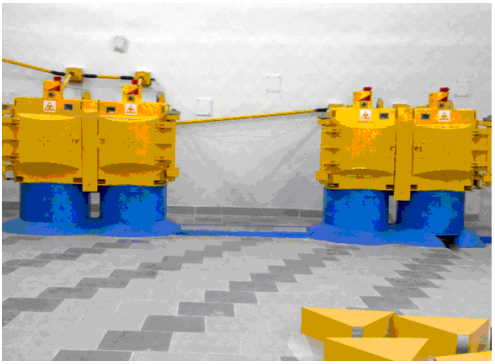

Fig. 1. General view of the GUR-120 irradiation facility

[1] Radiation technologies in agriculture and food industry/Editors: G.V. Kozmin, S.A. Geraskin and N.I. Sanzhrova. Obninsk: RIRAE,400 p. (2015)
[2] Yu.A. Kurachenko, A.V. Levchenko, Yu.G. Zabaryansky et al., Beta software for radionuclide vertebroplasty, Medicinskaya fizika, №1, pp. 51–57, (2017).
[3] Authors: X-5 Monte Carlo Team. MCNP – A General Monte Carlo N-Particle Transport Code. Version 5, Volume I: Overview and Theory. LA-UR-03-1987, 484 p. (2003).
[4] Calculated photon KERMA factors based on the LLNL EGDL (Evaluated Gamma-Ray Data Library) data file [electronic resource] https://searchworks.stanford.edu/view/11154547

PRECISION MODELING OF THYROID LESIONS IN RADIATION ACCIDENTS

E.N. Denisova, A.S. Snegiryov, G.V. Kozmin, Yu.A. Kurachenko

Russian Institute of Radiology and Agroecology (RIRAE), Obninsk, Russia
ellaizaden@mail.ru

The available computational capabilities (multi-core PCs, supercomputers, transport codes) allow us to consider the problem of dosimetric models' constructing in a complex, matching modeling of the subject area (source, irradiated object, environment) with modeling of the radiation transport. This approach is traditional for nuclear science and technology. Experience in solving these problems has allowed to create computing technologies that can be adapted to other areas. As an example of the precise domain model, the "one to one" core model can be considered, exhaustively images (in the selected software environment) the exact fuel assemblies geometry, their individual condition, the position of system control and protection rods etc. Modern transport codes, which allow to solve the radiation transport problems, usually have the ability to specify periodic structures [1], for example, reactor cells. This opportunity opens the way to precise ("voxel") domain modeling in the problems of radiation medicine and biology [2].

The paper considers the problem of the absorbed dose calculating in the thyroid gland (TG) in radiation accidents. So far as there are no any human "benchmark" (calculation or experimental) on the TG irradiation, the cattle case [3, 4] was analyzed. The aim was to determine the agreed values of the ^{131}I critical dose in the TG of cattle, leading to a serious dysfunction of the gland and its subsequent destruction. In order to achieve this goal, comprehensive studies were carried out to clarify the parameters of the compartmental model, based on reliable experimental and theoretical data. Voxel technologies are applied for modeling the subject domain (TG and its environment, Fig. 1). Finally, to solve the equation of the ^{131}I radiation transport, the Monte Carlo code [1] is applied, which takes into account the contribution of gamma and beta radiation of a source, and the contribution of all chains of secondary radiations up to total energy dissipation when calculating the dose.

As the main theoretical result, it is necessary to emphasize the conversion factor from the ^{131}I activity, distributed uniformly in volume of

the TG, to the average dose rate in the gland (Bq → Gy/s). This factor was calculated for both cows and calves in the selected domain configuration and TG morphology. The main practical result is a reliable estimation the lower bound of the absorbed dose in the cows' TG, which in a short time leads to its destruction under internal ^{131}I irradiation: ~ 300 Gy. The received results don't contradict the dosimetric data characterizing radiobiological consequences of radiation injury of a thyroid gland (~ 300 Gy) at the person and sheep [5].

No.	Thyroid size			
	External radius, cm		Height, cm	
	Cow	Calf	Cow	Calf
1	3.15	2.15	1.50	1.50
2	3.40	2.30	2.00	2.00
3	3.55	2.40	2.20	2.20
4	3.20	2.15	1.50	1.50
5	2.70	1.65	1.00	0.50

R = 2.4cm (cow), R = 1.4cm (calf)

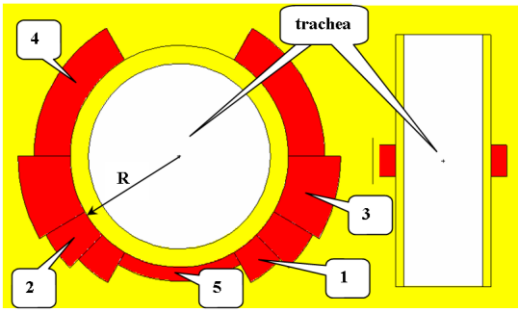

Fig. 1. Radial (left) and axial section of the TG computational model (not to scale; received by visualization of the MCNP5 code input); the table contains dimensions of TG cylindrical layers

[1] Authors: X-5 Monte Carlo Team. MCNP – A General Monte Carlo N-Particle Transport Code. Version 5, Volume I: Overview and Theory. LA-UR-03-1987, 484 p. (2003).
[2] Yu.A. Kurachenko, D.N Moiseenko, Voxel phantoms in the medical physics problems, Medicinskaya fizika, №3, pp. 27–34, (2012).
[3] E.V. Spirin, N.M. Lazarev, I.A. Sarapultsev, Formation of a dose of calves thyroid irradiation at ^{131}I receipt with a forage, Dokl. Russian Academy of Agricultural Sciences, vol. 4, pp. 54–55, (2004).
[4] A.N. Sirotkin, I.Ya. Panchenko, L.N. Tyumenev et al., Comparative behavior of ^{131}I in cows at different sources of its intake, In Sb. Biological action of external and internal sources of radiation (M: Medicine). 1972.
[5] A Toxicological Profile for Iodine. Agency for Toxic Substances and Disease Registry Division of Toxicology. USA, Atlanta, Georgia, 517 p. (2004).

THE DATABASE FOR THE AUTOMATED SYSTEM OF DIAGNOSIS OF A MELANOMA

E. Druzhinina, V Nikitaev, O Tamrazova, A Pronichev, V Sergeev, E. Polyakov

National Research Nuclear University MEPhI (Moscow Engineering Physics Institute), Kashirskoe shosse 31, 115409, Moscow, Russia

The relevance of work is caused by high degree of a case rate a melanoma, lack of enough highly qualified specialists in the field of recognition of a melanoma. The effectiveness of treatment of a melanoma depends on a stage at which it was found: the earlier the diagnosis is made, the it is more than chances of successful convalescence. However there is a variety of reasons because of which the melanoma is diagnosed at later stages. First, melanoma symptoms (especially at initial stages) are similar to symptoms of other cutifications, and not always look dangerous because of what he doesn't hurry to see a doctor for the patient. Secondly, the melanoma can longly not cause inconveniences even if initial external implications appeared.

Therefore it is important to frame the system of recognition of a melanoma for the help to doctors. Have huge value in the solution of this problem methods and agents of digital processing of images for automation of diagnostics of a melanoma. However, since system quite difficult, its creation is possible is divided into several stages, each of which is referred on detection of any qualitative and quantitative characteristics which are important for diagnostics of a melanoma (for example, netting, anomalies of a form, coloring, the size, structure, etc.).

Aim creation of a subsystem for structurization, storage and further use as knowledge bases for qualifiers of quantitative values of signs of objects (network, глобул, ячеек, hairs and areas of the birthmark) and also for object search in the set range.

During the research different types of objects on the dermatoskopichesky image of a neoplasm of a skin pigmental network, cells of pigmental network, a point and a globula, area of a birthmark were taped. The look and characteristics of these objects allow to define ma-

lignancy of a neoplasm. For example, the atypical pigmental network is one of signs of malignancy of a neoplasm of a skin.

The proposed solution is realized in the form of the program module in tongue of C ++ with use of Qt library. The application is based on the database of significant objects, in it there are tables with fields for values of signs, for example quantitative characteristics of color, perimeter, radius of a circumscribed circle etc for the corresponding objects. During work of system of the table are filled with the identified objects and their signs. The user can choose from tables or set manually (from the keyboard) values of one and/or several interesting signs, to set in a percentage ratio from the chosen value search range, to start search in range or search in the identifier. In the table corresponding to an object results of such search will appear.

Such subsystem can be useful to recognition of malignancy of a neoplasm, as a part of the training and clinical systems. Can form a basis for the qualifier and also trains in an associative perception of appearance of sign and its quantitative equivalent.

[1] Y. Zakharenko et al, The method of selection of leukocytes in images of preparations of peripheral blood and bone marrow. Journal of Physics: Confer-ence Series, 798(1), 012127, 2017

[2] A. Pronichev et al, The use of optical microscope equipped with multispec-tral detector to distinguish different types of acute lymphoblastic leuke-mia. Journal of Physics: Conference Series, 784(1), 012003, 2017

[3] V. Nikitaev et al, Application of texture analysis methods to computer mi-croscopy in the visible range of electromagnetic radiation. Bulletin of the Leb-edev Physics Institute, 43(10), 306-308, 2016

FORECASTING OF LONE ATRIAL FIBRILLATION PAROXYSMS DURING PREGNANCY

N. Dyatlov[1], F. Rakhmatullov[1], M. Mitrokhin[1], I. Moiseeva[1], L. Burmistrova[1] A. Kotlyarov[2]

[1] Penza State University, Ministry of Education and Science of the Russian Federation, 440026, Penza, Russia
E-mail: sakedas@gmail.com
[2]Obninsk institute for nuclear power engineering - National Research Nuclear University MEPhI (Moscow Engineering Physics Institute), 249040, Obninsk, Russia

The study of the features of the course of paroxysms of lone atrial fibrillation (AF) and trigger factors of its occurrence allows us to make a predictive model of AF development at any term of pregnancy according to the initial indices [1]. The obtained model can be used by clinicians to timely detect frequent and prolonged AF paroxysms associated with an increased risk of stroke and systemic embolism [2, 3]. To construct a mathematical model for predicting the number and duration of arrhythmia, we examined 90 pregnant women with lone AF. By 24-hour ECG monitoring method, 46 electrophysiological predictors of the onset of AF were obtained. To reduce the predictive features, eliminate duplicate indicators and simplify the model, a simple pairwise correlation method with a threshold value of 0.8 was used, as a result of which the number of signs was reduced to 15. Further selection of features was performed using an iterative procedure for analyzing the neighborhood component analysis (NCA), which calculates the contribution of each trait to the minimization of the mean error in the sample by the sliding control method [4]. The following two predictors of AF emergence were selected using NCA: mean nocturnal heart rate (HRnm), total daily supraventricular and ventricular extrasystoles (EStd). Next, a regression model with a distributed lag with the following form was constructed:

$$y_t = a_0 + a_1 \cdot y_{t-1} + a_2 \cdot x^1_{t-1} + a_3 \cdot x^2_{t-1},$$

where y is the predicted index (the number or duration of lone AF paroxysms), x - predictors (x^1 - HRnm, x^2 - EStd), t - conditional time (trimester number of pregnancy), a - model coefficients.

The coefficients of the model determined by the maximum likelihood method are given in Table 1.

Table 1 - Coefficients of the predictive model

Predictors	Projected indicator	Coefficients of the model			
		a_0	a_1	a_2	a_3
x^1 – HRnm x^2 – EStd	AF count	8.4861	-0.0361	0.0067	0.0046
	AF duration	-3.0097	0.1330	0.0447	0.0061

The quality of the obtained models was evaluated by the method of investigating the regression residuals for normality and the absence of correlation dependencies. The constructed histogram of the error distribution of the prediction of the number of AF paroxysms is well approximated by the normal distribution, x^2 value was 6.3, which is less than the critical value at the significance level 0.01. Thus, the described mathematical model is characterized by high accuracy, good prognostic significance and acceptable complexity of calculation, and can be recommended to the practical application to physicians.

[1] M. Mitrokhin, A. Kuzmin, N. Dyatlov, F. Rakhmatullov, N. Mitrokhina, A. Alimuradov, A. Tychkov, Investigation of models for prognosis of critical values of non-invasive electrophysiological parameters of pregnant women with abnormalities of heart rate, Conference of Open Innovation Association, FRUCT, vol. 21, pp. 238-243, doi: 10.23919/FRUCT.2017.8250188, (2018).

[2] N. Sauvé, É. Rey, A. Cumyn, Atrial Fibrillation in a Structurally Normal Heart during Pregnancy: A Review of Cases From a Registry and From the Literature, J Obstet Gynaecol Can, vol. 39(1), pp. 18-24, doi: 10.1016/j.jogc.2016.09.076, (2017).

[3] R. Rakhmatullov, L. Melnikova, A. Rakhmatullov. J. Shukin, Influence of thyrosol, bisoprolol and sotalol on structure and function of the thyroid gland, blood lipids in combination of subclinical thyrotoxicosis with atrial fibrillation, University proceedings. Volga region. Medical science, vol. 1(45), pp. 101-114, (2018).

[4] B. Alizadeh Savareh, A. Bashiri, A. Behmanesh, G. Meftahi, B. Hatef, Performance comparison of machine learning techniques in sleep scoring based on wavelet features and neighboring component analysis, PeerJ, e5247, doi: 10.7717/peerj.5247, (2018).

RESEARCH OF SEGMENTATION METHODS FOR HIGHLIGHING POINTS AND GLOBULES ON IMAGES OF SKIN NEOPLASMS

T. Ezhov[1], V. Nikitaev[1], O. Tamrazova[2], A. Pronichev[1], V. Sergeev[2]

[1]National Research Nuclear University MEPhI (Moscow Engineering Physics Institute), Kashirskoe shosse 31, 115409, Moscow, Russia
[2]RUDN University, ulica Miklukho-Maklay 6, 117198, Moscow, Russia
E. Polyakov e-mail address: kaf46@mail.ru

The relevance of this work is a possible solution to the problem of improving the technologies of early detection of malignant skin neoplasms for the timely treatment, by developing a system capable of classifying a skin neoplasm as malignant or benign.

The usage of digital image processing techniques to highlight objects on medical images is a particularly important part of the classification process of the depicted object in automated diagnostic system.

The process of image processing for highlighting objects on it includes the following steps: loading an image of a skin neoplasm into a digital image processing program, selecting the necessary parameters for image processing, adjusting the image processing parameters, obtaining the necessary image with selected objects, and analyzing it.

To solve the problem of image segmentation, there are several universal algorithms and methods. Since there is no common solution for the problem of image segmentation, these methods had to be combined with knowledge from the subject area in order to effectively solve this problem. In this work, it was decided to use the k-means segmentation method, because of its ease of implementation and high speed and MeanShift method due to the compliance of this method with the task.

The proposed solution is implemented as a separate C ++ program using the Qt library and the OpenCV graphics library.

In an experimental study, the efficiency of the implemented algorithms was investigated, and it was found that the accuracy of the selection of points and globules by the k-means algorithm was 76.5%, and by the MeanShift algorithm - 85%.

3rd International Symposium on
"Physics, Engineering and Technologies for Biomedicine"

COMBINED ACTION OF CHEMICALS AND IONIZING RADIATION ON CELL SURVIVAL

A.N. Filimonova[1,2], Yu.N. Anokhin[1,2]

[1]IATE MEPHI, Obninsk, Russia
[2] A. Tsyb MRRC, Obninsk, Russia
e-mail address: filimonowa.af@gmail.com

Actuality. Chemotherapy combined with ionizing radiation are often used in nuclear medicine. These factors synergistically enhances the action of each other. Some drugs for chemotherapy contain heavy metals in their composition, as the main component. It would be of interest to investigate experimentally their joint action to optimize the methods of combined therapy. At the present time, there are no systematic data that would confirm the universal patterns of the combined effects of chemotherapy drugs containing heavy metals with ionizing radiation.

Objective. Experimentally investigate the patterns of combined action of chemical preparations and ionizing radiation on the survival of cells.

Materials and methods. Diploid yeast cells of *Saccharomyces cerevisiae*, strain XS800, were used in the experiments. The cells were irradiated with ^{60}Co γ-rays (10.8 Gy/min). Cell survival was assessed by their ability to form a colony visible by the naked eyes. In the experiments, $K_2Cr_2O_7$ was used in various concentrations.

It was proved [1] that the mechanism of synergism in the combined use of chemical preparations with ionizing radiation is caused by the interaction of sub-lesions that are ineffective when the agents are used separately. The mathematical model of synergism predicts the conditions for maximum synergistic interaction. The model is tested for various biological objects [2], tests and acting agents.

Results. The results of determining the survival of diploid yeast cells *Saccharomyces cerevisiae* after simultaneous and separate application of $K_2Cr_2O_7$ with ionizing radiation, as well as theoretical curves calculated under the condition of independent summation of the effects pro-

duced by the factors used, were obtained. The pattern of the interaction of these agents is synergistic. Based on these results, we calculated the dependence of the synergistic enhancement ration on the drug concentrations.

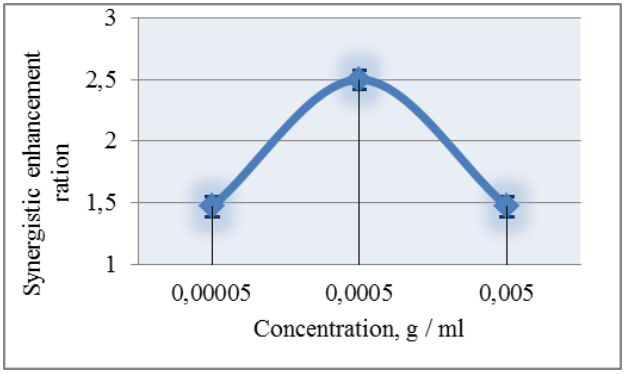

Fig.1. Dependence of the synergistic enhancement ration of simultaneous action of $K_2Cr_2O_7$ (in different concentrations) and ionizing radiation on drug concentration for diploid yeast cells of *Saccharomyces cerevisiae* of wild type (strain XS800).

Conclusions. The greatest value of the synergistic effect is observed at a concentration of 0.0005 g/ml and is equal to 2.5 and any deviation of the applied drug concentration from the optimal value leads to a significant decrease in the synergistic interaction of the factors studied. These data correspond to the predictions of the mathematical model of the synergistic interaction of various agents described earlier [1].

Literature

[1] Petin V.G., Zhurakovskaya G.P., Komarova L.N. Radiobiological bases of synergistic interactions in the biosphere. - Moscow: GEOS, 2012.
[2] M.D. Pronkevich. (Thabisimova M.D.), O.A. Vorobei, A.N. Filimonova. Participation of the restoration processes in the modification of the radiosensitivity of cells // Collection of scientific works of laureates of regional awards and scholarships, Kaluga, - 2017. - P. 93-103.

VOCAL FOLD SCARRING AND REPAIR THROUGH THE EYES OF ATOMIC FORCE MICROSCOPY

Anastasiya Frolova[1], Mikhail Svistushkin[2], Svetlana Kotova[1,3], Valery Svistushkin[2], Anatoly Shekhter[1], Peter Timashev[1,3,4]

[1] Institute for Regenerative Medicine, Sechenov University, Moscow, 119991, Russia
[2] ENT Department, Sechenov University, Moscow, 119991, Russia
[3] N.N.Semenov Institute of Chemical Physics, Moscow, 119991, Russia
[4] Institute of Photonic Technologies, Research center "Crystallography and Photonics", RAS, Troitsk, Moscow, 142190, Russia
nastyfr@yandex.ru
+7(903)715-05-41

Persistent voice impairment brings significant negative consequences not only to the health, but also to the social, mental and employment spheres of the human life activity [1]. Cicatricial lesions of the vocal folds are of significant clinical importance among all the benign laryngeal lesions. The regenerative medicine technologies open new opportunities in the repair of cicatricial lesions of the vocal folds, including the technologies using cell therapy approaches.

Here, we present a study dedicated to the effects of stem cells on the vocal folds restoration after cicatricial lesions. As an experimental model, we used a mature scar of the rabbit vocal folds, which was surgically excised with a simultaneous implantation of autologous bone marrow-derived mesenchymal stem cells (MSC) into the defect. The restoration of the vocal folds was studied 3 months post-implantation of stem cells and 6 months after the first surgery. The general morphological characteristics were estimated by means of hematoxyline-eosin and picrosirius red staining of paraffin sections. To assess the microarchitecture and viscoelastic properties of the collagen structures, we used atomic force microscopy (AFM). According to the data of optical microscopy and AFM, the scar tissue in the vocal folds with implanted MSC is closer in its structure to the normal mucosa of the vocal folds than that of the untreated scars. Such scars have also enhanced elasticity, comparable with

the elasticity of the intact mucosa. Thus, implantation of autologous MSC provides a more complete regeneration of the scarred vocal folds. AFM has proven to be an instrumental technique in the assessment of the microstructure restoration in such studies.

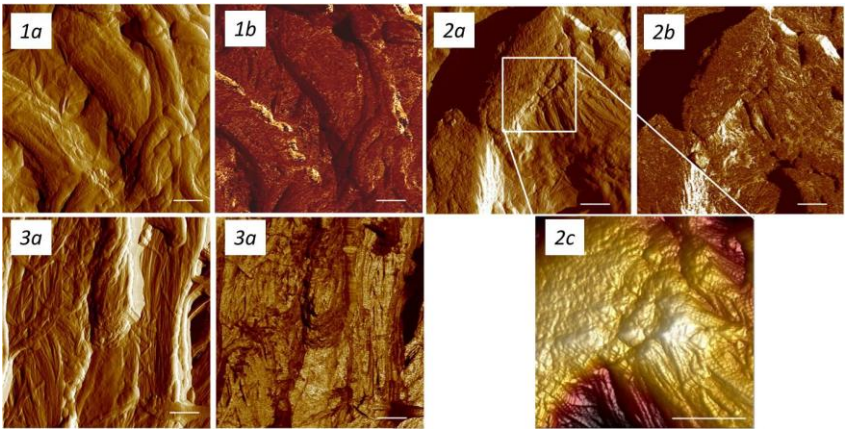

Fig.1. AFM images of the ECM of the intact (*1*), scarred (*2*) and stem cell-treated (*3*) vocal folds. *a* - topography and *b* – corresponding Young's modulus maps. 2c – details of the selected fragment in 2a, in a quasi 3D presentation, demonstrating the high compactness of the collagen fibrils' packing in the scarred tissue ECM. The twisted bundles of fibrils within the fiber are also notable. Bar=1 μm.

[1] Murry, T.; Medrado, R.; Hogikyan, N.; Aviv, J. The relationship between ratings of voice quality and quality of life measures. J. Voice, 18, 183-192, (2004)

The study is sponsored by the Russian academic excellence project "5-100".

EVALUATION OF ^{99}Mo AND ^{177}Lu FOR NUCLEAR MEDICINE IN LOW POWER REACTORS

E. Gubanova, A. Maksimushkina, H. Nepovinnykh, T. Osipova, S. Shkavrov, N. Usov, N. Epshtein

National Research Nuclear University MEPhI (Moscow Engineering Physics Institute), 115409, Moscow, Russia
E-mail: elizaveta.gubanova.1995@mail.ru

Radionuclides play an important role in our life, find many applications in industry, agriculture and respirator, as well as in medicine. The widespread use of radionuclides for nuclear medicine began in the early 1950s. Currently, radiopharmaceuticals are used mainly for diagnostic imaging studies (^{99m}Tc), but therapeutic applications have shown significant growth over the past few years. Thus, the calculation of activity, toxicity, assessment of the rate of production and the number of radionuclides is very important in the field of medicine for choosing the optimal scheme for the production of radiopharmaceuticals and conducting a course of treatment using therapeutic isotopes.

Of particular interest is the radionuclide ^{177}Lu. Currently, it is one of the most promising for radionuclide therapy. This is due to the fact that it has optimal characteristics for use in nuclear medicine: a sufficiently long half-life ($T_{1/2}$ = 6.7 days) for the production of pharmaceuticals and its transportation; energy of β-particles (maximum energy of 0.5 MeV), which allows you to affect small tumors and metastases of 1-3 mm in size, without affecting healthy tissue; soft accompanying γ-radiation with sufficient energy to visualize and track the drug in the body; the decay product of ^{177}Lu is the stable ^{177}Hf isotope. In this regard, the analysis and evaluation of various schemes for the preparation of this isotope is an urgent task at the moment.

The purpose and objectives of the study. The main goal of the work is the theoretical calculation of the ^{99}Mo and ^{177}Lu operating time at irradiation of various targets in the reactor.

To achieve this goal in the work solved the following tasks:

• an analysis of the current state of the market of medical isotopes; considered materials, methods and schemes for the production of isotopes and generators for medical purposes;

• algorithms have been developed for calculating the ^{177}Lu operating time in possible schemes for its production depending on the irradiation time, target composition and neutron flux;

• calculations of the ^{177}Lu operating time for various schemes, the optimal exposure time, and the comparison of the effectiveness of the development according to various schemes;

• algorithms have been developed for calculating the ^{99}Mo operating time in the reactor;

• calculations of the activity of ^{99}Mo under irradiation of uranium and molybdenum targets were carried out.

References

[1] C.J. Palestro. Molybdenum-99. Production and Its Impact on the Medical Community. U.S.NRC, 14 p. (2015).

[2] Nuclear Energy Agency, OECD, "The Supply of Medical Radioisotopes: An Assessment of Long-Term Global Demand for Technetium-99m" (2011).

FILTERING METHODS OF IMAGES OF SKIN IMPROVE-MENTS BASED ON SINGLE-DIMENSIONAL MASKS

E.Guguchkin[1], V. Nikitaev[1], O. Tamrazova[2], A. Pronichev[1], V. Sergeev[2], E. Druzhinina[1]

[1]National Research Nuclear University MEPhI (Moscow Engineering Physics Institute), Kashirskoe shosse 31, 115409, Moscow, Russia
[2]RUDN University, ulica Miklukho-Maklay 6, 117198, Moscow, Russia
E. Druzhinina e-mail address: kaf46@mail.ru

Recently, digital image processing for recognition of pathological processes has become one of the topical directions in the development of computer technology in medicine.

The relevance of this work is a possible solution to the problem of improving the technologies of early detection for the timely treatment of malignant skin neoplasms, by developing a system capable of classifying a skin neoplasm as malignant or benign.

The process of image processing for selecting objects on it includes the following steps: loading an image of a skin neoplasm, selecting the necessary parameters for image processing, adjusting the image processing parameter, obtaining the necessary image with selected objects, analyzing it.

One of the problems of automated image analysis of tumors is interfering with the analysis of the presence of hair on the skin.

To solve the problem of isolating the hairiness in images of skin tumors, a universal algorithm was developed based on pre-processing of images with a one-dimensional mask. The proposed solution is implemented as a separate C ++ program using the Qt library and the OpenCV graphic library.

In an experimental study, the effectiveness of the implemented algorithm was investigated. A qualitative assessment of the processed images was carried out: the program gave excellent results at 10%, good at 70% and bad at 20%.

STUDY OF COMPRESSION ALGORITHMS IMAGES OF CYTOLOGICAL PREPARATIONS

K. Hamadi[1], V. Nikitaev[1], O. Nagornov[1], A. Pronichev[1], E. Polyakov[1], S. Zaytsev[1], V. Dmitrieva[1], Yu. Ivanov, I. Shabalova[2], T. Djangirova[2]

[1]National Research Nuclear University MEPhI (Moscow Engineering Physics Institute), Kashirskoe shosse 31, 115409, Moscow, Russia
[2]Russian Medical Academy of Continuous Professional Education of the Ministry of Healthcare of the Russian Federation, Barrikadnaya str., 2/1, 125993, Moscow, Russia
The Institute of Biomedical Chemistry, 10 building 8, Pogodinskaya street, 119121, Moscow, Russia
K. Hamadi e-mail address: kaf46@mail.ru

Image compression is subdivided into lossy compression and lossless compression. Lossless compression is often preferable for artificially constructed images, such as graphics, program icons, or for special cases, for example, if images are intended for processing image recognition algorithms. Lossy compression algorithms with an increase in the compression ratio, as a rule, generate well-visible artifacts to the human eye.

The aim of the work is to investigate various methods of image compression with loss and without loss in the task of forming archives of images of cytological preparations.

As a result of the study, it was determined that the most effective in terms of speed and volume of compression is a wavelet algorithm for both lossless and lossy compression.

With lossless compression, the wavelet algorithm is more efficient than the LZW algorithm 1.5 times and 3 times more efficient than the RLE algorithm. With compression with a large compression ratio (60-90), the efficiency of the wavelet algorithm is almost the same as with JPEG2000, but it also allows you to perform the correct compression with a compression ratio of 100.

This type of archiving has been known for quite a long time and it directly proceeds from the idea of using the coherence of domains. The algorithm is focused on color and black-and-white images with smooth

transitions. Ideal for X-ray type images. The compression ratio is set and varies in the range of 5-100. When you try to set a larger factor at sharp boundaries, especially passing diagonally, a "ladder effect" appears - steps of different brightness of several pixels in size.

The algorithm used by the wavelet splits the image into high-frequency and low-frequency parts. Compression efficiencies when using wavelets are achieved with small losses on high-frequency components (quantization), since their human eye is not able to determine.

The efficiency of the algorithm can be improved by using a Huffman algorithm.

The proposed solution is implemented as a software module in C ++ using the Qt library.

[1] Y. Zakharenko et al, The method of selection of leukocytes in images of preparations of peripheral blood and bone marrow. Journal of Physics: Confer-ence Series, 798(1), 012127, 2017
[2] A. Pronichev et al, The use of optical microscope equipped with multispec-tral detector to distinguish different types of acute lymphoblastic leuke-mia. Journal of Physics: Conference Series, 784(1), 012003, 2017
[3] V. Nikitaev et al, Application of texture analysis methods to computer mi-croscopy in the visible range of electromagnetic radiation. Bulletin of the Leb-edev Physics Institute, 43(10), 306-308, 2016

DECREASE OF GABA AND NAA IN THE HUMAN VISUAL CORTEX DURING VIDEOSTIMULATION. 1H MRS STUDY

A. Iakovlev[1], A. Manzhurtsev[24], P. Menshchikov[234],T. Akhadov[4], N. A. Semenova[234]

Lomonosov Moscow State University, Moscow, Russia [1]
Emanuel Institute of biochemical physics of RAS, Moscow, Russia[2]
Semenov Institute of chemical physics of RAS, Moscow, Russia[3]
Clinical and research institute of emergency pediatric surgery and traumatology, Moscow, Russia[4]
e-mail: yakovlevalekcej@bk.ru

Glutamate (Glu) and γ-aminobutyric acid (GABA) are the major neurotransmitters (excitatory and inhibitory, respectively) in the human brain. Disturbance in the balance of GABA and Glu concentrations is important in such diseases as epilepsy, schizophrenia, Parkinson's disease. In this study, we used spectral editing with the MEGA-PRESS pulse sequence to reveal effects of visual stimulation on the balance of Glu and GABA in the visual cortex of human. At first, we obtain the standard PRESS spectrum, called "off-series". After addition of frequency-selective pulse (δ = 1.9 ppm), we obtain the second edited spectrum ("on-series"), and the result of subtraction is a signal of GABA with macromolecules (MM) (δ = 3.01 ppm ($GABA^+$)). Additional frequency-selective pulse (δ = 1.5 ppm) removes the signal of macromolecules (GABA-). In this study, the GABA+ and GABA- measurements were compared. For stimulation the flashing checkerboard (8 hz) during 10 min was used. The spectra were accumulated in the rest and during the stimulation in 21 healthy patients All spectra was processed in Gannet 3.0. GABA+ spectra didn't reveal any changes in the GABA +MM signal intensity. Statistically significant GABA decrease and the reduaction in GABA/Glx, (glx – the superposition of Glu and glutamine) were ovserved in $GABA^-$ spectra. Thus the signal of MM mask the effect of stimulation on the GABA. NAA changes were assessed from PRESS spectra accumulated every 3 min of the stimulation period. The initial 3 min of stimulation caused to statistically significant NAA decrease. Then NAA level returned to the norm.

3rd International Symposium on
"Physics, Engineering and Technologies for Biomedicine"

ETCH TRACK DETECTOR METHODS FOR THE MEASUREMENTS OF SECONDARY COSMIC RADIATION DOSES ONBOARD THE INTERNATIONAL SPACE STATION

K.O. Inozemtsev[1,2], V.V. Kushin[2], S. Kodaira[3], T. Kusumoto[3], A. Strádi[4], J. Szabó[4], I. Ambrožová[5], R.V. Tolochek[1], V.A. Shurshakov[1]

[1] Institute of Biomedical Problems of the Russian Academy of Sciences (IBMP RAS), Moscow, Russian Federation
[2] National Research Nuclear University MEPhI (Moscow Engineering Physics Institute), Moscow, Russian Federation
[3] Radiation Measurement Research Team, National Institute of Radiological Sciences, National Institutes for Quantum and Radiological Science and Technology, Chiba, Japan
[4] Hungarian Academy of Sciences, Centre for Energy Research (MTA EK), Budapest, Hungary
[5] Department of Radiation Dosimetry, Nuclear Physics Institute of the CAS, Praha, Czech Republic
Presenting author e-mail address: koinozemtsev@imbp.ru

It is commonly known from previous experiments that trapped protons generate significant amount of secondary neutrons onboard a spacecraft in low-Earth orbit [1]. Besides that comparable number of charged fragments is formed in the same nuclear interactions [2]. Secondary charged particles were paid much less attention in comparison with neutron measurements despite their significant impact on electronic components and biological objects onboard.

The features of these nuclear fragments are their relatively low energies, small residual ranges and large values of linear energy transfer (*LET*). With this in mind, they require special methods for separate registration. Most of the currently used space radiation detectors are not convenient to solve this specific problem.

The aim of this work was to develop and compare methods suitable enough to distinguish primary and secondary components of high-*LET* cosmic radiation and to evaluate their flux, spectral and dose parameters.

Etch track detector (*ETD*) CR-39™ was used in the measurements of primary and secondary high-*LET* components. Additionally to that thermo-luminescent detector (*TLD*) ^{Nat}LiF:Mg,Ti was applied to measure the dose from low ionizing primaries. The original procedures for detector etching, scanning and track data analysis were designed and compared.

Two methods based on the procedures given in [3, 4, 5] were developed and applied in long-term experiment on board *ISS*. Both of them proved to be convenient in charged nuclear fragment measurements on a high background of primary radiation. The level of primary radiation exposure was quite close to the dose limits established by *NASA* for astronauts working onboard ISS.

The contribution of charged secondaries to the common flux and total dose equivalent turned out to be considerable especially at high *LET* range.

[1] V.I. Tret'yakov, et al., The First Stage of the "BTN_Neutron" Space Experiment onboard the Russian Segment of the International Space Station, Cosmic Research, vol. 48(4), pp. 285–299, (2010).
[2] V.V. Kushin, Measurement of LET distribution and absorbed dose from secondary particles on board the spacecraft, Radiation Protection Dosimetry, vol. 141(2), pp. 199–204, (2010).
[3] I. Ambrožová, et al., Contribution of different particles onboard ISS measured with track etched detectors, Radiation Protection Dosimetry, Radiation Protection Dosimetry, vol. 180(1-4), pp. 138–141, (2018).
[4] K.O. Inozemtsev, et al., Observation of fragmentation events caused by space radiation: Contribution to the LET spectrum as measured with CR-39 track detectors, Radiation Measurements, vol. 95, pp. 37-43, (2016).
[5] K.O. Inozemtsev, et al., On the consistency among different approaches for nuclear track scanning and data processing, Nuclear Instruments and Methods in Physics Research Section A, vol. 887, pp. 133-137, (2018).

DEVELOPMENT OF MICROSCOPE SOFTWARE MODULE FOR SCANNING OF PRODUCTS WITH AUTOMATIC FOCUSING

E. Ivanov, V. Nikitaev, A. Pronichev, E. Polyakov, S. Zaytsev

National Research Nuclear University MEPhI (Moscow Engineering Physics Institute), Kashirskoe shosse 31, 115409, Moscow, Russia
E. Polyakov e-mail address: kaf46@mail.ru

Automation of scanning products is considerable interest now, since this greatly speeds up and facilitates the work of the doctor with the product.

The difficulty is the lack of a "high-level" API for the operation of the microscope. The difficulty of auto focus is that the computer does not distinguish between unfocused and focused image of the product.

The aim of the work is to develop a program with a graphical interface for convenient control of the microscope and automatic focusing on the studied product.

To solve the problem of autofocusing, a combined evaluation function 1 of focusing quality (defocusing curve) was used, the absolute maximum of which corresponds to the best focus. This function is calculated by the Laplace method 2 and the algorithm 3 based on the calculation of the standard deviation of the brightness of the image pixels. To control the microscope, a software module was developed in C ++ 11/14, which is a wrapper over a low-level "C" microscope interface used in the ATLANT diagnostic complex

The considered approach allowed to focus effectively on products in an automatic mode and to analyze them effectively.

$$F_k = \frac{L_k + G_k}{2}.$$

(1) the value of the focal curve in the K-th frame

$$L_k = \sum_{i=2}^{M-1} \sum_{j=2}^{N-1} |\nabla L(i,j)_k|.$$

(2) the expression under the sum sign is a module of the Laplace operator of the K-th frame at the point (i, j)

$$G_k = \sum_{i=1}^{M} \sum_{j=1}^{N} \left(f_k(i,j) - \overline{f_k}\right)^2,$$

(3) standard deviation of brightness

$$\overline{f_k} = \frac{1}{MN} \sum_{i=1}^{M} \sum_{j=1}^{N} f_k(i,j).$$

(4) average image brightness

Acknowledgments
The reported study was funded by RFBR according to the research project № 18-29-09115.

[1] Y. Zakharenko et al, The method of selection of leukocytes in images of preparations of peripheral blood and bone marrow. Journal of Physics: Conference Series, vol. 798, № 1, p. 012127, (2017).
[2] A. Pronichev et al, The use of optical microscope equipped with multispectral detector to distinguish different types of acute lymphoblastic leukemia. Journal of Physics: Conference Series, vol. 784, № 1, p. 012003, (2017).
[3] V. Nikitaev et al, Application of texture analysis methods to computer microscopy in the visible range of electromagnetic radiation, Bulletin of the Lebedev Physics Institute, vol. 43, № 10, pp. 306-308, (2016).

BIOPHYSICAL METHOD OF STRUCTURAL RESONANCE THERAPY IN TREATMENT OF ACUTE PANCREATITIS

Yu.V. Ivanov[1], S.G. Anaskin[2], I.D. Korniletskiy[2], D.Yu. Agibalov[2]

[1] Federal state budgetary institution of science "State research center of the Russian Federation-Institute of biomedical problems of the Russian Academy of Sciences", Moskow, Russia
[2] National Research Nuclear University MEPhI, Moskow, Russia
Presenting author e-mail address: ivanovkb83@yandex.ru

Randomized comparative perspective placebo-supervised clinical trial with assessment of an opportunity and efficiency of use in complex treatment of patients with acute pancreatitis of a new method of structural resonance therapy is carried out.

It is the new domestic method of treatment based on synchronization of rhythms of the operating factor and the corresponding functional system [2, 3]. In this plan the structural resonance therapy based on use of electromagnetic radiation and electric current in a certain frequency rhythm of functioning of living matter that promotes optimization of activity of a bioobject at the subcellular, cellular, fabric, organ, system and organismal levels [5] is represented interesting. In experiments the anesthetizing, antiinflammatory, antiedematous, reparative, immunomodulatory and trophic effects of magnetotherapy are proved [4]. Scientific biophysics established existence of certain oscillating motions of cells of various human organs which are possible for registering by means of the device - a biopotentsialograf. In the further analysis the integral frequency of self-oscillations of 0,0108 Hz was received (the period 93 seconds) and it is proved that each body is reduced rather this frequency a certain number of times, multiple 2 or 3. Based on properties of oscillatory processes in nonlinear systems devices were developed for holding sessions of structural resonance therapy. Researchers assume that in operating time of the device of structural resonance therapy the given signal of strictly certain frequency on a body of the person creates strictly certain magnetic field which recovers, normal functioning of bodies and fabrics the Operating modes of such devices necessary for achievement of the required

medical effect at various diseases were fulfilled and established experimentally [1, 5, 6].

The research included 144 patients undergoing treatment in department of surgery of Federal scientific clinical center of FMBA of Russia in the period from 2012 to 2017 with the clinical diagnosis acute pancreatitis.

Use of a method of structural resonance therapy in complex therapy of patient's acute pancreatitis allows to reduce terms of stopping of the main clinical symptoms of a disease and quicker to normalize laboratory indicators that leads to reduction of terms of hospitalization and according to expenses on drug treatment. The method of structural resonance therapy pathogenetic is reasonable, simple performed by and does not demand big financial expenses that does possible its broad use in clinical practice for patients with acute pancreatitis allows. The first experience of use of a method of structural resonance therapy showed lack of any negative side effects that does possible its broad use in clinical practice for patients with acute pancreatitis allows.

[1] Bezbakh I. V., Kuzovlev O. P., Tsakhilova S. G. Use of structural resonance therapy in recovery treatment of patients with a chronic salpingo-oophoritis//Zhurn. Russian society of obstetricians-gynecologists. – 2006. - No. 3. - Page 26-29.
[2] Gubareva V. V., Kuzovlev O. P., Kotenko K. V., Laktionova L. V. Use of structural resonance therapy for treatment of a hypomenstrual molimina at women with neuroendocrinal disturbances//Zhurn. physical therapy, balneology and rehabilitation. – 2007. - No. 1. - Page 50-61.
[3] Kuzovlev O. P., Hazina, L.V., Blinnikov I. L. A new perspective technique – structural resonance electromagnetic therapy//Zhurn. perspectives of traditional medicine. – 2003. - No. 2. – Page 44 – 50.
[4] Kuzovlev O. P., Blinkov I. L., Meyzerov E. E., etc. Structural resonance (electro- and electromagnetic) therapy: A grant for doctors. - Moscow, 2004. – 243 pages.
[5] Kuzovlev O. P., Hazina L. V., Akayev U. B. Experience of use of structural resonance electromagnetic therapy in gynecologic practice: Materials VII of the International forum "New Technologies of Recovery Medicine and Balneology". – Moscow, 2000. - Page 79-80.
[6] Hazina L. V., Korchazhkina N. B. Structural resonance therapy of patients with a lumbosacral radiculopathy//Zhurn. physical therapy, balneology and rehabilitation. – 2010. - No. 6. – Page 39 – 42.

THE AUTOMATIC SYSTEM OF THE ANALYSIS OF TISSUE SPECIMENS IN INTRAOPEATSIONY DIAGNOSIS OF NODAL FORMATIONS OF THE THYROID GLAND

Yu.V. Ivanov[1], S.G. Anaskin[2], I.D. Korniletskiy[2], D.Yu. Agibalov[2]

[1] Federal state budgetary institution of science "State research center of the Russian Federation-Institute of biomedical problems of the Russian Academy of Sciences", Moscow, Russia
[2] National Research Nuclear University MEPhI, Moskow, Russia
Presenting author e-mail address: ivanovkb83@yandex.ru

The problem of accurate intraoperative diagnosis of thyroid nodular diseases is described in detail. The authors propose a new domestic automated system of rapid analysis of histological preparations ATLANT-Biopsy developed by them for wide clinical application and on its basis — a computer Atlas of thyroid tumors. The technique of intraoperative diagnostics with the help of this system, principle of its work, advantages in comparison with traditional methods are described.

Now treatment of nodal formations of a thyroid gland continues to remain one of urgent problems in modern endocrinology.

Frequency of identification of nodal educations at ultrasound examination of a thyroid gland at the patients inspected with the preventive purpose reaches 11 - 50% [2, 5]. Unfortunately, the share of not representative aspirates reaches 4% - 25% [3, 6]. It demands carrying out repeated biopsies which almost in 50% of cases lead to obtaining information on morphology of nodal education [4]. It is essential to increase reliability of a cytologic research complex use of ultrasonography with color Doppler mapping in combination with a polyposition puncture fine-needle aspiration biopsy helps [1, 2]. Use of an aspiration fine-needle biopsy at a presurgical stage considerably improves detectability of malignant damages of a thyroid gland.

In the work we use the automated system of the analysis of tissue specimens ATLANT-Biopsy and on its basis — the computer atlas of tumors of a thyroid gland. The ATLANT-Biopsy system consists of a microscope with the color television camera of high resolution, the

computer, video signal input equipment mounted on it in the computer and the television monitor. The image can be transferred in a digital form on communication channels for consultations with specialists of other medical institutions.

In 2015 within the «Cito-Biopsiya» project the ATLANT-Biopsy systems are installed in Federal Scientific-Clinical Center FMBA of Russia and N. N. Blokhin National Medical Research Centre of Oncology with ensuring communication between these systems and consultation by specialists of Oncological scientific center of the N. N. Blokhin National Medical Research Centre of Oncology by results of the analysis of the digital images transferred on the corresponding communication channels. Since 2015 are carried out Federal Scientific-Clinical Center FMBA of Russia urgent histologic researches with use of this information system. Time of carrying out a research on the ATLANT-Biopsy system was reduced to 30 minutes.

The ATLANT-Biopsy system can be installed in the central regional or regional hospitals, providing replenishment of the atlas with images of the tissue specimens received as in the hospital, and directed from other medical institutions for diagnosis and consultations.

[1] Vetshev P. With, Chilingaridi K. E., Cherepenin M. Yu. Miniinvasive technologies in treatment of high-quality formations of a thyroid gland//Surgery. - 2002. - No. 7. - Page 61-64.
[2] Li SL. Nodal craw: clinical inspection and treatment in the USA//Modern aspects the surgeon, endocrinology: Materials XI (XIII) of the Russian symposium on surgery, endocrinology. Lectures, T. 1. - S.-P.,2003. - Page 90-99.
[3] Seliverstov O. V., Halts V.A.Retsidivny craw//Modern aspects surgeon, endocrinology: Materials IX (XI) of the Russian symposium on surgery, endocrinology. - Chelyabinsk, 2000. - Page 388-391.
[4] Cherenko See Missile defense need of change of medical tactics at an uzovy craw//Materials V of the congress of SFULT. - Dnipropetrovsk, 1994. - Page 117.
[5] Ezzat S., Sarti D.A., Cain Dr., Braunstein G.D. Thyroid incidentalomas: prevalence by palpation and ultrasonography.//Arch. Intern. Med.-1994. - Vol. 154. - P. 1838-1840.
[6] Gharib H. Fine-needle aspiration biopsy of thyroid nodules: advantages, limitation and effect//Mayo Clin. Proc. - 1994. - Vol. 69. - P. 44-49.

3rd International Symposium on
"Physics, Engineering and Technologies for Biomedicine"

BREATH ACETONE DETECTION WITH THE NEW COLORIMETRIC SENSOR: INTERPRETATION OF THE PILOT STUDY RESULTS

M. Dmitrienko[1], E. Kolomina[1], A. Ivanova[1, 2]

[1] Association of Medicine and Analytics Co Ltd, 199034, 18 line V.O. 3, St.Petersburg, Russian Federation
[2] St. Petersburg state institute of technology (technical university), 190013, St. Petersburg, Moskovsky Ave., 26, Russian Federation
e-mail:ivanovanastia1928@gmail.com

Background:

Fatty acids act as the main source of energy for tissues during the glucose deficit (low carbohydrates diet, periods of high physical activity, starvation etc.) [1-3]. Fatty acids may be oxidated with the formation of the ketone bodies; therefore the level of the acetoacetate**,** D-β-hydroxybutyrate, and acetone in biologic fluids and exhaled air will increase. Ketosis can be monitored by β-ketones in blood and by acetone in exhaled air.

Methods:

The aim of the pilot study was to assess the correlation between the fat burning and breath acetone concentration. Blood β-ketones monitor, electrochemical sensor-based acetone device and new colorimetric sensor for acetone detection have been used. Three healthy volunteers participated in this study. Two of them (FBV-1 and FBV-2) were trying to enter the fat burning state. The third (RV) was for controls. Duration of the study was 16 days.

Results:

Results are shown on the figure 1, where:
- bc-level of β-ketones, μmol/l
- acl (es) - level of acetone in exhaled air measured by electrochemical sensor (ES) , ppm
- acl (cs) - level of acetone in exhaled air measured and by colorimetric detector (CD), ppm.

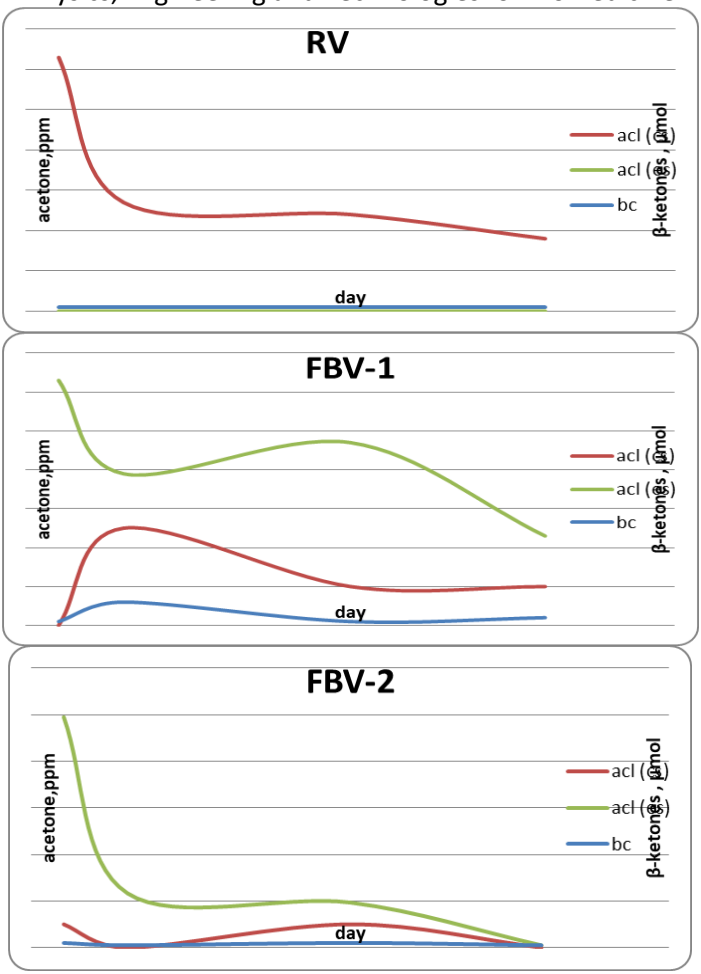

Fig. 1. Correlation between fat burning and breath acetone concentration in the course of the 16 days study

The data we received was questionable due to the difference between the volunteers. None of them was a professional sportsman; their daily activity was individual, various BMI and ratio of fat or muscles affected the fat burning process.

Volunteer (RV) (Fig.1.) tried to stick to a diet, balanced by protein, fat and carbohydrates, but no restrictions of daily calorie intake. This volunteer had episodes of overeating, was not physically active during the study. There was no noticeable progress in the weight loss.
Volunteer (FBV-1; BMI 26.8) (Fig.1.) followed the LCHF diet with a 20% calories restriction, having high-intensive interval training, activity of walking ~9k steps using the stairs per day, and etc. BMI has changed to 25.3. The state of ketosis has been reached. The higher acetone in the breath air has been found in the first few days and persisted for longer, when the body has adapted to the ketone production and switched from glucose to ketone bodies as a source of energy. The level of the acetone got stabilized, that indicates the state of deep ketosis.
Volunteer (FBV-2; BMI 21.45) (Fig.1.) followed the nutrition balanced diet with a 20% calories restriction. There was a mixture of high-intensive interval training with power training, activity during the day by walking ~9k steps, using the stairs and etc. Weight loss has reached 2.5 kilos, BMI has changed to 21.1. The state of ketosis was there, but it was not deep, on the contrary to FBV-1 here it was caused by the exceeding physical activity, rather than diet and was interrupted when the body received carbohydrates nutrition.

Conclusions:

The results vary because of the difference in initial physiological characteristics and the variety of the diet nutrition in the study. All of the volunteers were women and had natural hormonal changes during the cycle, which also affects fat burning. Despite the difference in the results, correlation between fat burning and breath acetone concentration was detected by blood β-ketones meter and the new colorimetric sensor for acetone.

[1] J. Anderson, Measuring Breath Acetone for Monitoring Fat Loss: Review, Obesity, vol. 23(12), pp. 2327-2334, (2015).
[2] Andreas T. Güntner, Noriane A. Sievi, S. Jonathan Theodore, T. Gulich, M. Kohler, Sotiris E. Pratsinis, Non-invasive body fat burn monitoring from exhaled acetone with Si-doped WO3 sensing nanoparticles, Anal. Chem., vol. 89(19), pp. 10578 – 10584, (2017).
[3] Y. Yamada, S. Hiyama, DoCoMo Breath Acetone analyzer, NTT DOCOMO Technical Journal, vol. 14(1), pp. 51-57, (2012).

ENGINEERING OF MATRIX-STRUCTURED CALCIUM CARBONATE MICROPARTICLES WITH DESIRED DISPERSION CHARACTERISTICS

Daria Kalenichenko[1], Galina Nifontova[1], Alyona Sukhanova [1,2], Igor Nabiev [1,2]

[1] Laboratory of Nano-Bioengineering, National Research Nuclear University MEPhI (Moscow Engineering Physics Institute), 115522 Moscow, Russia
[2] Laboratoire de Recherche en Nanosciences, EA4682-LRN, Université de Reims Champagne-Ardenne, 51100 Reims, France
Presenting author e-mail address: dasha09941kalenichenko@gmail.com

The water-insoluble inorganic matrix-structured microparticles may serve as the drug delivery systems ensuring controlled release of incorporated pharmaceutical substances [1]. Calcium carbonate is proved to be one of the most promising inorganic matrix-forming materials, providing stable, biocompatible and biodegradable matrices [2].

Calcium carbonate microparticles are porous and, hence, have a highly developed surface area sufficient for adsorbing both high-molecular-weight compounds (proteins, DNA, other polymers) and the low-molecular-weight molecules (including pharmaceutical substances), which makes them universal drug-delivery vehicles [1, 3]. The matrix structure of calcium carbonate microparticles ensures time-delayed, prolonged release of the active substance from them. The dispersion characteristics, microstructure, and shape of calcium carbonate microparticles are determined by the compositions and concentrations of salt solutions used for their synthesis; the viscosity, pH, and temperature of the reaction mixture; and the duration and intensity of its stirring [4, 5]. The size of the microparticles is an important parameter of quality defining the method of their administration to the patient. The purpose of this study was to develop the technology of obtaining calcium carbonate microparticles with dispersion characteristics that would be optimal for their administration by injection.

The calcium carbonate microparticles were obtained by crystallization from 0.33 M sodium carbonate (Na_2CO_3) and calcium chloride

($CaCl_2$) solutions with glycerol added to the reaction mixture as a gelatinizing agent. The viscosity of the reaction mixture was varied by changing the weight/volume glycerol content. The reaction mixture was stirred for 15, 30, or 60 min. The structure and shape characteristics, as well as the size distribution of the particles, were estimated using optical microscopy.

The study has shown that the use of 30, 40, and 45% (w/o) glycerol as a gelatinizing agent makes it possible to obtain microparticles 3.2 ± 0.5, 2.6 ± 0.49, and 2.3 ± 0.5 μm in diameter, respectively, whereas the mean diameter of the microparticles obtained without a gelatinizing agent is 6.2 ± 1.7 μm. The microparticles fabricated with the use of glycerol have a narrower size distribution, an almost regular spherical shape, and a positive surface ζ-potential of +13.6±2.15, +13.0±0.7, and +7.84±1.41 mV, respectively. We have found that the addition of glycerol to the reaction mixture requires longer stirring (at least 15 min) to receive microparticles with the specified characteristics.

Thus, the calcium carbonate microparticles obtained in this study are characterized by the mean diameter and size distribution suitable for administration by injection. These microparticles has a matrix-structure that can be loaded with pharmaceutical substances what make them promising for development of drug delivery systems with the controlled time-delayed (prolonged) release.

This study was supported by the Ministry of Science and Higher Education of Russian Federation (state contract no. 16.1034.2017/ПЧ), by the Ministry of Higher Education, Research and Innovations of France, and by the Ph.D. NanoCab program of the Region Grand Est, France.

[1] S. Maleki Dizaj, M. Barzegar-Jalali, M. H. Zarrintan, K. Adibkia, F. Lotfipour, Calcium carbonate nanoparticles as cancer drug delivery system, Expert Opinion on Drug Delivery, 12, 1649–1660, (2015).
[2] Y. Zhao, Z. Luo, M. Li, Q. Qu, X. Ma, S.-H. Yu, Y. Zhao, A preloaded amorphous calcium carbonate/doxorubicin@silica nanoreactor for pH-responsive delivery of an anticancer drug, Angewandte Chemie International Edition, 54, 919–922, (2015).
[3] C. Peng, Q. Zhao, C. Gao, Sustained delivery of doxorubicin by porous $CaCO_3$ and chitosan/alginate multilayers-coated $CaCO_3$ microparticles, Colloids

and Surfaces A: Physicochemical and Engineering Aspects, 353, 132–139, (2010).
[4] D. B. Trushina, T. V. Bukreeva, M. N. Antipina, Size-controlled synthesis of vaterite calcium carbonate by the mixing method: aiming for nanosized particles, Crystal Growth and Design, 16, 1311–1319, (2016).
[5] G. Nifontova, M. Zvaigzne, M. Baryshnikova, E. Korostylev, F. Ramos-Gomes, F. Alves, I. Nabiev, A. Sukhanova, Next-generation theranostic agents based on polyelectrolyte microcapsules encoded with semiconductor nanocrystals: Development and functional characterization, Nanoscale Research Letters, DOI: 10.1186/s11671-018-2447-z, (2018).

BIOMIMETIC NANOSTRUCTURES: MONOLAYERS, FILMS AND VESICLES BASED ON COMPLEXES OF AMPHIPHILIC COMPOUNDS, POLYMERS AND NANOPARTICLES

V.P. Kim[1], K.V. Potapenkov[1], G.B. Khomutov[1,3], A.V. Sybachin[2], A.A. Yaroslavov[2], I.V. Taranov[3], V.A. Cherepenin[3], Y.V. Gulyaev[3]

[1] Faculty of Physics, M.V. Lomonosov Moscow State University, Moscow, Russian Federation
[2] Faculty of Chemistry, M.V. Lomonosov Moscow State University, Moscow, Russian Federation
[3]Kotel'nikov Institute of Radio Engineering and Electronics, Russian Academy of Sciences, Moscow, Russian Federation
e-mail: vp.kim@physics.msu.ru

Creation of new functional biocompatible and bioactive materials and efficient systems for the encapsulation, drug delivery and controlled release of various substances in water environments, including live systems, is an actual task of biophysics, chemistry and for a number of aplied sciences, a solution of which is essentially important for practical bio-medical applications. In this work, we have prepared and characterized novel nanocomposite biomimetic functional nanosystems on the basis of Langmuir-Blodgett films and liposomes based on membrane complexes including lipids, functional amino-containing amphiphilic compounds, polymers (including biopolymers) and inorganic nanoparticles (Fe_3O_4 and Au).

Our research team carried out work on the synthesis of the original amphiphilic water-insoluble amine compound - stearoylspermine, that based on stearic acid and natural polyamine spermine molecules, which was formed by a peptide (amide) bond between them. It was also shown the prospect of using this compound in bionanotechnologies due to functional amino groups, the amphiphilic nature and non-toxicity properties, to create liposomes which were sensitive to electromagnetic influences.

In order to investigate the binding of stearoylspermine with functional inorganic nanoparticles and polymer biomolecules we have performed experiments using Langmuir-Blodgett monolayer method. As a result, nanocomposite films based on stearoylspermine molecules, DNA molecules and magnetite nanoparticles were formed on an aqueous subphase surface and transferred on the substrates. Synthesis of magnetite nanoparticles was carried out by Massart method [1].

The method of synthesis of two-component liposomes containing molecules of phosphatidylcholine and stearoylspermine consisted in ultrasonication of those substances in a water. Complexation of liposomes with magnetite, gold nanoparticles and polymers (DNA molecules) was carried out in an aqueous solution. Thus, functional nanocomposite vesicles based on liposomes, nanoparticles and polymers were successfully synthesized. The size of the vesicles was about 200 nm.

The example of the binding of synthesized liposomes with DNA molecules has shown the possibility of functionalization the liposomes by polymer molecules. Such functionalization promotes an increase in the stability of the capsules and a prolonged therapeutic effect in live organisms.

In addition, liposomes were synthesized in an aqueous solution of the NaCl salt to study the possibility of loading. Thus, that model low-molecular substance was capsulated inside the liposomes, and the salt residues in the external environment of the liposomes were removed by dialysis.

Functionalization of liposomes based on phosphatidylcholine and stearoylspermine by gold nanorods was carried out. Such structures are more sensitive to external electromagnetic influences due to an anisotropic elongated form of conducting nanorods.

In conclusion, the developed vesicles can be the basis for the development of new means for controlled drug delivery.

The work was supported by Russian Foundation for Basic Research (Grant 18-29-02080).

[1] Massart R., Preparation of aqueous magnetic liquids in alkaline and acidic media. IEEE Transactions on Magnetics. V. 17. P. 1247−1248. 1981.

INVESTIGATION OF NEURAL SYSTEM POSSIBILITIES IN RECOGNITION OF MELANOMA

S. Kobelev[1], V Nikitaev[1], O. Tamrazova[2], A. Pronichev[1], V. Sergeev[2], E. Polyakov[1]

[1]National Research Nuclear University MEPhI (Moscow Engineering Physics Institute), Kashirskoe shosse 31, 115409, Moscow, Russia
[2]RUDN University, ulica Miklukho-Maklay 6, 117198, Moscow, Russia

Diagnosis of melanoma is based on the study of dermoscopic images of melanocytic skin lesions. To determine the degree of malignancy of the tumor, it is possible to analyze the mutual arrangement of its structural elements [1]. This approach is an alternative to the rule "ABCD", used in most of the works.

The purpose of this work is to evaluate the capabilities of neural networks in the recognition of melanoma.

The studies were conducted with the data of The International Skin Imaging Collaboration (ISIC). The sample of 123 images with classes "benign" (78) and "malignant" (45) was divided randomly into training and test samples in a ratio of 75% to 25%. For the study, a python system was developed with the "Scikit-learn" library. With the initial data, preprocessing of data was carried out, which consisted in normalizing the values of the characteristics for the mean and variance. The activation function is f (x) = x ("identity"). The algorithm for optimizing the balance is the stochastic gradient "adam". The number of neurons of the inner layer is 100

The exact characteristics of the trained model on the test set for classes: "benign" - 74%, "malignant" - 75%. The average value was 74%. Other characteristics of the system are provided in Table 1.

In the future it is supposed to continue work on searching for informative signs, removing artifacts, increasing the sample and optimizing the model.

Table 1. Exact characteristics of the trained model on the test set for the classes "Benign", "Malignant"

	Precision	Recall	F1-score	Support
Benign	74%	89%	81%	19
Malignant	75%	50%	60%	12
Avg/Total	74%	74%	73%	31

[1] M. Zhuchkov, A. Bulinska, H. Kittler, Application of the algorithm «Chaos and Clues» in assessing dermatoscopy images of pigmented skin lesions, Dermatology (Suppl. Consilium Medicum), pp. 5–13, (2017).

THE PREVALENCE OF ANTIBIOTIC-RESISTANT BACTERIAL CARRIAGE AMONG CHILDREN OF EARLY CHILDHOOD, PRESCHOOL AGE AND SCHOOL-AGE CHILDREN

S. Kolesnikova[1], E. Tulyakova[1] , E. Burmistrova and O. Berseneva[1]

[1] *National Research Nuclear University MEPhI (Moscow Engineering Physics Institute), 115409, Moscow, Russia*
E-mail: sgkolesnikova@mail.ru

Among staphylococci, that are opportunistic microorganisms and are part of the normal human microflora, there are pathogenic strains that can cause purulent inflammatory diseases. In case of incorrect treatment tactics, they are not completely sanation from the body and partially survive in the affected tissues (as a rule, it is the mucous membranes of the upper respiratory tract). As a result, a person becomes a bacillicarrier and the source of distribution of pathogenic forms of microorganisms. The formation of antibiotic resistance also plays a significant role in the emergence of bacterial carriage, since this is determines the survival of bacteria. In pre-school and school institutions, in conditions of great crowding, children are in close contact with each other, as a result, the risk of transmission of resistant and pathogenic strains increases from bacterial carriers to healthy children. The number of contacts increases with age, accordingly, an increase in the risk of the condition of bacterial carriage. The acquisition of a pathogenic strain does not always lead to the appearance of a purulent inflammatory disease, however, such a microorganism has an adverse effect on the biotope, in which it exists, and this can lead to the development of respiratory allergies, recurrence of upper respiratory tract infections, bronchopulmonary diseases, chronic tonsillitis, the formation of a state of «children with recurrent respiratory infection (RRI)» and other consequences. Thus, the study of the prevalence of antibiotic resistance and pathogenic strains of staphylococci in children's groups of different age groups is relevant and worthy of attention.

The object of the study are children of several age groups: children of early childhood from 1 to 3 years, preschool age from 4 to 7 years and school age from 13 to 17 years. In total, 77 children took part in the screening study. The purpose of this work is to identify carriers of pathogenic and antibiotic-resistant staphylococci isolated from the microflora of the oral cavity of the studied groups of children which considered to be healthy and attending preschool and school institutions, and comparative analysis of results. An important part of the work is to determine antibiotic resistance of isolated pathogenic forms and comparison of data in different age groups. The results of the study may be in demand in practical health care, in particular, in pediatric practice.

[1] The order of MH of the USSR No. 535 of April 22, 1985 «On the unification of microbiological (bacteriological) research methods used in clinical diagnostic laboratories of medical institutions». Access from the ConsultantPlus legal reference system (reference date: 15.05.2018)
[2] A. S. Labinskaya Microbiology with technique of microbiological studies: the textbook, Moscow, Medicine Publ., 1978. 394 c.
[3] Methodical instructions of MUK 4.2.1890-04 «The definition of sensitivity of microorganisms to antibacterial preparations». Approved. and enacted as sec. of state sanitary physician of Russian Federation G. G. Onishchenko G. 04.03.2004

DEVELOPMENT OF FORMATION SYSTEM FOR PANORAMENT IMAGES FOR CYTOLOGICAL ANALYSIS

A. Koltsov, V. Nikitaev, A. Pronichev, E. Polyakov

National Research Nuclear University MEPhI (Moscow Engineering Physics Institute), Kashirskoe shosse 31, 115409, Moscow, Russia
A. Koltsov e-mail address: kaf46@mail.ru

Cytological examination is a highly specialized, full-fledged, globally recognized method of morphological verification of diagnosis, and at the same time it is one of the least automated and standardized types of laboratory diagnostics.

Actively developed and successfully developed in practical courses, cytology information technology, including in very different degrees.

The purpose of this work is to create tools for the formation and adjustment of the results of scanning cytological preparations using computer microscopy for cytological diagnosis tasks.

To solve the panorama stitching tasks, it is proposed to use step-by-step image processing, first remote background binarization based on histogram analysis, then fill-fill, then select objects and calculate their geometric features, as well as the gradient of the object, then compare the selected objects to two frames and look for similar objects.

The proposed solution is implemented as a software module in C ++ using the Qt library.

The program allows you to upload the original images in the video catalog, then the multi-layer panorama is automatically assembled. The data structure for loading includes naming files of 2048x2048, indicating the frame offset in the panorama relative to the upper left corner of the panorama in the file name. The offset coordinates are specified in the file name as follows: "y = 0" and "x = 0" for the first frame, for the second "y = 0" and "x = 2048", etc. The result of the program in the form of a stitched panorama, it can visually check the quality of the stitching of the panorama, for this it can increase and decrease the scale of the pa-rama, choose a sharper layer, in his opinion, and display the borders of the original frames. In some cases, the panorama is not cor-

rectly stitched, and for such cases it is possible to manually correct the panorama stitching: move one frame or group of frames. After a visual check, the user can save the results in the form of: properly cropped frames with their position in the panorama "y = 0" and "x = 0" specified in the file name, or in a text file that contains the name of the file and its position in the panorama at the moment of saving.

An experimental study and assessment of the effectiveness of work in real conditions were carried out, which showed that the program meets the actual requirements. The program works well with those directories in which frames with a large number of individual objects are well allocated from the background. If there are few objects in the frames, there is a high probability of errors during automatic stitching and problems with manual correction.

3rd International Symposium on
"Physics, Engineering and Technologies for Biomedicine"

THE RATIO BETWEEN ABSORBED DOSE, KERMA AND IONIZATION KERMA FOR SMALL-SIZE PHOTON BEAM

M. Kolyvanova[1], G. Galjautdinova[1], V. Klimanov[1,2]

[1] *State Research Center - Burnasyan Federal Medical Biophysical Center of Federal Medical Biological Agency, Moscow, Russia*
[2] *National Research Nuclear University MEPhI, Moscow, Russia*
vaklimanov@mail.ru, kolyvanova@physics.msu.ru

The relationships between the absorbed dose (D), kerma (K) and the ionization kerma (Kcol) for photon radiation in different media are of fundamental importance in radiation dosimetry [1]. Square radiation fields with sizes from 4x4 to 40x40 cm2 are usually used in conventional radiotherapy. For such fields, the ratio between the depth distributions D and Kcol for megavolt beams has the typical form. The presence of a constant ratio between the absorbed dose and the ionization kerma makes it possible to correctly recalculate the readings of last one into the absorbed dose. However, the pattern varies very significantly at the transition to the beams with small cross sections, and the region where disappears dynamic equilibrium. authors of several works to pay attention to the effect of small fields, for example in [2]. However, in [2], in fact, no concrete results are given of the relationship between D, K and Kcol on the transverse dimensions of the fields in the accumulation region. This problem was investigated in this paper for 6 MV photon beams with small circular cross sections in water with a spectrum calculated in [3].

The result showed, that, unlike traditional sizes, in small fields up to $R_0 \leq 1.0$ cm, the curves for D, K, and Kcol do not intersect with an increase in the depth of the point of interest, i.e. region, where $\beta \geq 1$ is absent, while at the same time the ratio Kcol / K for the considered spectrum of bremsstrahlung photons in the region of small fields is kept constant:

$$K_{col}/K = 0.993 \pm 0.0005 \qquad (1)$$

The results obtained in this work are of interest for clinical dosimetry of small photon beam. Since in the absence of electronic equilibrium the calculation of kerma values is simpler than the calculation of the absorbed dose, these results will also be useful in the development of systems for independent calculation of the absorbed dose for small photon fields.

[1] R. Loevinger, A formalism for calculation of absorbed dose to a medium from photon and electron beams, Med. Phys., vol. 8, pp. 1-12, (1981).
[2] S. Kumar, D. Deshpande, A.E. Nahum, Monte-Carlo-derived insights into dose–kerma–collision kerma inter-relationships for 50keV–25MeV photon beams in water, aluminum and copper, Phys. Med. Biol., vol. 60, pp. 501 -519, (2015).
[3] D. Sheikh-Bagheria, DW. Roger, Monte Carlo calculation of nine megavoltage photon beam spectra using the BEAM code, Med. Phys., vol. 29(3), pp. 391 – 402, (2002).

3rd International Symposium on
"Physics, Engineering and Technologies for Biomedicine"

SYNERGISM OF COMBINED ACTION OF ULTRAVIOLET LIGHT AND IONIZING RADIATION

L.N. Komarova [1]

[1] *Obninsk Institute for Nuclear Power Engineering, Obninsk, Russia*

Quantitative estimation of synergistic interaction of 254 nm ultraviolet (UV) light and X-rays damage in V79 Chinese hamster cells was accomplished using experimental data obtained by others. The age-response variations in survival of V79 cells following the combined application of a fixed dose of X rays and a dose of UV radiation show enhanced cell killing at all cell ages. The greatest interaction was observed in the middle of the DNA synthetic phase. To interpret the results observed, a simple mathematical model of the synergistic interaction for lethal effects produced by a simultaneous combined action of UV light and ionizing radiation was applied. The model suggests that the synergistic interaction of UV light and ionizing radiation is expected to result from some additional lethal damages arising from the interaction of some sublesions induced by both agents. These sublesions are considered ineffective when each agent is taken alone. One of the main conclusion of this model is the dependence of the synergistic effect on the ratio of lethal damages (N2/N1) produced by ionizing (N1) and UV light (N2) applied alone. In accordance with the model's consequences, within a definite range of N2/N1, the synergistic enhancement ratio increases, reaches its highest value and then decreases with the N2/N1 increasing. An interesting result, which can be derived from the model, is the conclusion that for a lower intensity of UV light a lower dose rate of ionizing radiation should be used to provide the greatest synergy. This prediction is completely held, the results have already been published before for a number of agents combined with heat. It can be concluded on this basis that for a long duration of interaction, which are important for problems of radiation protection, low intensities of environmental factors may, in principle, synergistically interact with each other or with other detrimental environmental agents.

MICRODISTRIBUTION OF DEPOSITED DOSE IN BIOLOGICAL TISSUE IN THE PRESENCE OF GOLD AND GADOLINIUM NANOPARTICLES UNDER PHOTON BEAM IRRADIATION

Konobeev I.A., Sheino I.N.
State Research Center - Burnasyan Federal Medical Biophysical Center of Federal Medical Biological Agency, Moscow, Russian Federation
beo0@mail.ru

Currently various methods for enhancing radiosensitivity of tumor cells to ionizing radiation are being developed. Among them a relatively new class of radiosensitizers that are developed on the basis of nanoparticles of high-Z elements such as gold ($_{79}$Au) with already proven *in vivo* biological effectiveness and gadolinium ($_{64}$Gd) [1]. Biological effectiveness caused by localization of deposited energy due to Auger cascade that accompanies interaction of photons with biological tissue in the presence of high-Z elements.

The purpose of this work is to investigate distribution of deposited dose in biological tissue in the presence of gold and gadolinium nanoparticles of different sizes depending on the energy of primary photons (up to 6 MeV).

Materials and methods. Due to disproportion of sizes of phantom and nanoparticles calculations were carried out in two stages. At the first stage spectra of photons and secondary particle flux (photons, electrons and positrons) were calculated at fixed depth in tissue-equivalent material. At the second stage calculations of dose distributions were carried out at nanoscale using spectra obtained at the first stage as equivalent source. Both calculations were performed via Geant4 tool using special DNA models for electrons.

Results. It is shown that spectrum of photon flux passing through biological tissue undergoes shift to lower energies area due to Compton scattering. It is shown that interaction of secondary electrons and positrons produced by photon flux in biological tissue with nanoparticles cannot lead to sufficient increase in additional dose.

[1] Bergs J.W., Wacker M.G., Hehlgans S. The role of recent nanotechnology in enhancing the efficacy of radiation therapy, BBA - Reviews on Cancer, vol. 1856 (1), pp. 130-143, (2015)

3rd International Symposium on
"Physics, Engineering and Technologies for Biomedicine"

CREATION OF MEDICAL DATABASE FOR DECISION SUPPORT SISTEM FOR MRI DIAGNOSIS OF ONCOLOGICAL DISEASES OF THE HUMAN BRAIN

V. S. Kozlov

NRNU MEPhI, Moscow, Russian Federation
vova_29@mail.ru

Decision Support systems (DSS) are an intellectual tool aimed at improving the efficiency of physicians in the diagnosis of various diseases using medical images [1]. Due to the specificity of the results obtained by various diagnostic methods, DSS are developed taking into account the specifics of a particular class of images and diagnosed diseases. This work will be devoted to the creation of a database of tomographic images of DSS diagnosis of cancer of the human brain.

One of the most common and accurate methods of obtaining medical images is Magnetic Resonance Imaging (MRI), a method based on measuring the electromagnetic response of atomic nuclei to excitation by a certain combination of electromagnetic waves in a constant magnetic field of high intensity. With the help of MRI it is possible to obtain pre-ascending contrast images of soft tissues, visualizing anatomical structures and allowing to detect tumors, as well as other pathological changes in the human body. In view of the prevalence and effectiveness of the MRI method, there is a need to build DSS specialized in this area.

The decision support system consists of three main components: database, model database and software subsystem, which consists of three subsystems: database management system (DBMS), model database management system (MBMS) and computer-to-user interface management systems (see figure 1).

When working with medical images, it is important to highlight significant signs that are useful for diagnosis. In this paper, we consider the possibility of using intelligent methods for finding useful properties of images [2].

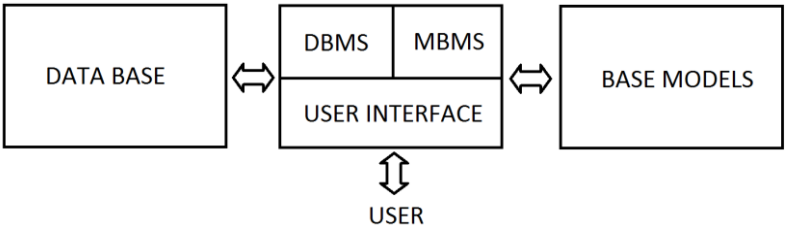

Fig.1. A simplified scheme DSS

Thus, because of the specificity of the methods of obtaining images and peculiarities of the manifestation of various diseases on them, requires the development of new DSS, taking into account all these factors. The most important element of the DSS is the database, and the main problem of its creation is the search for image properties related to various diseases.

[1] V. G. Nikitaev, Expert Systems in Information Measuring Complexes of Oncological Diagnoses, Measurement Techniques, № 6, pp. 67-70, (2015).
[2] Interactive Medical Image Segmentation Using Deep Learning With Image-Specific Fine Tuning, IEEE TRANSACTIONS ON MEDICAL IMAGING, vol. 37, № 7, pp. 1562-1573, (2018).

MOBILE MONITORING SYSTEM DETECTING THE PRECURSORS OF CARDIOVASCULAR DISEASES

I. Kozlovskaya[1], O. Bulkina[1], V. Lopukhova[1], A. Shubina[1], Yu. Karpov[1], E. Lukoshkova[1], V. Ermishkin[1], A. Bogomolov[2], V. Nevezhin[2]

[1]National Medical Research Centre for Cardiology, Moscow, Russia
[2]Financial University under Government of Russian Federation, Moscow, Russia
Presenting author e-mail address: ilkozlovskaya@yandex.ru

One of the priorities in the State Program of the Russian Federation "Development of Health" for 2018-2025 is "Informatisation of health care, including the development of telemedicine" [1]. The aim of telemedicine, inter alia, is the application of methods based on the the patients' individual characteristics. Improvement of miniature sensors of human physiological parameters and wearable devices contributes to the personalization of medicine. Wearable devices can generate plain automatic recommendations and transmit the measurements to the doctor through the smartphone. With the help of such portable devices data sets may be collected, which could contribute to improvement of healthcare quality and development of the artificial intelligence.

The giants in the development of information technology (IBM, Google, Apple, etc.) consider the creation of breakthrough technologies in the field of mobile medicine one of their priorities. For example, Apple is investing in the technology of smart gadgets to detect signs of cardiovascular pathology. In their recent presentation of Apple Watch 4 the company demonstrated a gadget with integrated heart rate sensor and electrodes to register the ECG. The watch can advise the owner to consult a doctor if he has a suspicion of atrial fibrillation. Apple Watch 4 has been approved by American Association of Physicians and the FDA and may be sold as a medical device.

The studies are also on in Russia. Working team involving the specialists of the Institute of Clinical Cardiology and the Financial University under the Government of Russian Federation is currently developing a Mobile Personal Medical System to identify precursors of cardio-

vascular diseases. The project includes medical research focused on the analysis of the patients' individual medical history and dynamic features of their ECG followed by identification of personal zones of stability of their parameters, as well as zones of instability and pathology. The processing of medical data on basis of BigData technology and artificial intelligence will allow developing a methodology and algorithms to alert patients about the likelihood of a possible sudden deterioration of the state and the onset of a crisis in the cardiovascular system. The software based on these algorithms will be transferred to the mobile phone platform. Together with smart bracelets or patches with ECG sensors it will perform a mobile medical system useful not only for the individual user, but for healthcare in general.

The significance and scientific novelty of the project as a whole is determined by the creation of conditions for partial replacement of physician functions with artificial intelligence in combination with automatic ECG analysis.

An important practical result of the project will be the creation of a telemonitoring patient alert system. The introduction of the proposed system into clinical practice will contribute to reduction of cardiovascular mortality and increase in the life expectancy, improvement of quality and accessibility of medical care in Russia, including rural areas and remote areas, drop of the load on physicians in polyclinics and other healthcare facilities. Obtaining a large amount of information during long-term remote observation will open the way to the development of new methods of treatment.

References

[1] Bogomolov AI, Nevezhin VP, Zhdanov G.A. Artificial Intelligence and Expert Systems in Mobile Medicine // Chronoeconomics, No. 3 (11). June 2018. P. 20-28.

SYSTEM FOR RECOGNITION OF PIGMENT NETWORK LINES ON DERMATOSCOPIC IMAGES OF MELANOCYTIC SKIN LESIONS

A. Kozyreva[1], V. Nikitaev[1], O. Tamrazova[2], A. Pronichev[1], V. Sergeev[2]

[1]National Research Nuclear University MEPhI (Moscow Engineering Physics Institute), Kashirskoe shosse 31, 115409, Moscow, Russia
[2]RUDN University, ulica Miklukho-Maklay 6, 117198, Moscow, Russia
A.Kozyreva e-mail address: a.v.kozyreva2015@gmail.com

Melanoma is a malignant tumor that develops from pigment cells - melanocytes. It is the most dangerous and aggressive form of skin tumors. It leads to a rapid appearance of metastases, which cause the formation of secondary tumors. As other types of malignant tumors, melanoma is often recognized in later stages, because it cannot cause inconvenience for a long time.

There are several criteria for assessing the malignancy of the skin tumor. The most commonly used system is the ABCDE feature system: Asymmetry - an irregular form of tumor, Border - uneven edges, Color - uneven coloring, Diameter - large size, Evolution - tumor change. Also, signs of malignancy are such structural formations within the tumor as points, globules, pigment network in case of their uneven coloring and distribution on neoplasm.

This work is aimed at identifying pigment network lines on dermatoscopic images of melanocytic skin lesions and calculating the characteristics of the selected lines (color, thickness). The proposed solution consists of several stages of image processing. The first step is the conversion of a color image to a halftone one. The second step is the use of coordinated filters, oriented in four directions – vertical, horizontal and two diagonal. The third step is the adaptive binarization of Otsu. The fourth step is the screening of artifacts based on the size of the objects. Then the recognized lines are divided into segments, the characteristics of each of them are calculated. The values obtained are used to construct histograms that show the distribution of the characteristic values over the image.

The implemented sequence of algorithms allowed to successfully recognizing the pigment network lines on most test images. However, if there is a hair on the image, the result may be incorrect, because hair is also well distinguished by the proposed algorithm. To solve this problem, it is necessary to introduce additional processing that would allow hair to be removed from the images.

Thus, the proposed system accurately identifies the lines of the pigment network on dermatoscopic images of skin lesions. It can simplify the visual analysis of the pigment network for color and morphological heterogeneity, which will make it easier to recognize melanoma.

[1] Ralph P. Braun, Harold S. Rabinovitz, Margaret Oliviero, Alfred W. Kopf, Jean-Hillaire Saurat, Luc Thomas, Dermoscopic Examination, Color Atlas of Melanocytic Lesions of the Skin, pp.7-22 (2007).
[2] Naser Alfed, Fouad Khelifi, Bagged Textural and Color Features for Melanoma Skin Cancer Detection in Dermoscopic and Standart Images, Expert Systems with Applications, vol.90, pp.101-110 (2017).
[3] S. Pathan, K.G. Prabhu, P.C. Siddalingaswamy, A methodological approach to classify typical and atypical pigment network patterns for melanoma diagnosis, Biomedical Signal Processing and Control, vol.44, pp.25-37 (2018).

THREE STEPS FOR THE DETERMINATION OF FLAVONOID CONTENTS AS AN APPROACH TO STANDARDIZATION OF STEVIA LEAVES FOR BIOMEDICINE

E. Kurdyukov[1], E. Semenova[1], I. Moiseeva[1], S. Kolesnikova[2], A. Kuznetsova[1], O. Rodina[1], Ya. Moiseev[1]

[1] Penza State University, Ministry of Education and Science of the Russian Federation, 440026, Penza, Russia
[2] National Research Nuclear University MEPhI (Moscow Engineering Physics Institute), 115409, Moscow, Russia
E-mail: e.e.kurdyukov@*mail.ru*

Stevia leaves (*Stevia rebaudiana Bertoni*) is well known in Russia as a sweetener and food supplement. Besides sweetness stevia has a lot of therapeutic activities such as immunomodulating, anti-microbial, antioxidant, and has outstanding potential as a herbal drug [1]. To use as a medicine herbal plant has to be carefully standardized. Today there is no quality standards and specification for stevia leaves in Russia [2-4]. The main purpose of the investigation is to develop approaches to the assay of flavonoid contents in stevia.

Materials and methods. The objects of the study were stevia rebaudiana bertolli leaves grown in Krasnodar and Penza regions. Flavonoids were extracted from stevia leaves with ethanol-water mixtures. Flavonoid contents were determined by direct specific Shinoda test and UV-spectrophotometry.

Results. This study proposes three steps procedure to determine flavonoid contents in stevia leaves. Flavonoids are slightly soluble in water, so we used 70% ethanol for the extraction. Shinoda reaction with magnesium and HCl is suitable as a first simple direct chemical test for flavonoids. Red color indicates the formation of anthocyanidin product with the extended conjugation.

Spectral methods are used widely in medicinal plant analysis [5-7]. The next step for the quality control of stevia leaves was UV-spectrophotometry of the ethanol extracts. We conducted UV spectral

study and carefully indentified characteristic wavelengths for the absorption maxima at 330 nm and shoulder at 290 nm. These maximas and shoulders were identical in extracts of stevia from Krasnodar and Penza. Aluminum chloride colorimetric assay was developed as a third step of determination of flavonoid complex. The percentage content of total flavonoids was around 2-3% (calculated by rutin as a standard).

This complex flavonoid analysis of stevia leaves will help to design standardization techniques for the raw stevia plant and herbal medicine.

[1] R. Lemus-Mondaca, A. Vega-Gálvez, L. Zura-Bravo, Kong Ah-Hen. Stevia rebaudiana Bertoni, source of a high-potency natural sweetener: A comprehensive review on the biochemical, nutritional and functional aspects, Food Chemistry, vol. 132 (3), - pp. 1121-1132 (2012).
[2] T. Zhuzhzhalova, Change in the chemical composition of stevia during cultivation in the Central Chernozem Region / T. Zhuzhzhalova, G. Podporinova, M.Zimin // Introduction of Non-Traditional and Rare Plants: Mater. VI Intern. scientific-practical. Conf. (May 24-27, 2006). - Belgorod, pp. 41-43, (2006)
[[3] E. Semenova, E. Kurdyukov, A. Shpichka, Antimicrobial activity of extracts from stevia raw material, Sb. Art. VI International. sci. Conf. "Actual problems of medical science and education" APNMO-2017 (Penza, September 14-15, 2017), Penza, PGU, pp. 144-146, (2017)
[4] E. Kurdyukov, E. Semenova, Macro- and micromorphological features of Stevia rebaudiana Bertoni stevia leaves during the introduction in the Middle Volga region, Scientific bulletins of the Belgorod State University. Ser. Medicine and Pharmacy, № 26, pp. 137-145, (2017)
[5] Phytochemical analysis of medicinal plant raw materials / I.M. Korenskaya, N.P. Ivanovskaya, I.E. Izmalkova, A.A. Maltseva, S.A. Karakozova .- Voronezh: Publishing and Printing Center of Voronezh State University, 77 p., (2012)
[6] A. Kurkina, Flavonoids of pharmacopoeial plants: monograph / A. V. Kurkina. - Samara: Etching, GBOU VPO SamGMU Ministry of Health and Social Development of Russia, - 290 p., (2012)
[7] A. Lobanova,. Investigation of biologically active flavonoids in extracts from plant raw materials / AA Lobanova, VV Budaeva, GV Sakovich // Chemistry of plant raw materials, N 1, pp. 47-52, (2004)

RESEARCH OF BIOMECHANICAL PROPERTIES OF TISSUE SPHEROIDS BY USING OF LASER MICRODISSECTION AND METHODS OF TENSIOMETRY

A. Kurishev

3D Bioprinting Solutions, Moscow, Russia;
Department of Biophysics, Moscow State University, Moscow, Russia
+79629079114, kurishartt@gmail.com

Mechanical properties of biological objects play an important role in the most diverse processes of cell activity within the body - both in normal and in pathologies. The area of science that studies such impacts is biomechanics. Biomechanical properties depend on cell-substrate interactions, extracellular matrix, and other types of cell-to-cell interconnections. The most suitable model object for studying this branch of science are tissue spheroids.

Recently, the field of cell biomechanics has been dynamically developed due to studying the residual stress in the tissues of living organisms. Deformation and reorganization of tissue occurs faster than tissue growth, which implies the presence of internal mechanical forces that maintain a constant stress [1]. In the main work on blood vessels, Fung and collaborators showed [2] the fundamental importance of residual stress in tissues. The residual stress is defined as the internal stress in the body, when all external mechanical influences are reduced to zero values. The state is considered here as an unloaded state of model object.

At present, the most common method for measuring residual stress is to create incisions in tissues *ex vivo* and to observe any subsequent changes in shape that may reveal the presence of residual stress. Using this experimental method, Fung demonstrated the presence of residual stress in the cardiovascular system. In our case, using the example of tissue spheroids, we proceed from the hypothesis that the surface tension of cells makes the main contribution to the residual stress of the entire tissue. Therefore, if we apply laser microdissection and make a series of uniform shallow incisions of the same length, which is shown in Figure 1, therefore we will put down the level of internal stress. In the

subsequent measurement, the Young's modulus due to the induced deformation should be smaller, so the stiffness of the spheroids will also decrease.

The aim of this research is to investigate the possibility to influence on residual stress and speed up the fusion of tissue spheroids. It's very important to control the velocity of fusion of a pair of spheroids, because it finds application in 3D bioprinting and biomedicine [3].

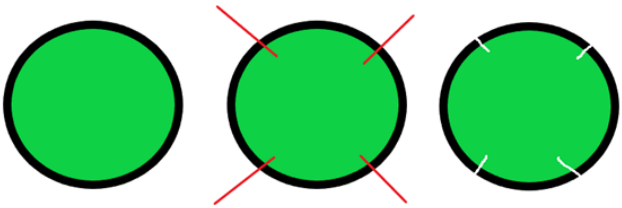

Fig.1. Experimental scheme of a laser microdissection

Tissue spheroids which are composed of cartilage cells (chondrospheres) were chosen as a model experiment object with the proposal to use this type of spheroid in regenerative medicine. Chondrospheres were obtained by biofabrication methods from a primary culture of sheep chondrocytes using low-adhesive culture microplates (Corning, USA). The material properties of the tissue spheroids were measured using a commercial Microsquisher tensiometer, according to the company's protocol (CellScale, Toronto, Canada). The residual stress was evaluated by measuring the open angle that was formed after microsurgical cutting of tissue spheroids in accordance with the previously described protocol. All quantitative data were systematically analyzed using statistics.

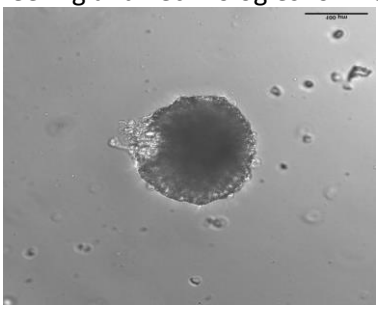

Fig.2. One cut on the surface of tissue spheroid

According to experimental results, it can be concluded that this approach can be useful in future research on the fusion of tissue spheroids and contributes to modeling experiments in tissue engineering.

References:

1. Colin T, Dechristé G, Fehrenbach J, Guillaume L, Lobjois V, Poignard C. Experimental estimation of stored stress within spherical microtissues : What can and cannot be inferred from cutting experiments. J Math Biol. 2018 May 7.

2. Mironov V, Visconti RP, Kasyanov V, Forgacs G, Drake CJ, Markwald RR. Organ printing: tissue spheroids as building blocks. Biomaterials.2009Apr;30(12):2164-74 Jan 26. Review. 2009

3. Chuong, C.J., Fung, Y.C.: On residual stresses in arteries. Journal of Biomechanical Engineering 108(2), 189–192 (1986)

THE EFFECT OF SEMAX AND SELANK ON HEMISPHERIC BRAIN ASYMMETRY IN RATS WITN DIFFERENT MOTOR LATERALIZATION PROFILE UNDER THE CONDITIONS OF THE AMYGDALA BASOLATERAL NUCLEUS DESTRUCTION

I. Latynova[1], M. Fedorova[1], Zh. Vishnyakova[1], S. Mozerov[2]
[1] Penza State University, Ministry of Education and Science of the Russian Federation, 440026, Penza, Russia
[2] National Research Nuclear University MEPhI (Moscow Engineering Physics Institute), 115409, Moscow, Russia
E-mail: latynovai@mail.ru

Among the correction means of impaired brain function there is increasingly considered a special class of substances – regulatory peptides that affect almost all physiological functions of the body. In addition to a wide range of pharmacological properties, peptides have the following advantages: the absence of toxic and side effects, hormonal activity, as well as a mild modulatory nature of the action [4]. Such drugs include peptides Semax (analogue ACTH4-10) and Selank (derived tuftsin). In clinical studies it is found that Semax and Selank have neuroprotective properties, their therapeutic efficacy in vascular lesions of the brain and in the treatment of traumatic brain injuries [1, 3]. However, the neurochemical and neurophysiological mechanisms of neuroprotective and mnemotropic action of Semax and Selank have not been studied. No target organs have been identified through which the pharmacological effects of peptides are mediated.

The aim of the study was to study the effect of peptides on hemispheric brain asymmetry in rats with different motor lateralization profile under the conditions of the amygdala basolateral nucleus destruction.

Materials and methods. The experiments were performed on male white mongrel rats. In animals, the development of a conditional food-producing reflex was carried out [2]. The degree of interhemispheric asymmetry was determined by the method of manipulative movements [5]. Animals were assigned to one of the groups: "right-handers", "left-handers" and ambidekstr. Bilateral destruction of the amygdala basolat-

eral nucleus was carried out electrolytically [6]. The study of changes in motor lateralization in the conditions of destruction in each of the groups with triple injection of the peptide was carried out for 5 days.

Results. It is shown that the destruction of the amygdala basolateral nucleus causes a change in interhemispheric relations in rats, which consists in suppressing motor skills to the previously preferred side. The studied peptides contribute to the restoration of impaired brain function and change motor asymmetry in rats. We revealed the dependence of the effect of Semax and Selank to measure motor asymmetry profile from the motor lateralization of animals. Semax changes hemispheric relations more active in "right-hander" and "left-hander" rats. Selank changes hemispheric relations more active in "left-hander" rats.

The results show that Selank and Semax mediate their effects through amygdala. Manifestation of their neuroprotective effects can be carried out through the regulation of functional hemispheric asymmetry of the brain. The obtained data are interesting in the development of ideas about the role of the peptidergic system in the manifestation of the functional activity of the brain and serve as the basis for the search and development of neurotropic drugs of peptide nature.

[1] Ashmarin, I. P. Nootropic adrenocorticotropin analog 4-10-Semax (15-years of experience developing and studying) / I. P. Ashmarin, V. N. Nezovybatko, N. F. Myasoedov, A. A. Kamensky, I. A. Grivennikov, M. A. Ponomareva-Stepnaya, L. A. Andreeva, A. Y. Kaplan, V. B. Koshelev, T. V. Razina // Zh. higher. nerve. deyat. – 1997. – Vol. 47. – N 2. – Pp. 420-429.

[2] Buresh, J. Techniques and basic experiments for study of brain and behavior / J. Buresh, O. Buresova, D. P. Houston. – M., 1991. – 268 p.

[3] Kozlovsky, I. I. compensatory properties selenka with mnestic disorders caused by neurotoxic effects on noradrenergic system of rat brain / I.I. Kozlovsky, F. Y. Belozertsev, T. P. Semenova, A. V. Zuykov // Experimental. and clinical Pharmacol. – 2008. – Vol. 71. – N 2. – Pp. 3-7.

[4] Khavinson, V. Kh., Peptide regulation of basic body functions / V.Kh. Havinson, G. A. Ryzhak // Vestnik Roszdravnadzor. – 2010. – N 6. – P. 58-62.

[5] Chuyan, E. N. Change in motor asymmetry coefficient in rats during adaptation to hypokinetic stress / E. N. Chuyan, O. I. Gornaya // Physics of the living. – 2009. – Vol. 17. – N1. – Pp. 165-168.

[6] Paxinos, G. The rat brain in stereotaxic coordinates / G. Paxinos, C. Watson. – Fourth Edition, Academic Press, 2007.

CONJUGATION OF NOVEL 4,5,9-TRI-SUBSTITUTED ACRIDINE DERIVATIVES AND QUANTUM DOTS

P. Linkov[1,2], K. Vokhmintcev[1], M. Cochard[3], B. Brassart[4], P. Samokhvalov[1], J. Sapi[3], and I. Nabiev[1,2]

[1] National Research Nuclear University MEPhI (Moscow Engineering Physics Institute), 31 Kashirskoe sh., 115409 Moscow, Russian Federation
[2] Laboratoire de Recherche en Nanosciences, Université de Reims Champagne-Ardenne, 51 rue Cognacq Jay, 51100 Reims, France
[3] Institut de Chimie Moléculaire de Reims, Université de Reims et Champagne-Ardenne, 51 rue Cognacq Jay, 51100 Reims, France
[4] UMR CNRS/URCA 7369, Matrice Extracellulaire et Dynamique Cellulaire (MEDyC), Université de Reims Champagne Ardenne, 51100 Reims, France
valinkov@gmail.com

The current strategy for the development of advanced methods of tumour treatment focuses on targeted drug delivery to tumour cells. Conjugation of a fluorescent imaging probe with a pharmacological agent ensures real-time tracking of the delivery process of the active substance. Photoluminescent (PL) nanocrystals, quantum dots (QDs), due to their unique characteristics, such as the size-tunable light emission, high brightness and photostability, can be used as biomedical fluorescent labels for visualization [1]. One of the strategies in cancer treatment is stabilization of G-quadruplex telomere of DNA. Acridine-based compounds are mostly studied in the G-quadruplex ligand family. Acridine can stabilize G-quadruplexes, thereby inhibiting the activity of DNA-related enzymes [2]. Engineering of nanoprobes based on QDs and acridines will benefit from the unique properties of both components and may be an interesting task for modern bio-nanotechnology.

Here, we addressed the problem of fabrication of PL pharmacological nanoprobes based on acridine ligands and QDs through the conjugation of these components followed by the high-performance purification fom the low-molecular-weight impurities. The pre-synthesized 4,5,9-substituted acridine derivatives with two polyamine side chains and highly luminescent CdSe/ZnS/CdS/ZnS core/multishell QDs have been

used [3]. The QDs were transferred to the aqueous phase by exchange of hydrophobic ligands to hydrophilic polyethylenglycol (PEG) derivatives functionalized with –OH and –COOH terminal groups. Here, hydroxyl groups ensured high solubility of QDs whereas the carboxyl groups were suitable for their conjugation with the amino groups of the acridine ligands by the formation of peptide bond. Conjugates of water-soluble QDs and acridine derivatives were prepared via carbodiimide chemistry approach, using EDC/NHS (1-ethyl-3-(3-dimethylaminopropyl)carbodiimide hydrochloride /N-hydroxysuccinimide) crosslinking reagent. The obtained conjugates were purified from low-molecular compounds via size exclusive chromatography using Sephadex G100 as the stationary carrier. It was shown that Sephadex G100 had a high separation efficiency for QDs, conjugates and small molecules that allowed obtaining the pure conjugates. Chemical composition and the molecular ratios of the components were analyzed by UV-vis spectrometry. As a result, we obtained a series of conjugates with molecular ratios of acridine-to-QD varying from 1 to 10 and possessing the bright PL in the visible region.

To conclude, we have shown that the QD-acridine conjugation followed by size exclusive chromatography is a highly efficient method for engineering of multifunctional small-sized nanoprobes for biomarkers detection, visualization and bioimaging.

This work was supported by the Russian Foundation for Basic Research (project no. 16-34-60253 mol_a_dk) and by the University of Reims Champagne-Ardenne (France).

1. P. Samokhvalov, et. al. Basic principles and current trends in colloidal synthesis of highly luminescent semiconductor nanocrystals. Chemistry - Eur. J. 19, 1534-1546, (2013)
2. M. Laronze-Cochard, et al. Synthesis and biological evaluation of novel 4,5-bis(dialkylaminoalkyl)-substituted acridines as potent telomeric G-quadruplex ligands, Eur. J. Med. Chem. 44, 3880–3888, (2009)
3. P. Linkov, et al. Ultrasmall quantum dots for fluorescent bioimaging in vivo and in vitro, Opt. Spectrosc, 122, 8–11, (2017).

3rd International Symposium on
"Physics, Engineering and Technologies for Biomedicine"

FUNCTIONAL MAGNETIC RESONANCE SPECTROSCOPY STUDY OF ASPARTATE IN ACTIVATED CORTEX AT 3T

A. Manzhurtsev [1,2], P. Menshchikov[3,2,1], O. Vasiukova[4], M. Ublinskiy[2,1], N.Semenova[1,3,2], T. Akhadov[2],

[1]N.M. Emanuel Institute of Biochemical Physics of the Russian Academy of Sciences, Moscow, Russia
[2]Clinical and Research Institute of Emergency Pediatric Surgery and Trauma, Moscow, Russia
[3]N.N. Semenov Institute of Chemical Physics of the Russian Academy of Sciences, Moscow, Russia
[4] National Research Nuclear University MEPhI (Moscow Engineering Physics Institute), Moscow, Russia
andrey.man.93@gmail.com

Purpose. Aspartate (Asp) is a neurotransmitter whose levels are reported to be decreased in activated brain zones at 7 Tesla. Previously we demonstrated that Asp can be measured more accurately using MEGA-PRESS pulse sequence at 3T. The fMRS of Asp is performed at 3T for the first time.

Materials and Methods. Eleven healthy subjects (20-28 y.o.), Philips Achieva dStream 3T and Head-Neck SENSE coil. Videostimulation: monitor, mirror, 8-Hz flashing checkerboard. The spectroscopy voxel (20x40x30 mm) located in visual cortex. Asp signal was obtained with $Asp_{MEGA\text{-}PRESS}$ sequence: TE=90 ms, TR=2000 ms, NSA=288, 27 ms editing pulses applied at δ_{On}=3.89 ppmand δ_{Off}=5.21 ppm (9.5 min). Spectrum in rest was obtained, then spectrum during visual stimulation. Asp peak was processed in jMRUI (AMARES), Asp intensity (I_{Asp}) was found. PRESS spectra from OFF-series were compiled, creatine (I_{Cr}) was found in LCModel. Asp was normalized on Cr: $I_{Asp}/I_{Cr} = Asp_{Cr}$. For each participant the relative effect of stimulation on Asp_{Cr} was calculated: $rel.Asp_{Cr}=Asp_{Cr}(stimulus)/Asp_{Cr}(rest)$. $rel.Asp_{Cr}$ was compared with 1 with Mann-Whitney (MW) criterion.

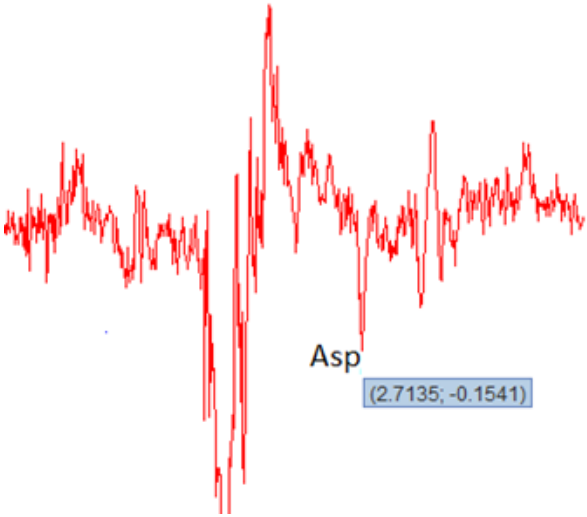

Fig.1. Typical Asp spectrum

Results. The Asp peak at 2.71 ppm has high SNR and is easily approximated by a single peak in AMARES (jMRUI). The statistically significant (p-value<0.05) decrease of rel.Asp_{Cr} by 4% was revealed.

Conclusion. The SNR of Asp peak in $Asp_{MEGA\text{-}PRESS}$ 24 mL spectrum is much greater than at 7T without spectral editing and is sufficient enough for the confident quantitative analysis. The decrease of Asp by 4% in response to neuronal activation is in good accordance with previous findings at 7 Tesla.

FUNCTIONAL MAGNETIC RESONANCE SPECTROSCOPY OF GLUTAMATE AT 3T

A. Manzhurtsev [1,2], P. Menshchikov[3,2,1], M. Ublinskiy[2,1], O. Vasiukova[4], N.Semenova[1,3,2], O. Bozhko[2], T. Akhadov[2],

[1]N.M. Emanuel Institute of Biochemical Physics of the Russian Academy of Sciences, Moscow, Russia
[2]Clinical and Research Institute of Emergency Pediatric Surgery and Trauma, Moscow, Russia
[3]N.N. Semenov Institute of Chemical Physics of the Russian Academy of Sciences, Moscow, Russia
[4] National Research Nuclear University MEPhI (Moscow Engineering Physics Institute), Moscow, Russia
andrey.man.93@gmail.com

Purpose. Functional MRS of glutamate (Glu) is of high interest since it is the main excitatory neurotransmitter. There is a problem of separating Glu and glutamine signals in MRS, especially at 3 Tesla. We used TE average to measure local Glu change in response to continuous visual stimulation at 3T.

Materials and Methods. Twelve healthy subjects (18-27 y.o.), Philips Achieva dStream 3T and Head-Neck SENSE coil. Videostimulation: monitor, mirror, 8-Hz flashing checkerboard. The spectroscopy voxel (20x40x30 mm) located in visual cortex. Glu signal was obtained with TE averaged sequence: TE=35, 45, ..., 185 ms, TR=2000 ms, NSA=16, total averages: 256, t=8.5 min. Spectrum in rest was obtained, then spectrum during visual stimulation. Spectral processing: LCModel, program based on FID-A was written to simulate TEavg brain in vivo spectra; basis set for LCModel was created, Glu/Cr and NAA/Cr values were obtained. The stimulation/rest values on Glu/Cr and NAA/Cr were found and compared with value=1 (Mann-Whitney criterion).

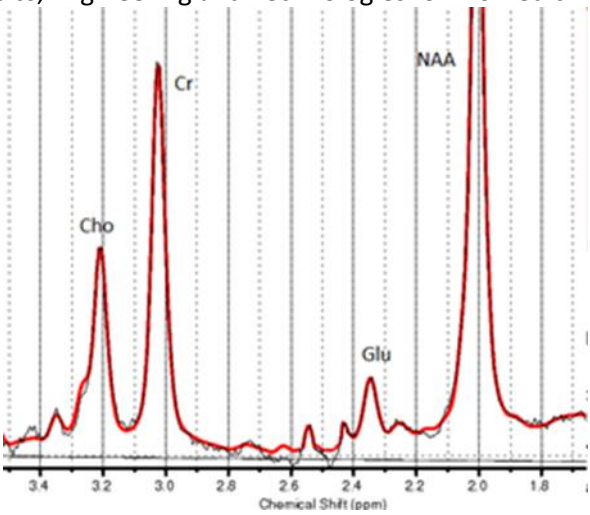

Fig.1. Typical TEavg spectrum

Results. Glu peak at 2.35 ppm was perfectly fitted by the simulated basis set. The increase (by 5%, $p<0.05$) of Glu/Cr was revealed, NAA/Cr: unchanged.

Conclusion. For the first time TEavg was used for functional MRS of glutamate. It allowed to confidently observe the growth of Glu at 3 Tesla during continuous visual stimulation, which is in agreement with published data obtained at 7 Tesla. The stability of NAA in this study (that is often reported to be decreased in neuroactivation) might be the manifestation of neuronal adaptation.

3rd International Symposium on
"Physics, Engineering and Technologies for Biomedicine"

MONTE CARLO MODULATION OF LEKSELL GAMMA KNIFE PERFEXION

T. Medjadj[1], A. Ksenofontov[1], A. Dalechina[2]

[1] National Research Nuclear University (Moscow Engineering Physics Institute) MEPhI, Moscow, Russia
[2] OJSC Neurosurgery Business Center (Moscow Gamma Knife Center), Moscow, Russia
Toufik.medjadj@yahoo.fr

Leksell Gamma Knife is a device for stereotactic radiosurgery used to treat several types of intracranial diseases. In this study we present a simple and accurate MC modulation of the LGK system model 'Perfexion' based on published data in the literature. This model will be used to calculate Gamma Knife collimator output factors, to evaluate treatment plan from Leksell GammaPlan system and to study clinical cases by using voxelised phantom obtained from DICOM RT images.

The latitudinal and azimuth angles of the sources are taken from publication of Young-Bin Cho et al [1], the capsule dimensions and materials are taken from a schematic view of the source published by Al-Daweri and al [2]. The geometrical details of the collimator system are measured in a schematic diagram provided in a presentation by Petti [3]. These measurements were done using free image analysis software called Digimizer. To calibrate this software we used the bushing length as a reference.

The simulation is performed only for one sector (fig.1.). The Phase Space File (PSF) for each source in this sector were created for the collimators 8mm and 16mm, since the axis of these sources are not aligned with the axis of the collimator channel and represent small tilt. The particles in the PSF were, then, rotated around the z-axis to create the PSFs of the sources of the other sectors.

A successful simulation has been implemented without using detailed geometrical information from the manufacturer.

Good agreement was found between this simulation and TMR10. The relative output factors are within 3%. The dose distribution profiles are consistent, especially in the plateau region (fig.2.).

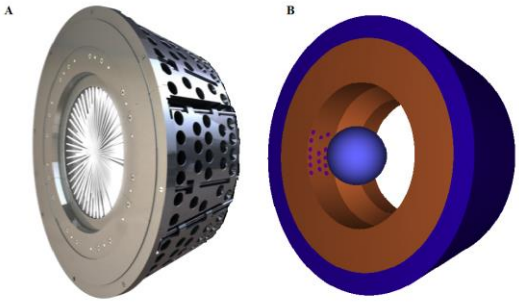

Fig.1. A: LGK-PFX radiation unit, B: Developed geometry using PENGE-OM, only one sector were simulated for each collimator size

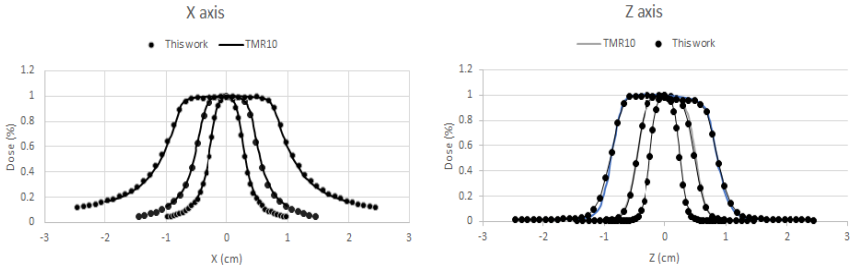

Fig.2. Comparison of profiles for all collimators between TMR10 and this work

[1] YB. Cho, M. van Prooijen, DA. Jaffray, MK. Islam, Verification of source and collimator configuration for GammaKnife Perfexion using panoramic imaging. Med Phys. 37(3):1325–31; 2010.
[2] FM. Al-Dweri, AM. Lallena, M. Vilches, A simplified model of the source channel of the Leksell GammaKnife tested with PENELOPE. Phys Med Biol. 49(12):2687–703;2004.
[3] P. Petti, Leksell Gamma Knife Perfexion QA considerations [presentation]. Available from: www.aapm.org/meetings/amos2/pdf/42-12073-2170-470.pdf

3rd International Symposium on
"Physics, Engineering and Technologies for Biomedicine"

RESTING-STATE FMRI: PREOPERATIVE MAPPING IN PATIENTS WITH BRAIN GLIOMAS

T. Melnikova-Pitskhelauri*, M.SharaevI, A.Smirnov*, E.Pogosbekyan[1], **E.Burnaev**[2], **L.Fadeeva**[1], I.**Pronin** [1], D.**Pitskhelauri**[1]

** - N .N. Burdenko National Scientific and Practical Center for Neurosurgery Moscow, Russia*
I - CDISE, Skolkovo Institute of Science and Technology Moscow, Russia
MelPitz@nsi.ru

Preoperative mapping is usually performed non-invasively by task-based functional MRI (t-fMRI) [1]. Because performing tasks for glioma patients could be hard or even impossible, attempts are made to replace t-fMRI with resting-state fMRI (rs-fMRI) when a subject is not performing any particular task in scanner. Rs-fMRI is thought to provide more general information about the functional architecture of the brain then t-fMRI [2,3].

In current work we propose a three-step approach to automatic and efficient functional brain areas mapping as well demonstrate in case studies on three patients with gliomas the potential applicability of constrained source separation technique (semiblind Independent Component Analysis, ICA) to brain networks discovery and the similarity of task-based-fMRI (t-fMRI) and resting state-fMRI (rs-fMRI) results.

Material and methods: 3 patients with brain glioma (females, age 25,26,57) were examined with MRI (Signa HDxt, 3T) with axial FSPGR BRAVO, t-fMRI and rs-fMRI protocols. For the t-fMRI: TR/TE/FA-3000ms/35ms/90°, FOV-240мм, matrix size 64x64, slice thickness 3мм, gap 0, in-plane pixel size 2,9mm x2,9mm and axial slices 50. For rs-fMRI: TR/TE/FA-2500ms/30ms/90°. Matrix size 64x64, FOV-240mm, slice thickness 3мм, no gap, in-plane pixel size 2,9mm x2,9mm and axial slice number - 50. Acquisition time for rs-fMRI – 12,5 min.

We applied blind and semiblind ICA-analysis for both methods t-fMRI and rs-fMRI. Pre-processed fMRI data were passed to GIFT software to create both blind and semiblind spatially-constrained ICA for

both task-based and rs-fMRI. For measure similarity between spatial maps we use Dice coefficient, which shows the ratio of overlapping voxels and all active voxels in two compared maps for each patient.

$$D = \frac{2|X \cap Y|}{|X|+|Y|} \quad (1)$$

Where X refers to active voxels of the first map, Y active voxels of the second map. In order to calculate Dice coefficient, IC spatial maps were binarized. For all comparison tasks binarization threshold on IC z-score maps was set to values of 1,2,3 in order to study its effect on maps similarity.

Results: in the experimental part we try to decide: how a particular RSN's spatial maps obtained from t-fMRI and rs-fMRI correspond to each other and how a particular RSN's spatial maps obtained from blind and semiblind ICA correspond to each other.

Based on the analysis of Dice coefficients (Table 1), there was a fairly high degree of overlap between the t-fMRI active areas, Broca and Wernicke and the language network obtained from rs-fMRI. The degree of motor areas overlap with sensorimotor network is less pronounced, but the activation sites correspond to anatomical landmarks – a complex of central gyri and supplementary motor area. In general, in comparisons of the functional brain areas obtained with t-fMRI and rs-fMRI, there is a greater specificity of semiblind ICA compared to blind ICA. RSNs of interest (motor and language) discovered by rs-fMRI highly correlate with t-fMRI reference and are located in anticipated anatomical regions. As a result, rs-fMRI maps seem as a good approximation of t-fMRI maps, especially in case of semiblind ICA decomposition.

Conclusion: our preliminary stage in the study of functional changes in neuronal activity caused by brain tumors showed the degree of concordance between spatial maps obtained from t-fMRI and rs-fMRI as well as produced by blind and semiblind ICA without any particular hypothesis or prior information. We hope that further our research of individual changes in sensorimotor and language networks based on functional rs-MRI will allow predicting the activity of neural network architectures and non-invasive mapping of functional areas for preoperative planning.

Table 1 ***Dice coefficients of similarity between spatial maps fordifferent comparison tasks and different z-score thresholds.***

Task ID	Patient ID	Threshold = 1	Threshold = 2	Threshold = 3
1_a	Patient1	0.35	0.31	0.30
1_b	Patient1	0.48	0.47	0.45
1_c	Patient1	0.43	0.38	0.35
1_d	Patient1	0.44	0.53	0.52
2_a	Patient2	0.30	0.22	0.15
3_a	Patient3	0.44	0.46	0.43

[1] - I.Z. Kapsalakis, E.Z. Kapsalaki, E.D. Gotsis, D. Verganelakis, P. Toulas, G. Hadjigeorgiou, I. Chung, I. Fezoulidis, A. Papadimitriou,J. S. Robinson, G.P. Lee, K. N. Fountas, "Preoperative Evaluation with fMRI of Patients with Intracranial Gliomas," Radiology Research and Practice, vol. 2012, pp. 1–17, 2012.
[2] - C. Briganti, C. Sestieri, P.A. Mattei, R. Esposito, R.J. Galzio, A. Tartaro, G.L. Romani, M. Caulo, "Reorganization of functional connectivity of the language network in patients with brain gliomas," American Journal of Neuroradiology, vol. 33, no. 10, pp. 1983–1990,2012.
[3] - P. Branco, D. Seixas, S. Deprez, S. Kovacs, R. Peeters, S. L. Castro, and S. Sunaert, "Resting-State Functional Magnetic Resonance Imaging for Language Preoperative Planning," Frontiers in Human Neuroscience,vol. 10, 2016.

METABOLIC CONCENTRATIONS IN ACUTE ANG LONG-TERM SEVERE TBI. ^{1}H MRS STUDY

P. Menshchikov[1,2], M. Ublinskiy[2], T. Akhadov[2], N.A. Semenova[1,2]

[1] Semenov Institute of chemical physics of RAS, Moscow, Russia
[2] Clinical and Research Institute of Emergency Pediatric Surgery and Trauma, Moscow, Russia
peeterem@gmail.com

Recent Apart from structural changes, there are strong changes in cerebral metabolite concentrations after severe Traumatic brain injury (TBI). For example, many previous ^{1}H MRS Studies reported significant decrease of N-acetyl aspartate concentration (NAA), major neuronal marker, in different brain locations and time intervals from the injury. Possible reasons of NAA reduction are not still completely known. Disruption of NAA synthesis from Asp may result to its decrease. It's became possible to measure simultaneously aspartate (Asp), NAA and glutamate (Glu) concentrations with novel J-edited method, based on MEGA-PRESS pulse sequence [1].

We studied 2 patients groups: Eight children (mean age - 14±2 years) with acute sTBI (23±4 hours after trauma) and seven patients with chronic sTBI (3 months after trauma). were Control group consisted of 11 healthy children (mean age - 15±1 years) without history of any TBI. ^{Asp}MEGA PRESS. The patients were examined under general anaesthesia. All investigations were performed on Phillips Achieva 3.0T scanner. ^{Asp}MEGA-PRESS pulse sequence with following parameters (TE/TR=115ms/1900ms, NSA-8×42, 40ms editing pulses applied at 3.89 ppm and 5.21 ppm) was used for Asp and Glu quantification. NAA, tCr GLX and Cho concentrations were quantified from PRESS spectra from the same localization. All Voxels in size of 25×25×30 mm were located in the frontal lobe (normal appearing brain tissue according to MRI examination).

Intergroup analysis revealed significant decrease in [NAA], [Asp], [tCr] in both patient groups. [Glu] significantly changes only in patients with acute TBI, while [Cho] is increased in long-term period. Asp/Glu

ratio significantly decreased in long term period after TBI and has trend to decrease in acute phase (p=0.09).

First time we simultaneously measure [Asp], [Glu] and [NAA] in the acute severe TBI. Our observation of a decrease in Glu is consistent with Glu release from neurons. TBI induces a rapid cascade of neuronal depolarization and release of the excitatory neurotransmitter Glu. Since Asp is also excitatory neurotransmitter, the same process of Asp excitotoxicity may occur, that can result in [Asp] reduction revealed. The lower Asp observed might also result from reduced availability of Glu, which is depleted rapidly from the neuron after TBI. Glu, main precursor of Asp, comes from the cytosol into the mitochondria through the mitochondrial transporter - glutamate aspartate transporter (Aralar1), which is part of the malate-aspartate shuttle (MAS). Significant decrease of [Asp] with an unchanged [Glu] as well as decreased Asp/Glu ratios found in our study may be a result of the inactivation of the glutamate transport into mitochondria, followed by inhibition of mitochondrial transamination. This conclusion can also be confirmed by the results of study2, where a significantly reduced synthesis of aspartate is accompanied by decreased consumption of glutamate and malate in mitochondria of knockout mice.

[1] P. Menshchikov, T. Akhadov, N. Semenova. Cerebral quantifi cation of N-acetyl aspartate, aspartate, and glutamate levels in local structures of the human brain using J-editing of 1H magnetic resonance spectra in vivo Russian Chemical Bulletin, International Edition, vol. 67(4), pp. 655—662 (2018)

This work is funded by RFBR Grant 17-04-01149 A

3rd International Symposium on
"Physics, Engineering and Technologies for Biomedicine"

QUANTIFICATION OF CEREBRAL WHITE AND GRAY MATTER ASPARTATE CONCENTRATIONS *IN VIVO*

P. Menshchikov[1,2], A. Manzhurtsev[2], T. Akhadov[2], N.A. Semenova[1,2]

[1] Semenov Institute of chemical physics of RAS, Moscow, Russia
[2] Clinical and Research Institute of Emergency Pediatric Surgery and Trauma, Moscow, Russia
peeterem@gmail.com

Recent studies [1] revealed using MEGA-PRESS for detection of Asp (^{Asp}MEGA-PRESS), where On editing pulse set to δ_{On}=3.89 ppm to affect CH- Asp resonance at 3.89 ppm and therefore to refocus the TE evolution of scalar couplings between the Asp spins and non-equivalent β-aspartyl proton ones at δ=2.80 and 2.65 ppm. As a result according to [1] in the edited spectrum (δ_{Off}=5.21ppm) we can observe strong total non-overlapped Asp signal at δ≈2.72 ppm using at least four suitable TE (90, 115, 140 and 150 ms). This theoretically makes it possible to measure T_2 of Asp from ^{Asp}MEGA-PRESS and consequently is an important step in mak TE dependence of the Asp signal $S_{Asp}^{Diff}(TE)$ in Diff spectrum describes as follows:

$$S_{Asp}^{Diff}(TE) = S_{0_{Asp}}^{Diff} \cdot \exp\left(-\frac{TE}{T_{2_{Asp}}}\right) \cdot \chi_{Diff}(TE) \qquad (1)$$

$\chi_{Diff}(TE)-$ function describing TE-dependence of the signal due to J-evolution, that strongly complicates T2 measurements. $\chi_{Diff}(TE)$ is non-periodic function, the analytical form of which cannot be obtained [1]. But $\chi_{Diff}(TE)$ can be expressed from phantom ^{Asp}MEGA-PRESS spectra:

$$ln\left[\frac{\frac{S_{Asp}^{phant}}{S_{tCr_2}^{phant}} \cdot \exp\left(-\frac{TE}{T_{2\,tCr}^{phant}}\right)}{\frac{S_{Asp}^{in\ vivo}}{S_{tCr_2}^{in\ vivo}} \cdot \exp\left(-\frac{TE}{T_{2\,tCr}^{in\ vivo}}\right)}\right] = ln\left[\frac{Asp_{phant}}{Asp_{in\ vivo}}\right] = ln\left[\frac{\frac{[Asp]^{phant}}{[tCr]^{phant}}}{\frac{S_{0\,Asp}^{in\ vivo}}{S_{0\,tCr}^{in\ vivo}}}\right] + \left(\frac{1}{T_{2\,Asp}^{in\ vivo}} - \frac{1}{T_{2\,Asp}^{phant}}\right) \cdot TE \quad (2)$$

$T_{2\,Asp}^{phant}$ and $T_{2\,Cr}^{phant}$ values were obtained from phantom (Asp – 6mM; Cr – 20mM) PRESS spectra (TE=35, 70, 90, 100, 120, 140ms, TR=10s)

using quantification with prior data in VESPA analysis tool. ^{Asp}MEGA-PRESS (TE=90, 115, 140 and 150ms, TR=2s) spectra were acquired from both the phantom (Asp – 6mM; Cr – 20mM) and *in vivo* (16 healthy volunteers, 8 spectra for each TE point, VOI in size of 50×25×25mm, ACC). Spectra were quantified using AMARES. Asp concentrations with were quantified from gray- (ACC 50×25×25mm,) and white-matter (left centrum semiovale (LCS) 50×19×27mm) dominant regions using ^{Asp}MEGA-PRESS (TE=90, 115, TR=2s). The spectra were fitting using prior data in VESPA analysis tool. Totally there were 29 healthy volunteers enrolled in the concentration estimation.ing this editing method quantitative.

$T_{2\,Asp}^{phant}$ and $T_{2\,Cr}^{phant}$values were quantified as follows: 453±43 and 327±27ms. According to expression (2) significant linear regression ($R^2=0.97$, $p<.01$) were found. Thus, $T_{2\,Asp}^{in\,vivo}$ were quantified as 197±27 ms. Asp concentrations quantified ACC and LCV were as follows: 2.66 and 0.88 mM respectively.

First time we measure T_2 relaxation time of Asp signal from novel edited ^{Asp}MEGA-PRESS scheme. The quantified value is in a good agreement with T2 value of appropriate group of NAA. Quantified concentrations is in good agreement with previous *in vivo* measurements on rats (GM, prefrontal cortex) as well as with estimation on humans with HERMES at TE=150 ms. Asp quantification is important task in understanding processes underlying NAA reduction, especially in the case of simultaneous quantification of NAA, Asp, Glu and NAAG quantification.

[1] P. Menshchikov, T. Akhadov, N. Semenova. Cerebral quantifi cation of N-acetyl aspartate, aspartate, and glutamate levels in local structures of the human brain using J-editing of 1H magnetic resonance spectra in vivo Russian Chemical Bulletin, International Edition, vol. 67(4), pp. 655—662 (2018)

This work is funded by RFBR Grant 17-04-01149 A

ROBUST SEGMENTATION TOOL FOR *IN VIVO* SINGLE VOXEL AND 2D ^{1}H MRS OF HUMAN BRAIN

P. Menshchikov[1,2], M. Melnikov[2], T. Akhadov[2], N.A. Semenova[1,2]

[1] Semenov Institute of chemical physics of RAS, Moscow, Russia
[2] Clinical and Research Institute of Emergency Pediatric Surgery and Trauma, Moscow, Russia
peeterem@gmail.com

Localized proton magnetic resonance spectroscopy (^{1}H MRS) is a unique non-invasive method for quantification of metabolic concentrations in all human tissues and organs. In contrast to the traditional NMR experiment, MRS uses medical magnetic fields (lower than 7Tesla) and large field of views (MR spectra are acquired using MRI scanners). Using such little fields decreases SNR, thereby increasing time of study or volume of interest (VOI) size. MRS is classified into 2 types: single voxel (spectra are acquired from one VOI) and 2D MRS (spectra are acquired from several voxels in one VOI). Average voxel volumes are 3000 and 1000 ml in the case of single voxel and 2D spectroscopy respectively. Such big volume include different tissue contaminants of brain – grey (GM) and white (WM) matter as well as cerebrospinal fluid (CSF). Due to the differences in H_2O and metabolic concentrations as well as different T_2 and T_1 relaxations times. Therefore, main objective of this study was creation robust method for quantification GM, WM and CSF contamination in voxels in case of 2D spectroscopy.

First solved task was writing MATLAB tool for creation of binary masks of chosen voxels in VOI (binary mask – image where pixels which belongs to voxel =1, other pixels =0). 3D T1 images and geometry information of spectra were used as input data. Correctness of the program was tested using experimental phantom spectra (FOV-200×200mm; voxels size 40×40×30mm) and images (3DT1 sagittal, TR/TE: 8.1ms/3.7ms, flipangle 8°, 179 slices) Binary mask completely coincides with voxel geometry (fig.1).

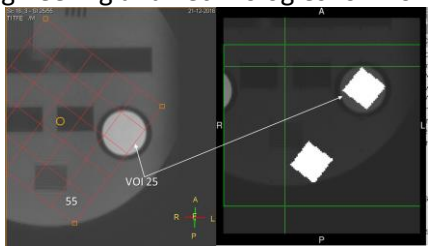

Figure 1. Comparison of binary mask and initial voxel geometry

FSL routine can segment T1 images into three contaminants – GM, WM, CSF using FAST algorithm. Resulted segmented images are presented on the fig.2.

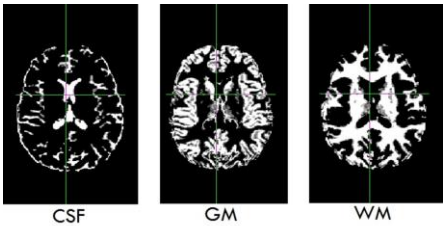

Figure 2. Segmented images.

The last step is to quantify contaminant using *$fslstats* function in the FSL routine with created mask.

This study for the first time revealed robust method for tissue segmentation spectroscopic in the voxel. Quantified GM, WM, CSF percentages can now be used for correction factors in the calculation of metabolic concentrations (1).

$$[M] = \frac{S_{met} \times (f_{GM} \cdot R_{H2O\_GM} + f_{WM} \cdot R_{H2O\_WM} + f_{CSF} \cdot R_{H2O\_CSF})}{S_{H_2O}(1 - f_{CSF}) \cdot R_M} \times \frac{\#H_{H_2O}}{\#H_{met}} [H_2O] \quad (1)$$

Calculated in this way concentrations do not introduce errors, associated with different tissue contamination of voxel, in the statistical analysis.

[1] Ross BD ^{1}H MRS in acute traumatic brain injury. J Magn Reson Imaging. vol. 8(4), pp. 829—840 (1998)

This work is funded by RFBR Grant 17-04-01149 A

3rd International Symposium on
"Physics, Engineering and Technologies for Biomedicine"

^{31}P-MR SPECTROSCOPY FOR BRAIN TUMORS PH-METRY

M. Mertsalova[1], L. Fadeeva[1], D.Piashina[2], A. Postnov[1,2], I. Pronin[1]

[1] Burdenko Neurosurgery Institute, 4-ya Tverskaya-Yamskaya Str., 16, Moscow, Russia
[2] National Research Nuclear University MEPhI (Moscow Engineering Physics Institute), Moscow, Russia
Presenting author e-mail address: mertsalova@nsi.ru

Evaluation of brain tumor metabolism is an important issue in brain tumor studies. Phosphorus magnetic resonance spectroscopy (^{31}P-MRS) allows noninvasive examination of metabolic changes occurring in pathologic brain tissue by measuring intracellular pH level based on obtained spectra of phosphorus-containing metabolites involved in cell membrane phospholipids turnover. The purpose of this study was pH-metry of brain tumors using 31P MRS.

All measurements were performed on 3T GE Signa3.0 MR System using a twin 1H-1P coil. The study included 10 patients with brain tumors (1 metastasis, 4 meningiomas and 5 glioblastomas) and 23 healthy volunteers aged from 23 to 28 y.o. (mean=25) as a control group. The phosphorus spectra were processed in the SAGE program. Calculation of intracellular pH was carried out according to the formula obtained by Petroff et al[1], where $^{\delta Pi}$ is the chemical shift of inorganic phosphate (Pi) relative to the peak of phosphocreatine (PCr):

$$pH = 6.77 + \log\frac{(\delta Pi - 3.29)}{(5.68 - \delta Pi)}$$

The definition of $^{\delta Pi}$ on the example of the phosphorus spectrum is shown in Figure 1.

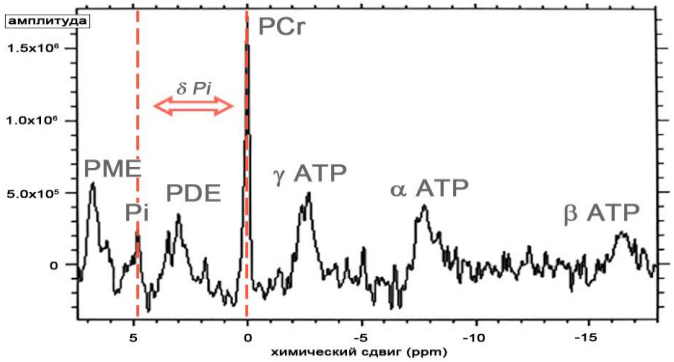

Fig.1. Determination of the chemical shift of inorganic phosphate relative to the peak of phosphocreatine on the example of the phosphorus spectrum of a healthy volunteer, male 25 years old.

The mean pH level of the control group of healthy volunteers (N=23) was 6.963 ± 0.044, pH level of metastasis (one patient) pH= 7,751, in group with glioblastomas (N=5) pH = 7,079 ± 0,056 and with meningiomas (N=4) pH = 7,065 ± 0,033 (table 1). There is a statistically significant difference between the control group and the groups with glioblastomas and meningiomas ($p<0.05$).

Table 1. Mean pH level of brain tumors

	Glioblastoma	Metastasis	Meningioma	Control
Mean pH level	7,079 ± 0,056	7,751	7,065 ± 0,033	6.963 ± 0.044

The results demonstrate a difference in pH level in normal and pathological tissues. However, in order to adapt this method to the clinic and determine its role in the non-invasive diagnosis of various brain lesions, further studies of the respective groups of patients are required.

[1] O. Petroff, J. Prichard, K. Behar, J. Alger, J. den Hollander, R. Shulman, Cerebral intracellular pH by 31P nuclear magnetic resonance spectroscopy, Neurology, vol. 35(6), pp. 781-781, (1985).

STRENGTH CHARACTERISTICS AND TRIBOLOGICAL PROPERTIES OF ISOTROPIC PYROLYTIC CARBON FRICTION PAIR IN TOTAL HIP REPLACEMENT

A. Mitroshin[1], S. Mozerov[2], A. Kibitkin[1], M. Ksenofontov[1], D. Kosmynin[1]

[1]Penza State University, Medical Institute, 440026, Penza, Russian Federation
[2]Obninsk institute for nuclear power engineering - National Research Nuclear University MEPhI (Moscow Engineering Physics Institute), 249040, *Obninsk, Russia*
E-mail: MAKsenofontov@mail.ru

The most common method of treating degenerative-dystrophic hip diseases is total hip joint replacements and every year the number of operations increases.

Strength characteristics and tribological properties of modern materials, such as metal, ceramics and polyethylene, allow using them for hip joint replacements of human joints. However, modern materials do not possess bioinerticity. We have proposed a new material for friction pairs of hip joint replacements - isotropic pyrolytic carbon, which has bioinerticity.

The purpose of the work. Justify the advantages of the friction pair from pyrolytic carbon with the help of mathematical modeling and torque evaluation, to study the strength and tribological characteristics of a carbon friction pair.

Materials and methods.

To determine the strength of the mobility node from pyrolytic carbon, mathematical modeling was used, which was carried out by the finite element method in the ANSYS 5.7 environment. The simulation conditions were set in accordance with GOST 31621-2012.

The study of the torque was carried out at the ElectroPuls E10000, designed to test the mechanical and tribological properties of the components of the hip joint replacement and was performed in accordance with GOST R 52640-2006.

Results.

Based on the results of the mathematical modeling, data were

obtained on the voltage value and the safety margin of pyrolytic carbon. The average tensile stress was 40.7 MPa, the safety factor was 6.1. The compression voltage was 79.6 MPa, the safety factor was 5.4.

As a result of the study of torque, this figure was 1.1 Nm, which does not exceed the required in accordance with GOST R 52640-2006 indicator of 1.5 Nm.

[1]. Fevang, B.T. Improved results of primary total hip replacement / B.T. Fevang [et al.] // Acta Orthop. – 2010. – Vol. 81, N 6. – P. 649–659.
[2] Pajarinen J, Kouri VP, Jamsen E, Li TF, Mandelin J, Konttinen YT 2013 The response of macrophages to titanium particles is determined by macrophage polarization. *Acta Biomater*. 9, 9229–9240.
[3] Jafari, S.M. Revision hip arthroplasty: infection is the most common cause of failure / S.M. Jafari [et al.] // Clin. Orthop. – 2010. – N 468. – P. 2046–2051.
[4] Pearl JI, Ma T, Irani AR, Huang ZN, Robinson WH, Smith RL, Goodman SB. 2011 Role of the toll-like receptor pathway in the recognition of orthopedic implant wear-debris particles. *Biomaterials* 32, 5535–5542.
[5] Q. Gu, Q. Shi, and H. Yang, "The role of TLR and chemokine in wear particle-induced aseptic loosening," Journal of Biomedicine and Biotechnology, vol. 2012, Article ID 596870, 9 pages, 2012.

MONTE-CARLO CALCULATION OF DOSE ENHANCEMENT FACTOR IN THE PARTICLE OF DNA LIQUID-CRYSTALLINE DISPERSION IN PRESENCE OF GOLD NANOPARTICLES

K.V. Morozov[1], V.N. Morozov[2,3], A.V. Belousov[1,2], G.A. Krusanov[2,4], M.A. Kolyvanova[2], A.A. Shtil[5]

[1]Lomonosov Moscow State University, Moscow, Russia
[2]State Research Center - Burnasyan Federal Medical Biophysical Center of Federal Medical Biological Agency, Moscow, Russia
[3]Emanuel Institute of Biochemical Physics, Russian Academy of Sciences, Moscow, Russia
[4]Skobeltsyn Institute of Nuclear Physics Lomonosov Moscow State University, Moscow, Russia
[5]Blokhin National Medical Center of Oncology, Moscow, Russia
Presenting author e-mail address: morozov.kv15@physics.msu.ru

High-Z nanoparticles, in particular gold nanoparticles (GNPs), are perspective for radiation theranostics. Preferential accumulation in tumor cells, high atomic number (Z_{Au} = 79), and mass attenuation coefficient of photon radiation compared to soft tissues, make GNPs applicable as radiosensitizers. Given that DNA is a major cellular target of radiation therapy, delivery of GNPs into the nuclei is important. The mechanisms of penetration of GNPs inside the cell nucleus and their intranuclear distribution are still unclear, however some notions may be obtained based on behavior of GNPs in model systems, for example, in DNA liquid-crystalline dispersions (LCD) [1]. Spatial distribution of GNPs in LCD is determined by the size of GNPs. [2, 3]. We performed a Monte-Carlo calculation of the absorbed photon dose inside the DNA LCD particle in the presence of 2 nm and 32 nm GNPs. Values of the absorbed dose in three models (Figure 1) were calculated using Geant4 toolkit: model A, 1 μm particle evenly filled with DNA (no GNPs); model B, 2 nm GNPs uniformly distributed within the DNA LCD particle; model C, 2/32 nm GNPs located on the border of DNA LCD particle. Models were placed in a water phantom. The radiation source was a photon beam (20-600 keV). The dose enhancement factor (DEF) was

calculated as a ratio of the doses absorbed by the DNA LCD particle in models B and C to the dose absorbed in model A.

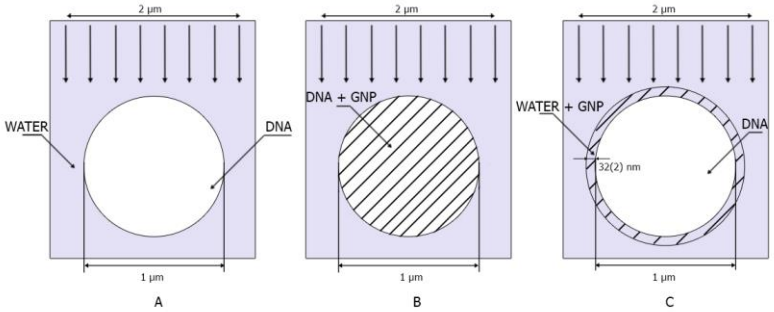

Figure 1. Scheme of Monte-Carlo simulations.

The highest DEF (from 13.2 to 1.1 depending on the photon energy) was obtained for model B. DEF values in model B were 1.1-7.6-fold bigger than in C depending on photon energy. For model C, DEF was weakly dependent on the GNPs'size. These results indicate the importance of the GNPs spatial distribution for the enhancement of absorbed dose in critical targets including the nuclei.

[1] – Yu.M. Yevdokimov, V.I. Salyanov, S.V. Semenov, S.G. Skuridin. DNA Liquid-Crystalline Dispersions and Nanoconstructions. CRC Press. Boca Raton, 2008.
[2] – S.G. Skuridin, V.A. Dubinskaya, V.M. Rudoy, O.V. Dement'eva, S.T. Zakhidov, T.L. Marshak, V.A. Kuzmin, V.I. Popenko, Yu.M. Evdokimov. Effect of Gold Nanoparticles on DNA Package in Model Systems. Doklady Biochemistry and Biophysics, vol. 432, pp. 141-143, 2010.
[3] – Yu. M. Yevdokimov, E.V. Shtykova, V.I. Salyanov, S.G. Skuridin. Linear Clusters of Gold Nanoparticles in Quasinematic Laters of DNA Liquid-Crystalline Dispersion Particles, Molecular Biophysics, vol. 58, pp. 148–156, 2013

FUNCTIONALIZATION OF POLYELECTROLYTE MICROCAPSULES FOR SMART TARGETED DELIVERY OF THERANOSTIC AGENTS

Galina Nifontova[1], Maria Baryshnikova[1,3], Alyona Sukhanova[1,2]

[1] Laboratory of Nano-Bioengineering, National Research Nuclear University MEPhI (Moscow Engineering Physics Institute), Moscow, Russia
[2] Laboratoire de Recherche en Nanosciences, EA4682-LRN, Universitŭ de Reims Champagne-Ardenne, Reims, France
[3] N.N. Blokhin National Medical Research Center of Oncology, Ministry of Health of the Russian Federation, Moscow, Russia
Presenting author e-mail address: galya.nif@yandex.ru

The development of theranostic agents for targeted delivery is of considerable importance in clinical diagnosis and personalized treatment of various diseases. Recently designed polyelectrolyte microcapsules demonstrated the great potential as a delivery systems of small drugs, therapeutic molecules, metal nanoparticles, and specific fluorescent nanoprobes [1, 2]. Conjugation of specific recognition molecules, such as antibodies and their functional fragments, with the microcapsule surface ensures site-specific targeted delivery of the carrier functional components [3, 4].

The purpose of this study was to develop an effective approach to the surface functionalization of polyelectrolyte microcapsules for smart targeted delivery.

We used hollow polyelectrolyte microcapsules obtained by layer-by-layer application of oppositely sized polymer polyelectrolytes on the surface of cores (calcium carbonate microspheres) and subsequent removal of the cores. The microcapsule surface was functionalized with heterobifunctional cross-linkers: (1) sulfosuccinimidyl 4-(N-maleimidomethyl)cyclohexane-1-carboxylate (SMCC) or (2) carbodiimide (EDC) in combination with N-hydroxysuccinimide (NHS). Before functionalization, the microcapsule surface was modified with polymers containing primary amine or carboxyl functional groups, respectively. The size distribution of the microcapsules and the effect of

the cross-linker type on the disperse characteristics of the microcapsules after the surface functionalization were estimated using optical microscopy. To test the effectiveness of the surface functionalization, we conjugated the microcapsules with monoclonal antibodies against human epidermal growth factor receptor 2 (HER2). The functional activity of these conjugates was determined as their capacity for specific interaction with HER2-expressing cancer cells. Optical microscopy was used to analyze the interaction between the antibody–microcapsule conjugates and the cells.

The polyelectrolyte microcapsules elaborated in this study have a narrow size distribution and a mean size of 5.2 ± 0.9 μm. We have found that functionalization of the microcapsule surface with SMCC leads to the formation of microcapsule aggregates with the size varying from 10 to 140 μm. The two-stage activation of the surface by means of the carbodiimide reaction makes it possible to preserve the dispersity of the microcapsules and their size distribution close to that of the original microparticles. The microcapsules with a carbodiimide-activated surface conjugated with monoclonal anti-HER2 antibodies have been demonstrated to specifically interact with HER2-expressing cancer cells.

Thus, carbodiimide-mediated functionalization ensures optimal dispersion characteristics of the polyelectrolyte microcapsules. Therefore, this method of surface activation is promising in terms of the subsequent conjugation with protein capture molecules and obtaining targeted bioconjugates of polyelectrolyte microcapsules serving as the basis for designing targeted theranostic agents.

This study was supported by the Ministry of Education and Science of the Russian Federation, State Contract no. 16.1034.2017/ПЧ.

[1] G. Nifontova, M. Zvaigzne, M. Baryshnikova, E. Korostylev, F. Ramos-Gomes, F. Alves, I. Nabiev, A. Sukhanova, Next-generation theranostic agents based on polyelectrolyte microcapsules encoded with semiconductor nanocrystals: Development and functional characterization, Nanoscale Research Letters, 13, 30, (2018).
[2] N. Gaponik, I.L. Radtchenko, G.B. Sukhorukov, A.L. Rogach, Luminescent polymer microcapsules addressable by a magnetic field, Langmuir, 20, 1449-1452, (2004).

[3] A. P. R. Johnston, M. M. J. Kamphuis, G. K. Such, A. M. Scott, E. C. Nice, J. K. Heath, F. Caruso, Targeting cancer cells: controlling the binding and internalization of antibody-functionalized capsules, ACS Nano, 6 (8), 6667–6674, (2012).

[4] R. Bilan, A. Ametzazurra, K. Brazhnik, S. Escorza, D. Fernбndez, M. Urнbarri, I. Nabiev, A. Sukhanova, Quantum-dot-based suspension microarray for multiplex detection of lung cancer markers: preclinical validation and

SELECTION OF OPTIMAL ANTIBODY FOR DETECTION OF HEPATITIS B SURFACE ANTIGEN VIA IMMUNOREAGENT SCREENING WITH SPECTRAL CORRELATION INTERFEROMETRY

D.O. Novichikhin[1], A.V. Pushkarev[2, 3], S.L. Znoyko[3], V. A. Bragina[3], A.V. Orlov[2, 3], P.I. Nikitin[1,3]

[1] National Research Nuclear University MEPhI, Moscow, Russia
[2] MIPT Moscow institute of physics and technology, Dolgoprudny, Russia
[3] A.M. Prokhorov General Physics Institute, RAS, Moscow, Russia
nammen@yandex.ru

Hepatitis B is a viral disease that affects liver and can cause both acute and chronic infections. Due to long incubation period up to 60 days, methods for early diagnostics of this disease is highly demanded in medicine, especially in view of potential epidemics. The commonly used marker of Hepatitis B is surface antigen HBsAg. This marker is traditionally detected by the enzyme-linked immunosorbent assay (ELISA), polymerase-chain reaction (PCR), or radioimmunoassay. Novel methods, which provide more convenience at similar or even better sensitivity, have been reported.

To achieve high sensitivity and specificity with these methods, thorough optimization of their parameters at each assay stage is required. The mentioned traditional methods register only final result of assay so that separate optimization at each stage is impossible. This deficiency is deprived by a label-free method of spectral-correlation interferometry (SCI), which permits registration in real time of dynamics of variations in thickness of a biolayer on the sensor chip surface due to intermolecular interactions [1-3]. As the sensor chips, SCI allows affordable and widely available microscope cover glass slips.

In the present research, we implemented screening of immunoreagents with using of the SCI method to select optimal antibodies for detection of HBsAg antigen by high-sensitive label-based methods. The optimization was carried out toward increasing the affinity and rate of adsorbtion on the surface with immobilized recombinant HBsAg. The figure below exhibits a characteristic sensogram, i.e., the dependence of biolayer thickness at each stage of the assay, which was obtained in real-time using an SCI biosensor.

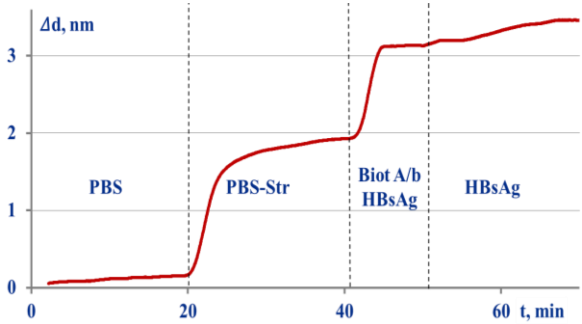

Fig. 1. Sensogram shows each stage of assay

The antibodies selected as a result of this research can be used for both early detection of hepatitis B, and for a wide range of other applications of *in vitro* diagnostics.

[1] P.I.Nikitin, B.G.Gorshkov, E.P.Nikitin, T.I.Ksenevich, Picoscope, a new label-free biosensor, Sensors and Actuators B: Chemical,Volumes 111–112, 11 November 2005, Pages 500-504

[2] P.I Nikitin, M.V Valeiko, B.G Gorshkov, New direct optical biosensors for multi-analyte detection, Sensors and Actuators B: Chemical, Volume 90, Issues 1–3, 20 April 2003, Pages 46-51

[3] А. В. Орлов, А. Г. Буренин, В. О. Шипунова, А. А. Лизунова, Б. Г. Горшков, П. И. Никитин, Разработка иммуноанализа с помощью интерферометрической регистрации его кинетики в реальном времени, Acta naturae, | ТОМ 6 № 1 (20) 2014, стр. 91-102.

3rd International Symposium on
"Physics, Engineering and Technologies for Biomedicine"

BREMSSTRAHLUNG OF HIGH-CURRENT ELECTRON ACCELERATOR FOR RADIOISOTOPE PRODUCTION

H.A. Onischuk[1], Yu.A. Kurachenko[2]

[1]A.Tsyb Medical Radiological Research Center – branch of the National Medical Research Radiological Center of the Ministry of Health of the Russian Federation (A. Tsyb MRRC), Obninsk, Russia
[2]Russian Institute of Radiology and Agroecology (RIRAE), Obninsk, Russia
elenaonischuk@yandex.ru

The possibilities of a powerful electron accelerator MEVEX [1] type in the radioisotope production (RP) by bremsstrahlung are examined. Use such an accelerator for neutron capture therapy is considered in [2].

It has turned out that this RP mode is the most perspective comparatively to RP in (n,γ) reactions, as yield of bremsstrahlung from a target is rather great. At the accepted accelerated parameters, namely, average current 4 mA and electron energy 35 MeV, the bremsstrahlung leak rate from heavy target is ~ $1.3 \cdot 10^{17}$ photon/s.

As an example, the results of calculations to estimate the ^{99}Mo production by bremsstrahlung in the reaction ^{100}Mo(γ,n)^{99}Mo ==> ^{99}Tc is presented below. The studied cylindrical targets have been optimized to get maximal yield of bremsstrahlung when electron beam (radius 0.5 cm) falls on an end face of the cylinder. At the chosen parameters of an electron beam the bremsstrahlung yield from optimal targets is almost identical for most heavy materials. Average energy of the bremsstrahlung is in the area of a giant dipole resonance. For technological reasons the eutectic lead–bismuth is preferable as a target; in this case this alloy will also be a coolant.

Let's compare our results with the data for photoreaction (γ,n) in [3] on producing ^{99}Mo at 14-kW electron accelerator with an energy of 40 MeV (i.e., the average current is 0.350 mA). For highly enriched (96 % ^{100}Mo) sample with a mass 14.4 g at the 24 hrs exposure ~ 25 Ci or 1.74 Ci/g activity is produced. Our data for the same exposure is 1.78 kCi and 5.72 Ci/g when the mass of the sample is 311 g, the average current

4 mA and 100 % ^{100}Mo). Unfortunately, specific irradiation geometry [3] is not available.

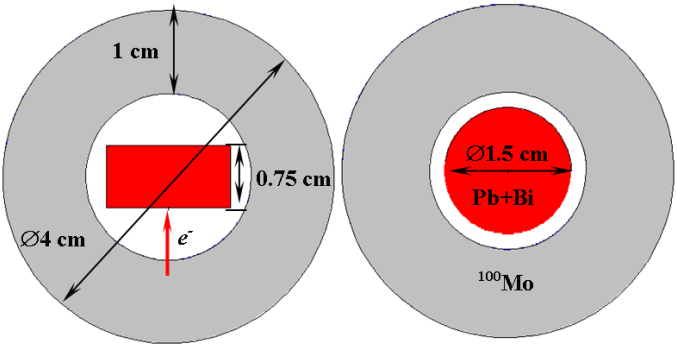

Fig. 1. Sections of the sphere calculation model of the ^{99}Mo production; arrow shows the direction of the electron beam (received by visualization of the MCNP5 code input file)

Equally effective is the production of the medical isotope ^{186}Re in ^{187}Re(γ,n)^{186}Re reaction: 2.98 kCi and 4.86 Ci/g at 48 hr exposure and sample of 100%^{187}Re.

As for (γ,p) reaction productivity, it is many times less: ^{99}Mo production in reaction Ru^{100}(γ,p)^{99}Mo at 24 hr exposure the total sample activity and specific activity are 1.54 Ci and 4.22 mCi/g accordingly.

[1] High Power Linacs for Isotope Production. MEVEX: The accelerator technology company. Internet resource http://www.mevex.com/Brochures/Brochure_High_Energy.pdf.

[2] Kurachenko Yu.A., Zabaryansky Yu.G., Onischuk H.A. Primenenie fotonejtronov dlya luchevoj terapii [Photoneutrons application for radiation therapy]. Medicinskaya radiologiya i radiatsionnaya bezopasnost'. 2017, v. 62, No. 3, pp. 33–42. (in Russian).

[3] Ralph G. Bennett, Jerry D. Christian, David A. Petti, et al. A System of ^{99m}Tc production based on distributed electron accelerators and thermal separation // Nucl. Technology. 1999. Vol. 126. P. 102–121.

NEUTRON BEAMS QUALITY PERFORMANCE CRITERIA FOR NEUTRON CAPTURE THERAPY

H.A. Onischuk[1,2], Yu.A. Kurachenko[3], Eu.S. Matusevich[2]

[1]A.Tsyb Medical Radiological Research Center – branch of the National Medical Research Radiological Center of the Ministry of Health of the Russian Federation (A. Tsyb MRRC), Obninsk, Russia
[2]Obninsk Institute for Nuclear Power Engineering, NRNU «MEPhI», Russia
[3]Russian Institute of Radiology and Agroecology (RIRAE), Obninsk, Russia
elenaonischuk@yandex.ru

Neutron beam performance criteria (BPC) for neutron capture therapy (NCT), formulated historically by the world community [1, 2], are naturally divided into "in phantom" and "in air" criteria [3]. The "in phantom" criteria characterize the effect of beam radiation on an organ or tissue. This is the dosimetric values in the irradiated tumor and tissue. The "in air" criteria are determined by the physical characteristics of the operative field at the beam outlet. These characteristics are localized in the area of the operating field at a channel outlet, but in the absence of the irradiated object.

Among the "in phantom" criteria the most important are:

- Advantage Depth (*AD*) – depth *x* in the tissue at which the dose in the tumor becomes equal to the maximal dose in the tissue;
- Advantage Ratio (*AR*) – the integral over the depth of the brain or other body:

$$AR = \int_0^{AD} \frac{D_{tumor}(x)}{D_{tissue}(x)} dx \qquad (1)$$

- Advantage Depth Dose Rate (*ADDR*) – dose rate in the tumor at the maximum depth of *AD*; it is $\check{D}_{tumor}$ (*AD*);
- and some others.

The "in air" criteria are radiation functionals (epithermal neutron flux density, "contamination" of the epithermal neutron beam by gamma radiation, by fast and thermal neutrons, beam directivity, etc.). These criteria are less universal due to dependence on concrete design of beam

extraction unit. Because of this dependence, the "in air" criteria cannot be categorical, unambiguous and exhaustive. But these criteria can significantly simplify the problem of beam computational design, excluding from the consideration complex problems of radiation transport "in phantom".

In the paper the both types of criteria are analyzed for "benchmark" neutron beams, reactor ones and beams of photoneutrons generated by bremsstrahlung of an electron accelerator. This analysis allowed us to revise the traditional paradigm of BPC based on the beam characteristics of existing research reactors. Specialized facilities for NCT (medical reactors [4], electron accelerators [5] and neutron generators) force to reformulate the BPC and open up new opportunities for NCT.

[1] Hungyuan B.Liu, Robert M.Brugger, and David C.Rorer. UPGRADES OF THE EPITHERMAL NEUTRON BEAM AT THE BROOKHAVEN MEDICAL RESEARCH REACTOR // BNL-63411. Available at: http://www.iaea.org/inis/collection/NCLCollectionStore/ _Public/28/014/ 28014354.pdf.
[2] Harling] O.K., Riley K.J., Newton T.H., et al. THE NEW FISSION CONVERTER BASED EPITHERMAL NEUTRON IRRADIATION FACILITY AT MIT // Nuclear Reactor Laboratory, MIT, 138 Albany St., Cambridge, MA 02139, USA. Available at: http://www.iaea.org/inis/collection/NCLCollectionStore/_Public/36/026/36026570.pdf.
[3] Kurachenko Yu.A., Kazanskij Yu.A., Matusevich Eu.S. *Kriterii kachestva nejtronnyh puchkov dlya luchevoj terapii* [Neutron beams performance criteria for radiation therapy]. *Izvestiya vuzov. Yadernaya energetika*. 2008, no. 1, pp. 139 – 149. (in Russian).
[4] Kurachenko Yu.A., Moiseenko D.N. *MARS i TAPIRO: reaktory maloj moschnosti dlya nejtrono-zahvatnoj terapii* [MARS & TAPIRO: small-capacity reactors for neutron capture therapy]. *Izvestiya vuzov. Yadernaya energetika*. 2010, no. 1, pp. 153 – 163. (in Russian).
[5] Onischuk H.A., Kurachenko Yu.A., Zabaryansky Yu.G. Photoneutrons for Radiation Therapy and Radionuclide Production. 2018, KnE Engineering, pp. 41–53. DOI 10.18502/keg.v3i3.1605.

EX VIVO BIODISTRIBUTION OF GALLIUM-68-LABELED POROUS SILICON NANOPARTICLES

V.K. Tishchenko[1], V.M. Petriev[1,2], A.A. Mikhailovskaya[1], O.A. Smoryzanova[1] A.V.Kabashin[2], I.N. Zavestovskaya[2]

[1] Tsyb Medical Radiological Research Centre, Obninsk, Russia
[2] National Research Nuclear University MEPhI (Moscow Engineering Physics Institute), Moscow, Russia
e-mail: petriev@mrrc.obninsk.ru

The introduction of nanotechnology in nuclear imaging has gained significant interest and could have promising potential for clinical use. Nanoparticles (NPs) possess unique properties that distinguish them from bulk material: large functional surface area, easily controllable surface chemistry which facilitates binding to small molecule drugs, imaging labels and targeting ligands [1]. Well-designed NPs with an optimal size can accumulate in tumor tissue due to enhanced permeability and retention effects.

Gallium-68 (^{68}Ga) is a promising radionuclide for PET due to its appropriate decay properties ($T_{1/2}$ = 67.7 min, β^+ = 89%, $E_{\beta max}$ = 1.9 MeV) and the availability from the ^{68}Ge/^{68}Ga-generator system. The purpose of this study was to evaluate the biodistribution of novel porous silicon NP labeled with ^{68}Ga (^{68}Ga-NPs).

For this purpose we used Wistar rats with subcutaneously transplanted cholangioma RS-1. Ten days after tumor transplantation the animals received single intravenous injection of 0.37 MBq of ^{68}Ga-NPs, or $^{68}GaCl_3$ in a volume 0.1 ml. Animals were sacrificed at different time intervals (5 min, 1, 3 and 5 h) after injection; tissue samples were isolated, weighed and counted using automatic gamma counter. Results were expressed as the percent of injected dose per gram of tissue (% ID/g). All animals procedures were performed in accordance with the national guidelines for the care of laboratory animals.

The uptake of ^{68}Ga-NPs in tumor tissue was 0.24±0.02 %ID/g at 5 min postinjection (p.i.) and climbed to 0.57±0.01, 0.83±0.03, and 0.87±0.07 %ID/g at 1 h, 3 h, and 5 h p.i., respectively. On the other

hand, the amount of free ^{68}Ga injected as $^{68}GaCl_3$ solution decreased from 0.34±0.07 %ID/g at 5 min p.i. to 0.07±0.01 %ID/g at 5 h p.i.

The highest level of radioactivity revealed in organs of mononuclear phagocyte system: liver (8.27–15.79 %ID/g), spleen (0.98–1.27 %ID/g), and lungs (0.98–1.80 %ID/g). ^{68}Ga-NPs were also determined in blood: up to 3.33±0.14 %ID/g at 5 min p.i. Then ^{68}Ga-NPs gradually decreased to 1.43±0.09 %ID/g at 5 h p.i. The uptake of ^{68}Ga-NPs in other organs and tissues didn't exceed 1 %ID/g.

In conclusion, the obtained results suggest that ^{68}Ga-NPs could be suitable for use as molecular imaging probes.

[1] S. Goel, C.E. England, F. Chen, W. Cai. F. Positron emission tomography and nanotechnology: a dynamic duo for cancer theranostics, Adv. Drug Delivery Rev., vol. 42, pp. 465-469, (2016).

BIODISTRIBUTION EX VIVO OF ^{213}Bi-KHEDP – A PROMISING BONE-SEEKING AGENT FOR TARGETED ALPHA THERAPY

V.K. Tishchenko[1], V.M. Petriev[1,2], A.A. Mikhailovskaya[1], O.A. Smoryzanova[1]

[1] Tsyb Medical Radiological Research Centre, Obninsk, Russia
[2] National Research Nuclear University MEPhI (Moscow Engineering Physics Institute), Moscow, Russia
e-mail: petriev@mrrc.obninsk.ru

α-Emitters are increasingly used for targeted alpha therapy because of their emission of high linear energy transfer (LET) particles with a relative short path length. The radioactive decay of bismuth-213 (^{213}Bi, $T_{1/2}$ = 46 min) results in the emission of high-LET α-particles by ^{213}Bi self and by its daughter ^{213}Po around 100 keV/μm. Due to the relative short half-life ^{213}Bi can deliver a high radiation dose rate to the target within a relatively short period of time. These physical characteristics make ^{213}Bi one of the most suitable radiation sources for medical applications.

Phosphonates are known to target bone tissue, especially the regions with an elevated bone turnover. These properties make them convenient for use as carriers of radionuclides in the targeting of primarily and metastatic bone tumors. In the present work we synthesized and studied the biodistribution of ^{213}Bi-monopotassium salt of 1-hydroxyethylidene diphosphonic acid (^{213}Bi-KHEDP) in intact mice.

All studies were carried out in intact healthy mice after intravenous injection via the tail vein of 0.37 MBq of ^{213}Bi-KHEDP or $^{213}BiCl_5$ in a volume 0.1 ml. Animals were sacrificed 5 min, 1 and 3 h post-injection (p.i.), the samples of different organs and tissues were collected for gamma count. The uptake was expressed as percentage of injected dose per gram of tissue (%ID/g).

It was shown that bones uptake of ^{213}Bi-KHEDP were higher than in the most soft tissue organs throughout the study. The maximum femur uptake of ^{213}Bi-KHEDP compared to $^{213}BiCl_5$ was 18.6±3.23 %ID/g

versus 1.38±0.25 %ID/g at 5 min p.i., respectively. The highest amounts of ^{213}Bi-KHEDP in skull, ribs, and spine were 16.2±3.76 %ID/g, 6.15±1.76 %ID/g, and 3.64±0.54 %ID/g, respectively. The bone-to-soft tissue ratios for ^{213}Bi-KHEDP were higher than the corresponding data for $^{213}BiCl_5$.

Among the soft tissue organs, only kidneys had a high uptake of ^{213}Bi-KHEDP and free ^{213}Bi during the study, which was consistent with the rapid renal excretion of both agents. Thus, the amount of ^{213}Bi-KHEDP was 46.8±4.12 %ID/g at 5 min p.i., and then increased to 77.2±2.94 %ID/g at 3 h p.i. At contrast, kidney uptake of $^{213}BiCl_5$ reached 141.6±39.3 %ID/g at 1 h p.i.

In conclusion, ^{213}Bi-KHEDP had a strong and selective bone affinity, indicating that this complex could be useful to deliver alpha-particle radiation to primary bone cancer and skeletal metastases.

THE INFLUENCE OF WHOLE BODY RADIATION EXPOSURE ON THE BIODISTRIBUTION OF MONOPOTASSIUM SALT OF 1-HYDROXYETHYLIDENE DIPHOSPHONIC ACID LABELED WITH RHENIUM-188

V.K. Tishchenko[1], V.M. Petriev[1,2], O.A. Smoryzanova[1]
E.D. Stepchenkova, I.N. Zavestovskaya[2]

[1] Tsyb Medical Radiological Research Centre, Obninsk, Russia
[2] National Research Nuclear University MEPhI (Moscow Engineering Physics Institute), Moscow, Russia
e-mail: petriev@mrrc.obninsk.ru

Bone metastases are common complications in advanced stages of various cancers, particularly of the prostate and breast carcinoma. They are often accompanied by pain, bone fractures, spinal cord compression, hypercalcemia, and rapid degradation in quality of life. Radiolabeled with β-emitting radionuclides phosphonates are of current interest in nuclear medicine for bone metastases therapy due to their high affinity to hydroxyapatite of osseous tissue.

Radionuclide is one of the important criteria that determine the utility of any bone-seeking agent. Rhenium-188 (^{188}Re) possess an excellent therapeutic potential due to its peculiar nuclear properties ($E_{\beta max}$ = 2.1 MeV, $T_{1/2}$ = 16.9 h). There is also a γ-emission of 155 keV that can be conveniently utilized to monitor the course of therapy using a γ-camera. Availability of ^{188}W/^{188}Re generator system offers immense advantages such as easy access and convenience when compared to other therapeutic radionuclides in clinical use.

There is no data how whole body radiation exposure changes the biodistribution of bone-seeking agents. The present study focuses on *ex vivo* evaluation of ^{188}Re-monopotassium salt of 1-hydroxyethylidene diphosphonic acid (^{188}Re-KHEDP) biodistribution in healthy rats and rats after total gamma irradiation.

Biodistribution experiments of ^{188}Re-KHEDP were carried out in female intact rats, which were divided in two groups. One group was injected with 0.37 MBq of ^{188}Re-KHEDP in a volume of 0.1 ml intrave-

nously into the tail vein. Another group of animals was exposed to whole body gamma irradiation by source ^{60}Co at dose of 2 Gy, a dose rate of 0.12 Gy/min. After 7 days the animals were also injected intravenously with ^{188}Re-KHEDP at the same dose. Then animals of both groups were sacrificed at particular time intervals (n = 4 for each time point) up to 48 h postinjection, desired organs were collected, washed and counted using gamma counter. The obtained results were expressed as the percent of injected dose per gram of the organ (%ID/g).

The results of biodistribution studies indicated selective bone accumulation of ^{188}Re-KHEDP in both groups of rats. Meanwhile, whole body gamma irradiation decreased the radioactivity level in bone tissue and other organs. The highest uptake of ^{188}Re-KHEDP in femur was 2.79±0.10 %ID/g and 1.78±0.26 %ID/g at 1 h postinjection (p.i.) in healthy rats and rats after gamma irradiation, respectively. The amounts of activity in skull, ribs, and spine were slightly lower as compared with femur. The concentration of ^{188}Re-KHEDP in blood was also lower in rats after gamma irradiation and didn't exceed 0.57±0.08 %ID/g at 5 min p.i. The amounts of ^{188}Re-KHEDP in other organs such as lungs, liver, spleen, thyroid, heart, stomach, intestine, and muscle were quite low (less than 1 %ID/g) throughout the study. High renal uptake (up to 2.22±0.28 %ID/g in group after gamma irradiation and 10.3±0.54 %ID/g in healthy rats) of ^{188}Re-KHEDP confirmed renal route of excretion.

In conclusion, it was shown that whole body radiation exposure influenced on the biodistribution of ^{188}Re-KHEDP decreasing its uptake in bones and non-osseous tissue.

OPTIMIZATION OF THE PHOTONIC CRYSTAL CHIP ACTIVATION PROCEDURE FOR ULTRASENSITIVE OPTICAL BIOSENSING

I.O. Petrova[1], I. Nabiev[1,2], V.N. Konopsky[3], A. Sukhanova[1,2]

[1] Laboratory of Nano-Bioengineering, National Research Nuclear University MEPhI (Moscow Engineering Physics Institute), Moscow, Russia
[2]Laboratoire de Recherche en Nanosciences, Université de Reims Champagne-Ardenne, LRN-EA4682, Reims, France
[3] Institute of Spectroscopy, Russian Academy of Sciences, Troitsk, Moscow region, Russia
Presenting author e-mail address: iopetrova17@gmail.com

The technique based on the use of photonic crystal surface waves is an innovative approach to ultra sensitive real-time flow detection of biological molecules in small volume liquid samples [1-3]. In order to ensure rapid and specific detection of analyte in solution, we optimized the procedure for chemical conjugation of specific protein capture molecules with the surface of the photonic-crystal chip. Two experimental approaches were chosen: (1) carbodiimide conjgation of protein using heterobifunctional zero-length crosslinker N-(3-dimethylaminopropyl)-N'-ethylcarbodiimide (EDC) and (2) direct conjugation of protein using glutaraldehyde (GA).

In the former case, the photonic crystal surface composed of silica was successively treated with (3-aminopropyl)triethoxysilane (APTES) and succinic anhydride before the chemical conjugation of the protein molecules. After that, the activated surface containing exposed carboxylic groups was functionalized with EDC and conjugated with the protein molecules.

In the latter case, the first stage of the surface activation also consisted in APTES treatment. Then, the chip surface was functionalized with GA, and the protein molecules were chemically linked. Figure 1 schematically shows the comparison of the two different experimental setup of photonic crystal surface activation.

We have demonstrated that the conjugation of the protein molecules via GA allows the number of steps of the photonic-crystal chip surface activation to be reduced while preserving the protein specific activity and the effectiveness of the subsequent detection of analytes in liquid samples.

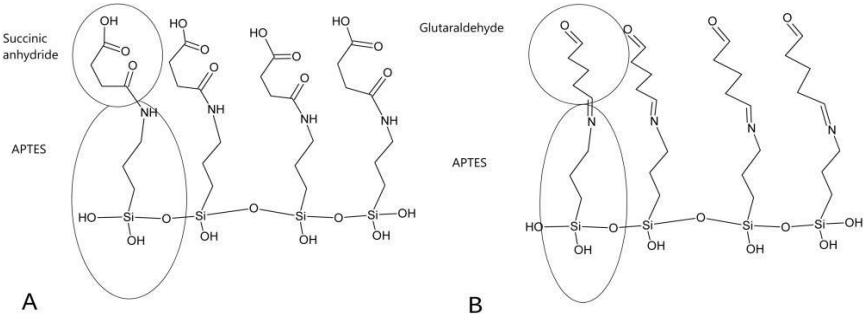

Fig. 1. Chemical activation of the photonic-crystal chip surface for subsequent conjugation of protein molecules using (A) carbodiimide or (B) glutaraldehyde

This work was funded by Russian Science Foundation, contract number 17-15-01533.

[1] V.N. Konopsky, E.V. Alieva, Photonic crystal surface waves for optical biosensors, Analytical Chemistry, vol. 79(12), pp. 4729-4735, (2007).
[2] V.N. Konopsky, E.V. Alieva, A biosensor based on photonic crystal surface waves with an independent registration of the liquid refractive index, Biosensors and Bioelectronics, vol. 25, pp. 1212-1216, (2010).
[3] V. Konopsky, T. Karakouz, E. Alieva, C. Vicario, S. Sekatskii, G. Dietler, Photonic Crystal Biosensor Based on Optical Surface Waves, Sensors, vol. 13(3), pp. 2566-2578, (2013).

3rd International Symposium on
"Physics, Engineering and Technologies for Biomedicine"

A CONTROL METHOD FOR ROTARY BLOOD PUMPS AS A BIVENTRICULAR ASSIST DEVICE UTILIZING PUMPING STATE IDENTIFICATION

D. Petukhov[1]

[1] *National Research University of Electronic Technology, Zelenograd, Russia*
petuhov@bms.zone

The control of rotary blood pumps as a biventricular assist device (BiVAD) is a complex task due to issues related to different systemic and pulmonary vascular resistance, which are results in flow imbalance between systemic and pulmonary circulation with pulmonary congestion or ventricular suction [1].

There are a limited amount of effective control methods for the Bi-VAD [2] and some of them are sensor-based [3], which requires close monitoring to prevent flow imbalance.

The aim of this study is to propose a control method for the rotary blood pumps as the BiVAD, which should provide required pump flow level and maintain certain pumping state ensuring the flow balance in systemic and pulmonary circulation.

The study was done with a previously developed lumped-parameter mathematical model of a cardiovascular system. The rotary blood pump was described by a mathematical model of Sputnik (JSC ZITC-MT, Russia) as follows:

$$LdQ/dt = aQ + b\omega^2 + cH + d\omega^2 Q, \quad (1)$$

where L is a parameter characterizing the fluid inertia effect on the pump, Q is pump flow, ω is pump impeller speed, H is differential pressure across the pump, a-d are coefficients.

The control method can be represented as a control system for the left ventricular (L) and the right ventricular (R) pumps in Figure 1. The control variable is the pump impeller speed, which new value $\omega(t+1)$ depends on the difference between Q_D and Q_P as well as the current pumping state obtained in the estimation unit. The pump flow Q_P for the

left and for the right pumps was estimated with the same mathematical model; pumping states identification was provided by the specific derivatives obtained from the mathematical model and correlated with the pumping states at pump speed changes.

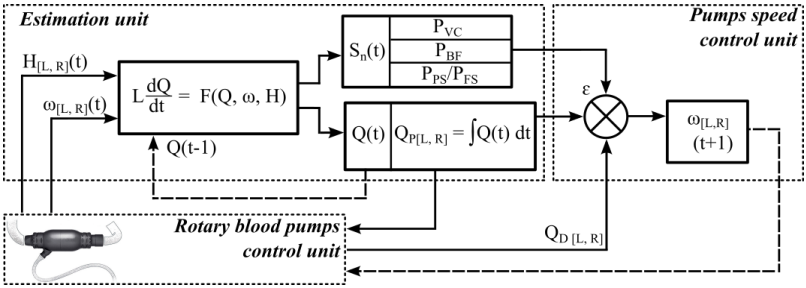

Fig.1. The control system for the rotary blood pumps (L – left, R – right) as the biventricular assist device

The balance of flows in systemic and pulmonary circulation was considered as the equality of pump flows and the maintenance of certain pumping state, such as partial ventricular support with intermittently opening aortic and pulmonary valves (P_{PS}). The numerical simulation results showed the possibility of maintenance of pump flow equality without adverse states such as full ventricular support (P_{FS}) or ventricular collapse (P_{VC}).

[1] A. Levin, N. Jaramillo, A. Garan et al. Outcomes of contemporary mechanical circulatory support device configurations in patients with severe biventricular failure, The Journal of thoracic and cardiovascular surgery. vol. 151, pp. 530-535, (2016).
[2] J. Pauls, M. Stevens, E. Schummy et al. In vitro comparison of active and passive physiological control systems for biventricular assist devices, Annals of biomedical engineering. vol. 44, pp. 1370-1380, (2016).
[3] Y. Wang, S. Koenig, Z. Wu et al. Sensor-based physiologic control strategy for biventricular support with rotary blood pumps, ASAIO Journal, vol. 64, pp. 338-350, (2017).

CYTOGENETIC EFFECTS IN LETTUCE SEEDS AFTER EXPOSURE TO ACCELERATED GELIUM IONS

N.G. Platova, R.V. Tolochek

The Russian Federation State Research Center – Institute of Biomedical Problems of the Russian Academy of Sciences, Moscow, Russia
nataliaspl@inbox.ru

Space radiation environment is characterized by complex composition. Space radiation will influence to humans and the biological life support systems of spacecraft. Helium ions present in the galactic and solar cosmic radiation spectrum. In this connection studying of biological action of helium ions of different energies and doses on biological objects is actual.

We used lettuce seeds of Lactuca sativa L., strain "Moskovskiy parnikoviy". Irradiations of the seeds were carried out at the Heavy Ion Medical Accelerator (HIMAC) at the National Institute of Radiological Sciences (NIRS, QST) in Chiba, Japan. Irradiations were carried out with ^{4}He beam with energy 230 MeV/n and LET 1,65 keV/mm (H_2O) in dose 1 Gy. Next year the seeds of the next crop were irradiated with ^{4}He beam with energy 180 MeV/n and LET 1,93 keV/mm (H_2O) in dose 50 mGy and 100 mGy.

After irradiation and transport to Moscow, the seeds were subjected to germination conditions. Seedlings with root length corresponded to the first mitosis were used for cytogenetic analysis. Student's t criterion was used. Cells with chromosomal aberrations and cells with multiple aberrations were considered. The chromosome and chromatid bridges and fragments were examined. Chromosomal aberrations are a test for definition of cell DNA damage [1]. Lettuce seeds are useful object for space radiation research [2].

The variant irradiated in a dose 50 mGy had percent of cells with chromosomal aberrations, and also percent of chromosomal bridges and fragments exceeding laboratory control ($p \leq 0,05$), whereas percent of cells with chromosomal aberrations at a variant irradiated in a dose 100

mGy was at a level of the control, that is probably connected with the effect of hyper-radiosensitivity and induced radio-resistance [3].

The variant irradiated in a dose 1Gy had percent of cells with chromosomal aberrations, percent of chromosomal bridges and fragments exceeding control ($p \leq 0{,}01$). The percent of cells with multiple aberrations, and also percent of chromatid bridges and fragments was at a level of the control.

Under germination of the seeds irradiated in a dose 50 mGy, some inhibition of germination of seeds in comparison with not irradiated control is noted. For the seeds irradiated in a dose 100 mGy, the curve of germination practically coincides with the curve of the laboratory control. For germination of the seeds irradiated in a dose 1 Gy, the inhibition of germination is observed under 24-26 hours from soaking. By 48 hours this variant is practically compared to the laboratory control.

Thus, helium irradiation of lettuce seeds leads to chromosomal damages depended on beam parameters and probably connected with the effect of hyper-radiosensitivity and induced radio-resistance.

This work was performed with the support of the Fundamental Research Program of the Russian Federation State Research Center – Institute of Biomedical Problems of the Russian Academy of Sciences (IBMP RAS). The portions of this work were made under the Memorandum between NIRS for QST and IBMP RAS.

[1] L.V. Nevzgodina Chromosomal aberrations as a biomarker for cosmic radiation // Fundamentals for the Assessment of Risks from Environmental Radiation. C. Baumstark-Khan et al. (eds). Kluwer Academic Publishers. pp. 203 – 208, (1999)

[2] E.V. Kaminskaya, L.V. Nevzgodina, N.G. Platova. Bio-objects and biological methods of space radiation effects evaluation // Aviakosmicheskaya i Ekologicheskaya Meditsina, vol. 43. № 5. pp. 8–12. (2009) (in Russian).

[3] M.C. Joiner, B. Marples, P. Lambin, S.C. Short, I.Turesson. Low-dose hypersensitivity: current status and possible mechanisms // Int. J Radiat. Oncol. Biol. Phys. vol. 49(2), pp. 379–389, (2001)

NANOCOMPOSITE MAGNETIC LIPOSOMES FOR TARGETED DELIVERY AND CONTROLLED RELEASE OF DRUGS: EFFECTS OF APPLIED ELECTRIC AND MAGNETIC FIELDS

K.V. Potapenkov[1], V.P. Kim[1], G.B. Khomutov[1,3], A.V. Sybachin[2], A.A. Yaroslavov[2], I.V. Taranov[3], V.A. Cherepenin[3], Y.V. Gulyaev[3]

[1] Faculty of Physics, M.V. Lomonosov Moscow State University, Moscow, Russian Federation
[2] Faculty of Chemistry, M.V. Lomonosov Moscow State University, Moscow, Russian Federation
[3]Kotel'nikov Institute of Radio Engineering and Electronics, Russian Academy of Sciences, Moscow, Russian Federation
e-mail: metalsonic@inbox.ru

One of the most important and actual problems of applied biophysics and nanobioengineering is development of biomedical technologies for efficient targeted delivery and controlled release of drugs in vivo. In this way, it is possible to achieve a significant increase in effectiveness of drug therapy, as well as to minimize side effects of drugs. There are several approaches to creation of controlled delivery and drug release means, for example, it is possible to use microparticles of mesoporous silicon, polymeric capsules and microspheres, as well as biomimetic lipid vesicles- liposomes. The liposome-based approach has advantages like non-toxicity and complete biocompatibility of lipids - in addition to liposomes, lipids are the main structural component of cell membranes. Another advantage of liposomes is ability to vary their size over a wide range, down to submicron. This allows to achieve the best distribution of carriers of the drug directly in the body.

A promising approach to development of controlled drug carriers is the approach based on creation of magnetic biomimetic constructions based on nanocomposite liposomes containing magnetic magnetite nanoparticles (Fe_3O_4) bound to the liposomal membrane [1]. Magnetite particles have magnetic and semiconductor properties and they can pro-

vide sensitivity to external electric and magnetic fields. Despite the fact that several approaches can achieve selectivity effect electroporation - opening liposomes by external electric field, the use of magnetic fields for controlled release of drugs has the advantage of being completely harmless to human. For experimental studying of the effect of a magnetic field on liposomes, we have conducted experiments in which an aqueous suspension of liposomes containing in the internal volume capsulated model NaCl solution was incubated in vitro within an hour between the poles of a permanent magnet producing a field intensity of 1.9 kOe. After then conductivity of solution was investigated. As in the case of electrical influences, the method of transmission electron microscopy was also used. Despite the observed jump in the conductivity of the solution, the destruction of the vesicles, as in the case of electrical pulse influences, did not occur. The release of the salt solution was explained by the change in the permeability of the lipid bilayer, since under the influence of an external magnetic field the magnetic vesicles were deformed, their shape was changed from spherical to ellipsoidal. A theoretical description of the processes is possible by solving the problem of deformation of a layer of a magnetic fluid in an external magnetic field from the position of finding the minimum of the potential energy of the system. Analysis of the formulae obtained by us for the energy of an ellipsoidal magnetic shell indicates that under external magnetic field the minima of the free energy of the magnetic liposome are attained precisely for the shape of an ellipsoid oriented along the major semi-axis along the field, rather than the geoid. The obtained results indicate to the possibility for use of magnetic deformation effect in controlled drug delivery.

The work was supported by Russian Foundation for Basic Research (Grant 18-29-02080).

[1] G. B. Khomutov, V.P. Kim, Y.A. Koksharov, K.V. Potapenkov, A.A. Parshintsev, E.S. Soldatov, N.N. Usmanov, A.M. Saletsky, A.V. Sybachin, A.A. Yaroslavov, I.V. Taranov, V.A. Cherepenin, and Y.V. Gulyaev. Nanocomposite biomimetic vesicles based on interfacial complexes of polyelectrolytes and colloid magnetic nanoparticles. Colloids and Surfaces A: Physicochemical and Engineering Aspects, 532:26–35, 2017

NEW MODIFICATION OF PROTOM PATIENT POSITIONING AND IMMOBILIZATION SYSTEM FOR PROTON THERAPY IN LYING POSITION

V.E. Balakin[1,2], M.A. Belikhin[1,2], A.A. Pryanichnikov[1,2], A.E Shemyakov[1,2].

[1] PhTC LPI RAS, Protvino, Russia
[2] Protom ltd., Protvino, Russia
Presenting author e-mail address: pryanichnikov.al@gmail.com

A new modification of Protom patient positioning and immobilization system represents the immobilization unit of proton therapy complex "Prometheus" [1] completed for treatment patients in lying position. Previous version of this system has been already used for irradiation patients with head and neck cancer. In the March 2017, the proton therapy complex "Prometheus" received the license for irradiation entire patient body. The new modification of the immobilization unit adds the possibility to change the chair to a special horizontal deck that allows using for lying patients, which is necessary to irradiate any patient with any cancer locations. Replacement of the chair on the horizontal deck and back occurs in the shortest possible time. That fact makes treatment possible in a seated and lying position using the same immobilization module. This unit has been adapted for proton therapy facility using the pencil beam scanning (PBS) technique. The modified version of Protom immobilization unit has the capability to irradiate patient from different direction and costs much cheaper than gantry based systems. This paper contains the first results of using presented system, a comparison of this unit with the standard immobilization methods and gantry based systems.

Purpose: To report the first experimental results of using new modification of patient positioning and immobilization system in laboratory conditions.

Materials and Methods: a modified patient positioning and immobilization unit, GAFCHROMIC™ EBT3 Dosimetry Film, X-Ray cone-beam computed tomography.

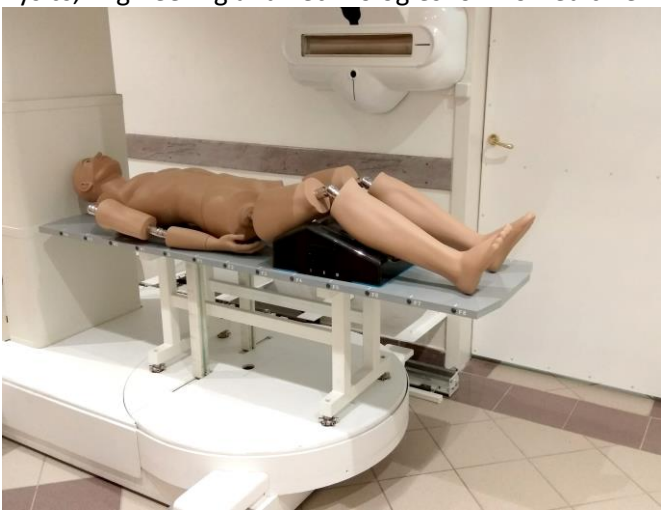

Fig.1. New modification of patient immobilization system.

Conclusion: the first experimental results demonstrate that modified Protom positioning and immobilization system is ready for clinical tests. New modified unit allows irradiation any localization of tumor in lying patient from different directions for better dose distribution.

Key words: proton therapy, pencil beam scanning, patient immobilization.

[1] Balakin V.E. et al., Clinical Application of New Immobilization System in Seated Position for Proton Therapy, KnE Energy & Physics | The 2nd International Symposium "Physics, Engineering and Technologies for Biomedicine", pp. 45–51, 2018.

THE CONDITION OF THE CORONARY RESERVE IN PATIENTS WITH ASYMPTOMATIC ATRIAL FIBRILLATION WITH SUBCLINICAL THYROTOXICOSIS

R. Rakhmatullov[1], A. Rakhmatullov[1], I. Moiseeva[1] , A. Kotlyarov[2]
[1] Penza State University, Ministry of Education and Science of the Russian Federation, 440026, Penza, Russia
E-mail: capitalofgreat@icloud.com
[2]Obninsk institute for nuclear power engineering - National Research Nuclear University MEPhI (Moscow Engineering Physics Institute), 249040, Obninsk, Russia

At present, problems of treatment patients with atrial fibrillation (AF) are one of the unresolved issues of modern clinical medicine [1]. The main pathogenetic mechanism of the onset of myocardial ischemia during AF paroxysm is the discrepancy between oxygen consumption in the myocardium and restriction of its delivery [2]. With the introduction of transesophageal electrophysiological study of the heart (TEEPS), it became possible to determine the degree of the coronary reserve in a non-invasive manner [3]. The aim of this study was to assess the degree of coronary reserve in patients with asymptomatic paroxysms of AF in subclinical thyrotoxicosis (ST). The study included 139 patients (62 men and 77 women) aged 58 to 67 years (mean age 62.7 ± 2.4 years), which were divided into 4 groups. The 1st group included 34 patients with asymptomatic AF paroxysms on the background of a combination of ischemic heart disease (IHD) with ST. The 2nd group included 32 patients with symptomatic AF on the background of a combination of IHD with ST. The 3rd group includes 38 people with asymptomatic AF in the presence of IHD. The 4th group included 35 patients with symptomatic AF on the background of IHD. All patients were treated TEEPS with a frequency of 15-20 imp/min exceeding the patient's heart rate. Every 2 minutes the stimulation rate was increased by 20 imp/min until the appearance of a horizontal depression of the ST segment on the ECG by not less than 0.2 mV. The maximum frequency of stimulation in all groups was 160 imp/min. An ECG was recorded in 12 leads. In all

groups, we evaluated the total ST segment depression in leads aVF, III, V3, V4 (mV). The results of the study are presented in the table 1.

Table 1 – Summary ST depression in groups of patients

Parameters	1st group	2nd group	3rd group	4th group	p
	n=34	n=32	n=38	n=35	
	1	2	3	4	
Summary ST depression in in the leads aVF, III, V3, V4 (mV)	0,44±0,056	0,42±0,051	0,38±0,044	0,35±0,036	p1-3 = 0,040, p2-4 = 0,045

We revealed that the depression of the segment is maximal in patients with asymptomatic AF with the combination of IHD and ST. It was also found that the total depression of the ST segment with asymptomatic AF is greater than in symptomatic. It should also be noted that the stratification of ST to symptomatic and asymptomatic AF significantly ($p<0.05$) increases the total depression of the ST segment. Based on the above data, it can be concluded that TEEPS with an assessment of total ST depression allows one to evaluate the degree of coronary reserve in patients with asymptomatic AF with ST.

[1] N. Dyatlov, The clinical course of the isolated atrial fibrillation in pregnancy, University proceedings. Volga region, vol. 1(45), pp. 62-76, doi: 10.21685/2072-3032-2018-1-7, (2018).
[2] R. Rakhmatullov, A. Rakhmatullov, Thyroid state in subclinical thyrotoxicosis, In the collection: Actual problems of diagnostics, treatment and rehabilitation of patients. Materials of the XIX anniversary interregional scientific and practical conference dedicated to the 40th anniversary of the PIUV - affiliated branch of the Russian Ministry of Health, pp. 367-369, (2017).
[3] A. Rakhmatullov, R. Rakhmatullov, Electrophysiological factors of the prediction of fibrillation of precurities in subclinic thyrootoxicose. In the collection: Actual problems of diagnostics, treatment and rehabilitation of patients. Materials of the XIX anniversary interregional scientific and practical conference dedicated to the 40th anniversary of the PIUV - affiliated branch of the Russian Ministry of Health, pp. 369-370, (2017).

OPTICAL METHODS IN THE DIAGNOSTICS OF FIBROSIS

Yu. Chursinova[1], I. Raznitsyna[1,2], D. Kulikov[1]

[1] Moscow Regional Research and Clinical Institute (MONIKI) named after M.F Vladimirsky., Moscow, Russian Federation
[2] National Research Nuclear University MEPhI (Moscow Engineering Physics Institute), Moscow, Russian Federation
Presenting author e-mail address: RaznitsynaIA@yandex.ru

Inflammation and hypoxia are typical processes that accompany various illnesses, including fibrosis disease. Earlier, we have showed that these local pathologies induce increased endogenous fluorescence of porphyrins, hence, they can be tracked by the laser fluorescence spectroscopy [1]. Also, the optic tissue oximetry allows assessment of local circulatory disorders caused by local inflammatory processes and hypoxia non-invasively. Thus, a complex of optical non-invasive diagnostic methods can provide the clinician with important information about the functional changes in tissues in various diseases, for example, fibrosis.

A modern understanding of the pathogenesis of fibrosis as a dynamically flowing and reversible process associated with inflammation and hypoxia is appeared [2]. The current view on the problem is aimed at the diagnosis of these processes, the timely impact on which increases the probability of successful treatment of fibrosis. It is known that the excess of collagen characterizing fibrosis can be fixed by the laser fluorescence spectroscopy, since this substance fluoresces in the UV range [3]. In the red and green ranges, it is also possible to detect fluorophores responsible for inflammation and hypoxia [4]. The optical tissue oximetry allows to determine the specific consumption of oxygen by tissues, which characterizes the activity of proliferative processes and the degree of fibrosis. Therefore, the simultaneously analysis of laser fluorescence spectroscopy results and optical tissue oximetry one could help in determining the leading pathological process and, accordingly, in selecting a personalized therapy.

Our investigation on modeling of bleomycin-induced fibrosis of mouse skin [5] allowed to find a correspondence between obtained data and known phases of the fibrogenic response [6]. The results of the study demonstrated the possibility of objective non-invasive dynamic monitoring of inflammation and hypoxia processes within the confines of fibrosis development using laser fluorescent spectroscopy and optical tissue oximetry.

[1] E.N. Petritskaya, D.A. Kulikov, D.A. Rogatkin. I.A. Guseva, P.A. Kulikova, Use of fluorescence spectroscopy for diagnosis of hypoxia and inflammatory processes in tissue, J. Opt. Technol., vol.82, N.12, pp.810-814, (2015).
[2] M. C. Manresa, C. Godson, C. T. Taylor. Hypoxia-sensitive pathways in inflammation-driven fibrosis, American Journal of Physiology-Regulatory, Integrative and Comparative Physiology, vol. 307, N 12, pp. R1369-R1380, (2014).
[3] O. D. Smirnova, D. A. Rogatkin, K. S. Litvinova. Collagen as in vivo quantitative fluorescent biomarkers of abnormal tissue changes, Journal of Innovative Optical Health Sciences, vol. 5, N. 02, P. 1250010, (2012)
[4] W. Franco et al. Review of applications of fluorescence excitation spectroscopy to dermatology, British Journal of Dermatology, vol. 174, N 3, pp 499-504, (2016).
[5] J. Avouac Mouse model of experimental dermal fibrosis: the bleomycin-induced dermal fibrosis, Arthritis Research. – Humana Press, New York, NY, pp. 91-98, (2014).
[6] D.C. Rockey, P.D. Bell, J.A. Hill. Fibrosis—a common pathway to organ injury and failure, New England Journal of Medicine, vol. 372, N 12, pp 1138-1149, (2015).

EXCITONIC-TO-PLASMONIC TRANSITION IN $CuInS_2$ NANOCRYSTALS

P. Samokhvalov[1], P. Linkov[1] and I. Nabiev[1,2]

[1] Laboratory of Nano-Bioengineering, National Research Nuclear University MEPhI (Moscow Engineering Physics Institute), 115409 Moscow, Russian Federation
[2] Laboratoire de Recherche en Nanosciences, LRN-EA4682, Université de Reims Champagne-Ardenne, 51100 Reims, France
Presenting author e-mail address: p.samokhvalov@gmail.com

Plasmonic nanostructures and nanoparticles (NPs) have emerged as a powerful tool in physics, chemistry and medicine. One of the recent hot topics in application of plasmonic NPs is the light-matter interaction in strong coupling regime [1], where they serve as the source of localized electromagnetic (EM) field. Coupling of excitonic quantum dots (QDs) with plasmonic NPs has been shown to significantly enhance the light output of the former through weak coupling effect, allowing a 5-fold increase of intensity of fluorescence signal [2].

In this work, we demonstrate the transformation of fluorescent excitonic $CuInS_2$ QDs into plasmonic NPs by a post-synthetic treatment and without modification of the chemical nature of the nanoparticles. Here, fluorescent $CuInS_2$ QDs were synthesized as described earlier [3], and subjected to a complete removal of thiol surface ligands by oleylamine. During such treatment, QDs exhibited partial loss of fluorescence without discernible modification of their absorbance spectrum. Surprisingly, further heating of these QDs in the aliphatic phase comprising of octadecene and oleylamine under vacuum, what is an intermediate stage of preparation of CdSe QD cores to the shell coating [4], led to a complete quenching of $CuInS_2$ QD's fluorescence and appearance of an intense low-energy peak in the absorbance spectrum (Fig. 1). This peak may be undoubtedly attributed to a plasmonic transition, as was reported earlier for copper-deficient $Cu_{2-x}Se$ nanocrystals [5]. The mechanism of such excitonic-to-plasmonic transition of $CuInS_2$ nanocrystals is still to be elucidated.

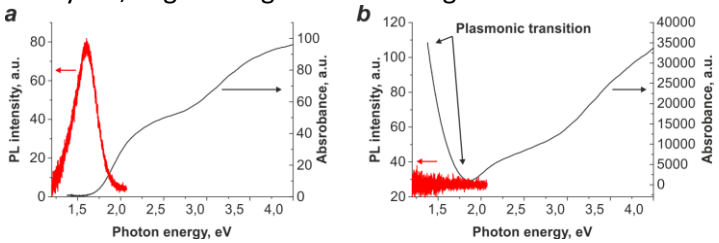

Fig.1. Absorbance and fluorescence (PL) spectra of oleylamine-capped $CuInS_2$ nanocrystals before (a) and after (b) heat treatment under vacuum.

To conclude, we have shown that a single synthetic approach could be applied to obtain either fluorescent or plasmonic $CuInS_2$ nanocrystals, depending on the post-synthetic treatment.

This work was supported by the Ministry of Education and Science of the Russian Federation, grant no. 14.587.21.0039 (ID RFMEFI58717X0039)

[1] D.S. Dovzhenko, S.V. Ryabchuk, Yu.P. Rakovich, I.R. Nabiev, Light–matter interaction in the strong coupling regime: configurations, conditions, and applications, Nanoscale, 10, 3589–3605, (2018).
[2] O. Kulakovich, N. Strekal, A. Yaroshevich, S. Maskevich, S. Gaponenko, I. Nabiev, U. Woggon, M. Artemyev, Enhanced Luminescence of CdSe Quantum Dots on Gold Colloids, Nano Lett., 2 (12), 1449–1452, (2002).
[3] L. Li, A. Pandey, D.J. Werder, B.P. Khanal, J.M. Pietryga, V.I. Klimov, Efficient Synthesis of Highly Luminescent Copper Indium Sulfide-Based Core/Shell Nanocrystals with Surprisingly Long-Lived Emission, J. Am. Chem. Soc., 133 (5), 1176–1179, (2011).
[4] V. Krivenkov, P. Samokhvalov, M. Zvaigzne, I. Martynov, A. Chistyakov, I. Nabiev, Ligand-Mediated Photobrightening and Photodarkening of CdSe/ZnS Quantum Dot Ensembles, J. Phys. Chem. C, 122 (27), 15761–15771, (2018).
[5] V. Lesnyak, R. Brescia, G.C. Messina, L. Manna, Cu Vacancies Boost Cation Exchange Reactions in Copper Selenide Nanocrystals, J. Am. Chem. Soc., 137 (29), 9315–9323, (2015).

QUALITY CONTROL OF DITERPENOID GLUCOSIDES AS A MAIN BIOACTIVE MARKERS OF *STEVIA REBAUDIANA* BERTONI LEAVES

E. Semenova[1], E. Kurdyukov[1], N. Glebova[1], A. Kuznetsova[1], I. Moiseeva[1], N. Gavrilova[1], S. Kolesnikova[2]

[1] Penza State University, Ministry of Education and Science of the Russian Federation, 440026, Penza, Russia
[2] National Research Nuclear University MEPhI (Moscow Engineering Physics Institute), 115409, Moscow, Russia
E-mail: sef1957@mail.ru

Stevia leaves and isolated steviol glycosides usualy used to treat diabetes and other immune desiases. Even stevia leaves powder around 20-30 times sweeter then sugar. There are at least eight different steviol glycosides in stevia [1]. The main stevia gucoside (stevioside) enhances insuin secretion and exerts antihyperglycaemic, insulinotropic, and glucagonostatic actions in rats and has high potency to become antidiabetic drug [2, 3]. To be a medicinal drug a herbal plant has to be carefully standardized. Today liquid chromatography is the most relible but very expensive method of stevioside assay [4, 5]. The object of the research was to work out a quality control procedure for dry stevia leaves as a herbal drug.

Dry stevia leaves were obtained from Penza and Krasnodar regions. The present pharmacopoeia study of herb medicine is performed in 5 sections - Definition, Characters, Identification, Tests and Assay. The first section consists of physical and organoleptic properties of plant. We propose to check sweet taste of stevia leaves as a first step of stevia analysis (Characters). Then in Identification section stevia leaves have to be identified by their macroscopic and microscopic description. To qualify stevia leaves we suggest stevioside identification by thin-layer chromatography, which is a simple and relatively cheap method.

We offer spectrophotometric method to evaluate steviol glycosides in stevia leaves. We performed extraction of diterpenoid glucosides by 95% ethanol and revealed absorbtion maxima on the UV spectrum (203

nm). This maximum was identical in extracts from stevia leaves grown in different Russia regions. The linear correlation between absorbtion at 203 nm and stevioside concentration was confirm with reference stevioside extract [6]. The concentration of diterpenoid glucosides in dry stevia leaves performed by UV-spetrophotometry at 203 nm was around 10%.

This quantitative and qualitative analysis of diterpenoid glucosides as a pharmacopogycal active constituents of stevia leaves will ensure quality of raw plant and consistancy of stevia formulation.

[1] R. Lemus-Mondaca, A. Vega-Gálvez, L. Zura-Bravo, Kong Ah-Hen. Stevia rebaudiana Bertoni, source of a high-potency natural sweetener: A comprehensive review on the biochemical, nutritional and functional aspects, Food Chemistry, vol. 132 (3), - pp. 1121-1132 (2012).
[2] Swati Madan, Sayeed Ahmad, G N Singh, Kanchan Kohli, Yatendra Kumar Raman Singh and Madhukar Garg, Stevia rebaudiana (Bert.) Bertoni A Review, Indian Journal of Natural Products and Resources Vol. 1 (3), pp. 267-286, (2010).
[3] E.E.Kurdyukov, E.F. Semenova, Macro- and micromorphological features of Stevia rebaudiana Bertoni stevia leaves during the introduction in the Middle Volga region, Scientific bulletins of the Belgorod State University. Ser. Medicine and Pharmacy, № 26, pp. 137-145, (2017).
[4] C. A. Kedik, S. V. Fedorov, N. A. Yanul, L. V. Prokhorova, E. V. Smirnova, A. V. Panov, Control of Stevioside Content in Vegetable Raw Materials by HPLC and TLC, Chemical-pharmaceutical magazine, No. 10, pp. 19-22, (2003).
[5] O.B. Rudakov, N.D. Verzilina, S.V. Fedorov, K.K. Polyansky, Control of stevioside in raw materials by the method of high-performance liquid chromatography, Dairy Industry, No. 7, pp. 54-55, (2004).
[6] N.D. Verzilina, Rheological features of extracts and syrups of stevia, yakon and Jerusalem artichoke / N.D. Verzilina, E.S. Hasanova, K.K. Polyansky // Collection of scientific works dedicated to the 95th anniversary of the Mazlumov's All-Russian Research Institute of Physical Culture, pp. 144-152, (2017).

INVESTIGATION OF THE DEPENDENCE OF LIGHT FLOW INTENSIFICATION FROM THE MEANS OF THE LIQUID FLUX POWER

Shachneva E.A.[1], Murashkina TI.[1], Badeeva E.A.[1]

[1] Penza State University, Penza
+79656375890, e-mail: e_shachneva@mail.ru

Nowadays, there are many methods and installations for the reproduction and measurement of fluid flow [1, 2]. But their main disadvantages are - the complexity of technical implementation and the unjustifiably high complexity of conducting experiments and measurements, the effect on the result of measuring electromagnetic interference.

In the paper [3], the authors proposed a new method and a fiber-optic sensor (VOD) for measuring the parameters of the liquid flow. The article [2] is devoted to the determination of the constructive and technological parameters of the sensor and, first of all, the sensing element (RE) in the form of a plate with a reflecting surface (reflector), which transforms the flow parameters into changes in the parameters of the optical signal [3]. At the moment, the task is to develop a program that calculates the strength of formula (1) to calculate the flow rate of the fluid F_s depending on the parameters being changed.

$$F_s = k_C 2\alpha R_C R_C = \frac{2k_C \alpha R_C^2}{l} \qquad (1)$$

where R_c – inner radius of bellows,

k_C – bellows rigidity,

α , l – displacement of plate or turn.

In the C # programming language, software was developed to simulate changes in fluid flow parameters.

From the source [3], the dependence of flow of the photodiodes on the angles of the deflection of the plate of the first and second channels $I_1=f_1(\alpha)$ and $I_2=f_2(\alpha)$, obtained in the process of real adjustment and opti-

cal adjustment of the optical system of the developed device for measuring the parameters of the liquid flow. Relying on these results, changing the values of the angle α occurred in the range from -3 to 3 degrees, also bellows with a radius of 3 to 20 mm were chosen, and, accordingly, the stiffness of the bellows, specified in GOST 201482 -76 single-layer metal measuring bellows.

The graph of the calculated dependence of the intensity of the light flux on the flow strength is shown in Fig. 1.

Fig. 1. Graphical display of the results of calculations in the form of the dependence of the intensity of the light flux on the strength of the fluid flow

In accordance with the calculations performed, it is determined that the developed water supply will be most effective at a force of a liquid flow from 2 to 3.5 N.

Literature

1. Fluid Flow Measurement in Astronauts Life Support Systems / T.I. Murashkina, E.A. Badeeva, E.A. Shachneva, etc.//Biomedical Engineering. – Vol. 49.- No 5.- January 2016. –pp.295-299.
2. E.A. Shachneva and T.I. Murashkina//Journal of Physics: Conference Series 735(2016)012036. - International Conference of Young Scientists and Specialists "Optics-2015" 12–16 October 2015, St. Petersburg, Russia.
3. Patent of the Russian Federation No. 2419765. IPC G01 B 21/00. A fiber-optic transducer of angular displacement / Murashkina TI, Pivkin AG, Serebryakov DI, Yurova OV Bul. № 15.opubl. 05/27/2011.

PARTICLES FROM STAR-SHAPED POLYLACTIDES AS A TOOL FOR PROLONGED PROTEIN DRUG RELEASE

Shpichka A.I[1], Shavkuta B.S.[1,2] , Bardakova K.N.[1,2], Kostjuk S.V.[1,3], Timashev P.S.[1,2,4]

[1]Institute for Regenerative Medicine, Sechenov First Moscow State Medical University, Moscow, Russia
[2]Institute of Photonic Technologies, Research Center "Crystallography and Photonics" RAS, Moscow, Troitsk, Russia
[3] Research Institute for Physical Chemical Problems of the Belarusian State University, Minsk, Belarus
[4] NNSemenov Institute of Chemical Physics, Department of Polymers and Composites, Moscow, Russia
ana-shpichka@yandex.ru, timashev.peter@gmail.com

To date, one of the focuses of the pharmaceutical industry is the new protein delivery systems that ensure the prolonged drug release. Polylactide is a good candidate as a carrier due to its biocompatibility, biodegradability and easy modification [1]. Our study aimed to assess applicability of polylactide particles for the prolonged drug release.

The particles were obtained from photosensitive methacryloyl chloride modified poly(D,L)-lactide differing in arm length. The photoinitiator, 4,4′-bis(diethylamino) benzophenone, was added to polylactides in dichloromethane. The mixture was placed into a specially designed silicone mold which was prepared via microreplication technique and consisted of four rows of four wells (100×100×100 μm). Then it was exposed to the UV-light to polymerize. The polylactide particle degradation was analyzed in three media: HCl solution (pH 1.1, 2 h), 0,05 M phosphate buffer saline (PBS) (pH 6.0, 2 h), and 0,05 M phosphate buffer saline (PBS) (pH 7.4, 4 h). The fluorescence signal reduction was measured via fluorimetry. To assess substance release, we used two compounds: fluorescein isothiocyanate and insulin. FITC release kinetics was measured after dipping the particles in 0.1% FITC for 12 h and washed with PBS. Then they were placed into PBS with constant mixing at 36-37°C for 12 h. We chose the following time points: 15 min, 30

min, 1 h, 2 h, 4 h, 8 h, 12 h. The FITC concentration was measured via a spectrophotometer using a calibration curve [3]. The insulin release was studied using bicinchoninic acid assay [4] during 24 h.

The polylactide particles from two studied polymers (P1 and P2) had good geometry and easy handling. The degradation rate in media imitating the gastrointestinal tract was different. The P2 particles degraded on 67.0±6.9%, and the P1 particles – 53.7±8.8%. After FITC loading, both particles types mainly released the substance during first 30 min, and the further release from 2 h till 8 h was linear. In 8 h, the FITC release was insignificant. However, the insulin release from P1 and P2 particles differed. The P2 particles had stable release during 24 h compared to the P1 particles which had insulin release kinetics similar to that for FITC. Therefore, only P2 particles are interesting for the further development of oral insulin dosage forms and are a good platform for delivery systems.

Thus, Thus, we showed that photo-crosslinked polylactide particles can be used as a drug carrier and provide sustained release.

This work was supported by the Russian Foundation for Basic Research, grant 17-34-80151.

[1] P. Fonte *et al.*, "Polymer-based nanoparticles for oral insulin delivery: Revisited approaches," *Biotechnol. Adv.*, vol. 33, no. 6, pp. 1342–1354, 2014.

[2] M. T. Cook, G. Tzortzis, D. Charalampopoulos, and V. V. Khutoryanskiy, "Microencapsulation of probiotics for gastrointestinal delivery," *J. Control. Release*, vol. 162, no. 1, pp. 56–67, 2012.

[3] B. Xu *et al.*, "Preparation of poly(lactic-co-glycolic acid) and chitosan composite nanocarriers via electrostatic self assembly for oral delivery of insulin," *Mater. Sci. Eng. C*, vol. 78, pp. 420–428, 2017.

[4] X. Y. Xiong, Q. H. Li, Y. P. Li, L. Guo, Z. L. Li, and Y. C. Gong, "Pluronic P85/poly(lactic acid) vesicles as novel carrier for oral insulin delivery," *Colloids Surfaces B Biointerfaces*, vol. 111, pp. 282–288, 2013.

ANALYSIS OF fMRI DATA IN CONN AND ICA

K. Shemarova

National Research University of Electronic Technology – MIET, Moscow, Russia
shemarova7may@gmail.com

Nowadays, doctors and neuroscience scientists working in the field of neurobiology have faced the problem of identifying active and passive neural networks in the human brain in order to display their zones, determine the network structure, its response to external stimulation, changes in time, etc. non-invasive diagnostic method, called as functional magnetic resonance imaging (fMRT), can help obtain the necessary data for the researchers and physicians.

There are many ways to process fMRI data. The choice of the algorithm depends on: the processing time and the obtaining quality of the data. The main purpose of this work is to compare the portability of patient's resting networks. Resting networks are chains of nerve cells that are active when a person is not engaged in mental activity. The analysis was performed in two programs: CONN (a functional connectivity toolbox of correlated and anticorrelated brain nemtworks) and ICA (Independent Component Analysis) .

Methods:

The data set was obtained from healthy men at the age of 40 years. A total of 158 sessions were conducted in 185 weeks.

CONN toolbox performs normalization of the "raw" fMRI data. At this stage, the image is spatially smoothed. The a CompCor method analyzes the characteristics of the main components to reduce the contribution of artifacts on the resulting images. Reproducement of the subject's displacement in the scanner using time curves. Analysis of the average and maximum deviations of the subject from the initial position in the tomograph. Establishment of a functional connection between the seeds and the rest of the brain.

ICA Is the data analyzer that works with resting networks as with a linear combination of signals that come from spatially independent sources. He estimates these sources, while increasing their mutual independence. One of the biggest advantages of the method is that it allows analyzing rs-fMRI data without a priori knowledge of sources. [1]

Results:

1. In the ICA, 50-65 resting networks were identified (taking into account artifacts);
2. In CONN, 50-70 resting nets were found on the same data set;
3. The number of significant networks varies between ICA and CONN in the range of 20 to 30;
3. Resting-state was found in 100% of cases;

Conclusions:

1 The treatment time per patient in CONN is five minutes per person. This slows down the processing of data.
2. CONN allows a more complete analysis of fMRI data.
3. The processing of the same set of data in ICA is several times faster.

[1] Choe AS, Jones CK, Joel SE, Muschelli J, Belegu V, Caffo BS, et al. (2015) Reproducibility and Temporal Structure in Weekly Resting-State fMRI over a Period of 3.5 Years. PLoS ONE 10(10): e0140134. doi:10.1371/journal.pone.0140134

SYNTHETIC MAGNETIC RESONANCE IMAGING IN NEUROVIZUALIZATION

A. Shevchenko[1], L. Fadeeva[1], I. Pronin[1], N. Zakharova[1]

[1]Burdenko Neurosurgery Institute, 4-ya Tverskaya-Yamskaya Str., 16, Moscow, Russia
Presenting author e-mail address: Shevchenko@nsi.ru

This work presents a comparison of synthetic images of the brain with conventional MR-imaging including: T1, T2, T2-FLAIR, T2-STIR. The study was performed on the magnetic resonance scanner General Electric Optima MR 450W, with a magnetic field strength of 1.5 T. Two the brains of healthy volunteers were examined. Synthetic MR images (T1, T2, T2-FLAIR, T2-STIR) were obtained, using a pulse sequence MAGIC, with the possibility of quantitative evaluation of the relaxation parameters: the longitudinal relaxation rate -R1 (1/T1,ms), the transverse relaxation rate -R2(1/T2,ms) and the proton density –PD (pu or water proton %).

The standard brain protocol of MRI surway included:

T1 MRI: axial and sagittal slices, 4.0 mm thick with a gap of 1 mm, FOV = 240 mm, TR = 600 ms, TE = 8.8, scanning time TA = 4 min.

T2 MRI: axial slices, 4.0 mm thick with a gap of 1 mm, FOV = 240 mm, TR = 3000 msec, TE = 88.3, scanning time TA = 4 min.

T2-FLAIR: axial slices, 4.0 mm thick with a 1 mm gap, FOV = 240 Ч 192, TR = 12,000 msec, TE = 97.8, scanning time TA = 4 minutes, voxel size 0.75 Ч 0.75 Ч 4mm

MAGIC protocol: 30 axial sections, 4.0 mm thick with a 1 mm gap, FOV = 240 Ч 192, voxel size - 0.75 Ч 0.75 Ч 4mm, ETL = 12, frequency band = 20.83 Hz. In total 8 images per slice were acquired with pulse sequence's parameters: autoTR = 4000 msec, TE = 22 or 95 msec, eff TE = 90.4 msec, TI-170, 670, 1840, 3840 ms.

Total number of images was 480. The scan time was 4.55 minutes. These images were used to build synthetic images, the tissue contrast of which can be varied.

The synthetic T1, T2, T2-FLAIR, T2-STIR images were imitating the tissue contrast in T1, T2, PD and also there was an opportunity to build the scatterplot of R1 and R2 on images. The duration of the synthetic images reconstruction to build parametric maps and graphs of R1 and R2 was 1-2 minutes.

The main physicochemical parameters of the main brain tissues were determined in ROIs located in the following brain anatomical structures:

white matter (T1 = 565 ± 26 ms, T2 = 79 ± 3 ms, PD = 61.3 ± 1.9 %)

gray matter of the cortex (T1 = 1255 ± 90 ms, T2 = 103 ± 7 ms, PD = 86.5 ± 3.5 %)

gray matter of the subcortex (putamen, thalamus)) (T1 = 831 ± 48 ms, T2 = 75 ± 4 ms, PD = 77 ± 2.9 %)

upper sagittal sinus (venous blood) (T1 = 576 ± 193 ms, T2 = 789 ± 17 ms, PD = 54.1 ± 15.7 %)

anterior cerebral artery (arterial blood) (T1 = 2742 ± 615 ms, T2 = 185 ± 53 ms, PD = 69.1 ± 15.0 %)

cerebrospinal fluid (lateral ventricles) (T1 = 4295 ± 9 ms, T2 = 1071 ± 305 ms, PD = 101.7 ± 2.3 %)

The duration of obtaining a synthetic images of diagnostic quality in the MAGIC program was 6 minutes. The duration of conventional image acquisition, using standard protocols was 12-14 minutes.

The quality of synthetic images (MAGIC) in our study were comparable(visually) with the one of conventional images($p>0,05$), the duration of MR investigation for synthetic imaging were shorter (6 vs 12min). The technique of synthetic images allows us to quantify (T1, T2, PD) - the "MR Fingerprint" of the brain tissues such as: gray, white matter, basal nuclei, cerebrospinal fluid. Fast multiparametric mapping can thus open the path to the creation of a multiproperty space that might allow a deeper characterization and understanding of the conditions and evolutions of determined pathologies.

[1] Ida Blystad, Jan Bertus Marcel Warntjes, Цrjan Smedby, Anne-Marie Landtblom, Peter Lundberg and Elna-Marie Larsson. Synthetic MRI of the brain in a clinical setting, Acta Radiologica, 2012. 53(10), pp. 1158-1163.

ACOUSTOGRAVIMETRIC SENSORS OF ACETONE VAPOR IN EXHALED AIR

V. Simonov

National Research Nuclear University "Moscow Engineering Physics Institute", Moscow 115409, Kashirskoye sh., 31, simonov.valer@yandex.ru,+7(903)1842037, ORCID iD - 0000-0002-5694-3986

Quartz crystal gravimetry has many applications, including in biochemistry and medicine. The piezoelectric (usually quartz) resonator (PR), which is extremely sensitive to changes in conditions at the surface boundary, helps to detect vapors and gases in micro concentrations, monolayers of small molecules, complex biopolymer matrixes, biomacromolecules or individual cells [1]. This work is aimed at increasing the sensitivity of sensors for the micro concentration of acetone vapor, which is a marker of such socially important diseases as diabetes, lung cancer, halitosis, etc.

In this work using the theory of oscillations of piezoelectric resonators with a sorption film on the surface[2] and through experimental studies of three dozen sensors realized on the basis of PR and polymethyl methacrylate (PMMA) film as a sorption sensitive element, it was shown that by choosing the optimal film thickness, by double-sided positioning of the film on the PR and using the method of smoothing the measured value of the frequency of the PR in time, it is possible to increase the sensitivity of the acoustogravimetric sensors by an order of magnitude. Figure 1 shows the experimental dependence of the threshold sensitivity parameter of the parameter P on the ratio of the film thickness h_f to the thickness of the sensor plate H. The minimum sensitivity threshold corresponds to the value h_f / H = 0.55%. This graph shows how many times the sensor with a non-optimal h_f / H ratio is less sensitive than with the optimal one. For example, for h_f / H = 0.05%, the gain in sensitivity is 7-8 times.

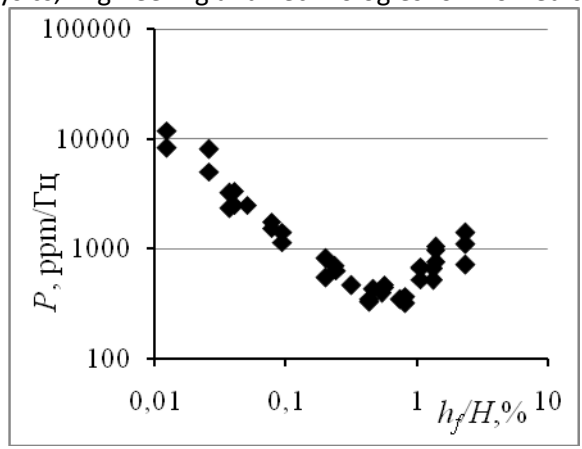

Fig.1. Dependences of the parameter P on h_f / H

The change in the temperature coefficient of the frequency caused by the film with the optimal thickness is $-0.55 \cdot 10^{-6}$ 1/°C, and the experimentally defined $-0.7 \cdot 10^{-6}$ 1/°C.

The results obtained in this study allow us to hope for the successful use of the sensors in question as a basis for a relatively inexpensive portable or stationary non-invasive device. In addition, the proposed methods for increasing the sensitivity of sensors are universal and can be used in combination with traditional methods, for example, using film materials with a higher adsorption capacity than PMMA.

The work was carried out under a project No. 16-07-0097-a with the support of the Russian Foundation for Basic Research under the Competitiveness Program of the NRNU MEPhI.

[1] R. Lucklum, P. Hauptmann, Acoustic microsensors - the challenge behind microgravimetry // Anal Bioanal Chem., V. 384. pp. 667-682, 2006.
[2] D. Johannsmann. Derivation of the compliance of thin films on quartz resonators from comparison of the frequency shifts on different harmonics: a perturbation analysis // J. of Applied Physics, V.89, № 11, pp.6356-6364, 2001.

THE INTELLIGENT SYSTEM OF RECOGNITION OF THE NETWORK STRUCTURE OF MELANOMA

A.Skripnik[1], V Nikitaev[1], O Tamrazova[2], A. Pronichev[1], V Yu Sergeev[2], S. Zaytsev[1], V. Dmitrieva[1], E. Druzhinina[1]

[1]National Research Nuclear University MEPhI (Moscow Engineering Physics Institute), Kashirskoe shosse 31, 115409, Moscow, Russia
[2]RUDN University, ulica Miklukho-Maklay 6, 117198, Moscow, Russia

Malignant melanoma of the skin is one of the leading oncological pathologies of the world's population in terms of increasing incidence. The average annual growth rate of the incidence of this tumor in the world is about 5% and can be considered one of the highest among all malignant tumors, second only to lung cancer [1]. The accuracy of clinical diagnosis by first-line physicians during initial treatment is 37% [2]. The purpose of this study is to develop methods and means of isolating the mesh structure of melanoma and counting its characteristics for medical decision support systems in the diagnosis of melanoma.

One of the well-known clinical symptom complexes of melanomas is dermatoscopic structures (pigment network, branching, points and globules). Computer processing of images of nevi will improve the accuracy of recognition of melanoma of the skin. The difficulty is the exact selection of the mesh structure border due to the lack of contrast of objects in the image and the presence of interference (hair, gel, skin defects).

There is no specific approaches identified that ensure reliable isolation of the boundary of the melanoma network structure in the course of the analysis of publications.

To solve the problem of separating the grid structure, it was suggested to use step-by-step image processing by applying the matrix filters from the openCV software package, first the Canny filter (cvCanny) to isolate the brightness transition boundaries and image binarization; filters median, erosion and build-up for a clearer delineation of boundaries on a binary image; algorithms cvFindCounturs and cvDrawCounturs for highlighting the mesh structure and filling them with the characteristics of arrays.

The proposed solution is implemented as a software module in C ++ using the Qt library.

This approach allowed us to distinguish the network structure of melanoma. According to the test results, the average error of the program is 35%. The correctness of the algorithm depends on the quality of the image of the nevus and the presence of interference. In addition, it is necessary to continue testing the algorithms for recognizing the boundaries, imposing matrices, since the current algorithms do not give an acceptable recognition accuracy in the automatic mode, especially in the case of eliminating contour breaks.

[1] Lememov V.G. (2001) Epidemiology, risk factors, screening for skin melanoma. Practical oncology, 4 (8): 3-11.
[2] Alexandrov H.H. Non-contact remote pyrometry and the use of hyperthermia and hyperglycemia in the complex treatment of malignant neoplasms / H.H. Aleksandrov, N.I. Zatsepin, E.G. Marshinki. -Minsk, 19S4.-C. 200-209.

PLANNING PROTON THERAPY ON CONE-BEAM CT IMAGES

A. Solovev[1], A. Chernukha[1], O. Lepilina[1], R. Shersnev[1], O. Golovanova[1], A. Shestopalov[2], S. Ulyanenko[1]

[1] A. Tsyb MRRC, Obninsk, Russia
[2] ZAO PROTOM, Protvino, Russia
Presenting author e-mail address: salonf@mrrc.obninsk.ru

Proton therapy is one of the most promising radiotherapy treatment modality offering the significant advantage of delivering dose at the exact point sparing healthy tissues around the target volume. However, the possibility of reducing the dose from diagnostic procedures now discussed, where the Cone-Beam CT offers a great improvement in comparison to the conventional CT examination.

In this study, we carefully investigated the possibility of generation and implementation of therapeutic proton treatment plans directly on CBCT images for head and neck patients. The CIRS phantom of head and neck provided by INR RAS, Troitsk, Russia has been used. The multiple sets of images obtained: spiral-CT on Siemens Somatom Emotion using H&N protocol, the Elekta XVI Cone-Beam CT facility, and built-in Cone-Beam CT of scanning proton beam therapeutic facility "Prometheus" with in-house reconstruction software used. All the images obtained in DICOM format and then transferred to Elekta XiO 5 to perform the delineation procedures. The number of corresponding volumes (PTVs from 80 to 750 ml) and some critical ROIs contoured and exported to DICOM RT. After that, all the DICOM RT datasets imported to the in-house proton therapy planning system of "Prometheus" facility. For proton therapy plans, the single, two opposite, four symmetric and five asymmetric directions has been used to generate an uniform absorbed dose distribution inside the PTV. The maximum allowed hotspot inside PTV was set to 105%. For five directions the built-in MFO optimization has been used, other plans generated using SFUD techniques. All the resulted dose distributions for all cases (from XiO in DICOM RT Dose format, for proton plans – in ASCII format) analyzed

using self-developed software using CERN ROOT, Python with numpy and scipy toolkits. The Gafcromic EBT3 film put inside the CIRS phantom and proton plans were delivered at "Prometheus" facility, the films were scanned at Epson Perfection V700, the resulted dose distribution obtained using previously developed software. In additional, the output of proton TPS has been simulated using Geant4 using the same CT and CBCT images. Finally, the TPS-to-TPS for CT versus CBCT images, TPS-to-film and TPS-to-Geant4 dose distributions analyzed using Gamma-index criteria with 3%/3mm acceptance level.

The preliminary results shows that head-and-neck patients can be safely planned for proton therapy using medical images from verified calibrated CBCT. The calculated Gamma-index is from 0.90 to 0.98 for all tested cases. Moreover, it might be assumed that all the uncertainties given by CBCT images in comparison to spiral-CT, serve as intrinsic pseudo-robust optimization for Monte-Carlo based TPS and optimization engines.

PERSPECTIVES FOR USING QUANTUM TECHNOLOGIES IN BIOMEDICINE

P.A. Tarasov[1], E.A Isaev[1,2] and G.V. Detkov[3]

[1] National Research University "Higher School of Economics", Moscow, Russia, E-mail: PTarasov@Hse.ru
[2] P.N. Lebedev Physical Institute of the Russian Academy of Sciences
[3] LLC "Information technologies and electronic communications", Moscow, Russia

In modern biomedicine, the flows of processed data are growing in an avalanche manner, which requires the use of ever more powerful and perfect resources [1]. Also, when transferring data, it is often necessary to ensure a high-quality level of cryptographic protection.

The goal of this article,- to make a brief analysis of existing quantum technologies, in terms of their applicability to the needs of biomedicine. For example, the use of quantum computers in the near future will allow solving problems with the processing of large data in biomedicine, and quantum communication technologies will provide in the future the necessary protection of transmitted biomedical information.

[1] Isaev E., Tarasov P. A., The utilization of information technology in biomedicine, Journal of Physics: Conference Series, Vol. 784, No. 012023, P. 1-5, (2017).

3rd International Symposium on
"Physics, Engineering and Technologies for Biomedicine"

BIONIC HEART: TRANSLATION PRINCIPLES

Dmitry Telyshev[1,2], **Maxim Denisov**[1], **Anna Satyukova**[3], **Tatyana Le**[3]

[1] *Institute of Biomedical Systems, National Research University of Electronic Technology, Zelenograd, Moscow, Russian Federation*
[2] *Institute for Bionic Technologies and Engineering, Sechenov University, Moscow, Russian Federation*
[3] *Bakoulev Scientific Center for Cardiovascular Surgery, Moscow, Russian Federation*
telyshev@bms.zone

Background: Since 2009 our research group has been developing promising implantable systems, namely, ventricular assist devices (VAD), for the treatment of heart failure among adults and children population. Such systems are widely used not only as a bridge to transplantation, but also as a means of destination therapy. To date, we have experience of more than 40 successful implantations for the adult population. Solving the problem of the miniaturization, adult VAD-H of the second generation and a pediatric VAD were developed. Both devices are at the stage of state registration.

Methods: The Sputnik VAD design (Sputnik 1) is based on an axial-flow blood pump with nonpulsatile flow. It can provide flow up to 10 l/min. The pump includes a moving part, namely, impeller (rotor with four blades) and a stationary part, namely, flow straightener with three blades and diffuser. The Sputnik 2 was developed with a set of changes in construction. The head pressure−flow rate (H−Q) and power consumption−flow rate curves for the Sputnik VADs were measured at different rotational speeds. The geometry of the PVAD Sputnik was designed and a rotor geometry effect on the H-Q curves of the PVAD Sputnik was investigated. Computational fluid dynamics (CFD) were used for operating condition simulation and the VADs were compared under the simulated physiological conditions. The haemolysis tests for the Sputnik VADs were done.

Results: The length of the implantable pump (Sputnik 2) was reduced from 81 mm to 70 mm and the maximum diameter was decreased

from 34 mm to 29 mm. Elimination of the taper expansion, new geometry of the diffuser and the rotor design changes allowed to reduce device energy consumption by 15%. Impeller diameter was changed from 15.6 mm to 13.8 mm, pump weight was reduced from 246 g to 205 g. The haemolisys index NIH reduced from 0.0099 ± 0.0015 (Sputnik 1) to 0.0031 ± 0.0011 g/100 L (Sputnik 1). The weight of the PVAD Sputnik is 102 g, the modeling results demonstrated that it is able to deliver 5–85 mmHg of pressure rise for a flow range of 0.5–4 L/min and rotational speeds of 9000-14,000 RPM.

3rd International Symposium on
"Physics, Engineering and Technologies for Biomedicine"

INTERACTIVE SEGMENTATION OF SKIN NEOPLASM IMAGES FOR HAIRS DETECTION

I. Trefilov[1], V. Nikitaev[1], O. Tamrazova[2], A. Pronichev[1], V. Sergeev[2], E. Druzhinina

[1]National Research Nuclear University MEPhI (Moscow Engineering Physics Institute), Kashirskoe shosse 31, 115409, Moscow, Russia
[2]RUDN University, ulica Miklukho-Maklay 6, 117198, Moscow, Russia
I. Trefilov e-mail address: kaf46@mail.ru

Elimination of hairs, which prevent correct analysis, on dermatoscopic images is very important phase in process of solving the problem of skin neoplasm diagnostics

Process of digital image processing for artifact detection includes following stages: creation of skin neoplasm image and correct image formatting and resizing, loading of image in digital image processing application, selecting required parameters for image processing, adjustment of each image processing parameter, obtaining the result with detected artifacts and the result analysis.

Work objective is interactive detection of hairs on images, which contain melanom. As a solution for detection and processing hairs on images, which contain melanom, next algorithm of staged image processing is proposed: applying of modified Prewitt operator on image, that is followed by thresholding, median filtering and dilatation. Proposed solution is implemented in C++ using Qt library.

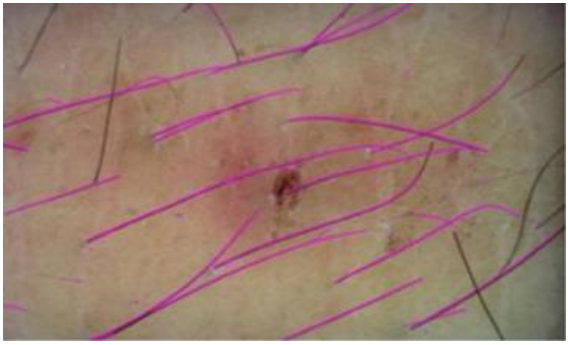

Fig. 1 Image with detected hairs after processing

Conducted experiment proves efficiency of proposed approach. The result of hair detection using algorithm mentioned above can be seen on Fig.1.

DOSIMETRY OF PROTON SCANNING BEAM WITH FBX DOSIMETRIC SYSTEM

Troshina M. V., Potetnya V. I., Koryakina E. V., Baykuzina R. M., Koryakin S. N., Ulyanenko S. E.

A. Tsyb Medical Radiological Research Center (MRRC)
branch of the National Medical Research Radiological Center of the Ministry of Health of the Russian Federation, Obninsk, Russia
Presenting author e-mail address: troshina-m-v@mrrc.obninsk.ru

The development of hadron therapy methods allows to increase the level of medical care for cancer patients [1]. The use of proton beams in radiotherapy and radiobiological studies requires accurate dosimetric measurements [2-4]. In addition to the use of ionization chambers recommended in TRS-398, methods such as film and gel dosimetry have now been used. Dosimetric films allow to quickly obtain a two-dimensional dose distribution of high resolution, gel dosimeters – three-dimensional distribution. In the case when it is necessary to determine the average values of absorbed dose or linear energy transfer in the irradiated volume, the most convenient way is to use aqueous solutions of chemical dosimeters.

The aim of this study is to determinate the absorbed dose with chemical dosimeter. A highly sensitive dosimetry system FBX (ferrous sulphate – benzoic acid – xylenol orange), based on the Fricke dosimeter was used. Irradiations were done at the therapeutic proton facility "Prometeus" (ZAO PROTOM, Russia) with scanning beam (located at MRRC). The clinical studies have been conducted now [1, 3] The 5 ml of the FBX dosimeter in polypropylene Eppendorf tubes (inner diameter 14 mm, height 54 mm) was irradiated with 110-130 MeV protons in a SOBP (diameter and height 30 and 50 mm, respectively, $LET_D \sim 2\text{-}2.5$ keV/μm) from one direction. The dose ranged from 1 to 5 Gy. The tubes with dosimetric solution were installed in a special holder in a cylindrical water phantom. The doses delivered to the FBX dosimeter were measured with a cylindrical ionization chamber TM30010-1, which was fixed in the same position as the tubes and irradiated under the same conditions. The optical density of FBX solution was measured on a single beam spectrophotometer SF-56 at a wavelength of 540 nm one hour past the exposure, the unirradiated sample being used

as a blank. The value of absorbed dose was calculated using the value of the radiation chemical yield of Fe^{3+} ions (G (Fe^{3+})) for photon radiation.

The average absorbed doses for 4 experiments measured by chemical dosimeter were by ~ 15% lower than the expected doses as predicted by the computerized treatment planning system. However, the doses measured using the ionization chamber fully corresponded to planned ones. The differences in the results of the two dosimetric systems are statistically significant ($p = 0.01$). The dose responses of the FBX dosimeter were linear for both radiations in the dose range studied. The observed differences in doses measured by the two methods agreed well if one takes into account the decrease in G(Fe^{3+}) value for FBX dosimeter irradiated with protons due to LET increase to ~ 2-2.5 keV/μm. So, the relative G(Fe^{3+}) value for protons was 0.86 of that for γ-radiation, or was equal 13.8 ions/100 eV.

Thus, the FBX solution can be used to quickly determine the average volume absorbed dose of protons in the dose range investigated, taking into account the established radiation-chemical yield G (Fe^{3+}) value, and also to estimate the important radiobiological and clinical parameter – the average in the volume LET of radiation [2].

The reported research was funded by Russian Foundation for Basic Research and the government of the Kaluga region of the Russian Federation (№ 18-44-400011).

[1] A.D. Kaprin, S.E. Ulyanenko, Hadron therapy – points of the development, Medicine: target projects, No. 23, pp. 56-59, (2016) (in Rushian).

[2] S.E. Ulyanenko, A.A. Lychagin, S.N. Koryakin, A.E. Chernukha, M.V. Troshina, I.N. Goulidov, A.N. Solovev, O.I. Lepilina, V.I. Potetnya, A.E. Shemyakov, V.N. Galkin, Simulation of dose and LET distributions within biological objects in proton fields, Medical Physics, vol. 77, no. 1, pp. 68-74, (2018) (in Rushian).

[3] S. Ulyanenko, V. Balakin, S. Koryakin, A. Lychagin, O. Lepilina, E. Isaeva, E. Koryakina, E. Beketov, M. Troshina, A. Solovev, Preclinical trials of the "Prometeus" scanning pencil proton beam, 55th Annual Conference of the Particle Therapy Co-operative Group (PTCOG), abstract: P 001, (2016).

[4] S.E. Ulyanenko , A.A. Lychagin , S.N. Koryakin, V.N. Galkin, The proton therapeutic facility with active scanning beam system Prometheus: radiological basics and perspectives, Research'n Practical Medicine Journal, vol. 4, no. S1, p. 107, (2017) (in Rushian).

3rd International Symposium on
"Physics, Engineering and Technologies for Biomedicine"

DOSIMETRY SUPPORT OF NUCLEAR MEDICINE

A. A. Trukhin[1,2], P.O. Rumyantsev[1], V.G. Nikitaev[2]

[1] Endocrinology research center, Moscow, Russian Federation
[2] National Research Nuclear University MEPhI, Moscow, Russian Federation
e-mail address: alexey.trukhin12@gmail.com

Implementation of medical physicist professional standard [1] is the up to date event. Developing standard prototype is divided in five labor functions. They are: physical and technical support of distant radiotherapy; physical and technical support of roentgenology and interventional radiology; physical and technical support of nuclear medicine; physical and technical support of medical use of non-ionizing radiation; physical and technical support of radiation protection.

According to labor function «Physical and technical support of nuclear medicine», this article shows the possible way of dosimetry support of nuclear medicine organization. It includes database organization, patient model development, pharmacokinetics investigation, theoretical model development, data analysis, ALARA (As low as reasonable achievable and AHASA (as high as safe applicable) principles implementation []. The block scheme is shown on Fig. 1.

Database organization consist of internal nuclear medicine documentary turnover process on local server. Patient model (Monte-Carlo code) develops in case of new clinical stuff training.

Pharmacokinetics investigations is one of main principles of dosimetry approach, called MIRD-scheme. Theoretical model develops to proof the diagnostic examination protocol validity. Data analysis shows the initial dosimetry parameters for therapeutic activity calculation [3]. ALARA and AHASA principles dictates in some cases to find the safest way to treat the patient and in some other cases tells us to treat patients using all possible means [2].

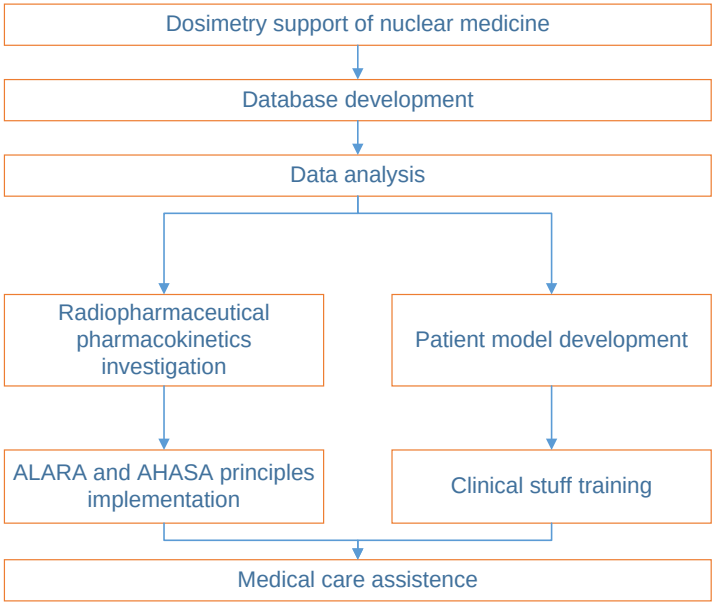

Fig. 1. Principal scheme of dosimetry support for nuclear medicine care assistance

[1] Прототип профессионального стандарта «Медицинский физик» http://www.russian-radiology.ru/node/249

[2] C. Hindorf, G. Glatting, C. Chiesa, O. Lindén, G. Flux. EANM Dosimetry Committee guidelines for bone marrow and whole-body dosimetry, 2010.

[3] T. Krohn, H. Hänscheid, B. Müller, F. F. Behrendt, A. Heinzel, F. M. Mottaghy, F. A. Verburg. Maximum dose rate is a determinant of hypothyroidism after 131i therapy of Graves' disease but the total thyroid absorbed dose is not. Journal of Clinical Endocrinology and Metabolism, 2014.

3D MRSI IN DIAGNOSIS OF BRAIN TUMOURS

A. Tyurina[1], A. Podoprigora[1], L. Fadeeva[1], V. Kornienko[1], I. Pronin[1]

[1] Federal State Autonomous Institution N.N. Burdenko National Medical Research Center of Neurosurgery of the Ministry of Health of the Russian Federation, 4-ya Tverskaya-Yamskaya Str., 16, Moscow, Russia

Magnetic resonance imaging (MRI) is widely used in diagnosing of brain tumours but the data obtained by the standard T1 and T2-weighted images are not always sufficient to get full confidence on the neoplasm biochemistry. The most difficult question is how to differentiate gliomas and metastatic lesions. Proton Magnetic Resonance Spectroscopy (H-MRS) is a functional technique based on an estimation of the main metabolite concentration in the tissue. Obtained spectra make it possible to determine the nature of the pathological process in those cases when the signal characteristics and morphological features of the detected focus are non-specific.

Nowadays a 3D proton MR spectroscopy (MRSI) is introduced in clinical practice along with single-voxel MRS (SV MRS) and 2D MRS (CSI). It allows obtaining data on the composition of metabolites for the whole volume of interest in one series.

The ratios of main metabolites peaks (NAA-N-acetylaspartate, Cr-creatine) to Cho-choline (3.0T MRI) in 15 healthy volunteers (age 26-56 years), 10 patients (age 28-62 years) with gliomas Grade I-II, 9 patients (age 35-65 years) with gliomas Grade III-IV, 3 patients (age 28-40 years) with meningiomas and 10 patients (age 40-65 years) with metastasis were measured.

Volumes of interest (tumour and adjacent areas) were selected by T1 FSPGR pulse sequence. HOS PROBE 3D sequence was performed to obtain MR spectra and ReadyView package (GE) was used to process spectral data.

In Low Grade I-II gliomas, the Cho/Cr values were 2.45 ± 1.44; Cho/NAA: 1.76 ± 1.2; NAA/Cr: 1.77 ± 0.57. In glioma Grade III-IV, the parameters of Cho/Cr were 3.36 ± 0.79; Cho/NAA: 2.27 ± 1.3;

NAA/Cr: 1.19 ± 0.61. In meningiomas the Cho/Cr values were 2,55 ± 1,18; Cho/NAA: 1,19 ± 0,16; NAA/Cr: 2,26 ± 1,29. In metastasis the Cho/Cr values were 0,53 ± 0,32; Cho/NAA: 3,87± 1,57; NAA/Cr: 1,25 ± 0,51. In group of healthy volunteers, the following ratios of the main metabolites were obtained: Cho/Cr: 1,19 ± 0.11; Cho/NAA: 0.53 ± 0.32; NAA/Cr: 2.53±0.20.

In Low Grade gliomas, the indices of the main metabolites of tumour growth have changed significantly compare with brain tissue, but in high-grade gliomas an increase in the ratio of Cho / Cr, Cho / NAA were the most pronounced. In meningioma and metastases the ratios of the main metabolites also had statistically significant differences which confirms these biomarkers of the pathological process.

3D proton-MRSI allows evaluating main markers of tumour malignance at different anatomic levels which can be used to determine the target point for biopsy, follow treatment management and differentiate tumours of various histological types.

MALFUNCTION OF CEREBELLAR CONNECTIVITY IN PATIENTS WITH MILD TBI. RSFMRI STUDY

M.V. Ublinskiy[1,2], P.E. Menshchikov[1,3], A.V. Manzhurtsev[1,2], N.A. Semenova[1,2,3], T.A. Akhadov[1,2]

[1]Clinical and Research Institute of Emergency Pediatric Surgery and Trauma, Radiology, Moscow, Russia.
[2]Institute of Biochemical Physics N.M. Emanuel RAS, Moscow, Russia
[3]Semenov Institute of Chemical Physics RAS, Moscow, Russia
Presenting author: M.V. Ublinskiy, maxublinsk@mail.ru

Objection: Mild TBI (mTBI) is the most common neurological damage in children that's why it is extremely important to identify and analyze biomarkers that can help in predicting patient's treatment and recovery in period of mTBI. Aim of this study is to verify a hypothesis that functional connectivity disturbances between intact cerebellum and DMN nodes are included in symptomatic manifestation of mTBI.

Methods: 28 MR negative patients with mTBI were studied in age from 12 to 17 years (mean age – 14.7 years). The control group consisted of 23 healthy children. All MRI studies were performed on a Philips Achieva dStream 3.0T scanner equipped with a 32-channel Philips dStream head coil. A 4 min rsfMRI gradient-echo echo planar imaging (EPI) sequence was acquired (TR=3000 ms, echo time [TE] = 30 ms, 80 dynamics with dynamic scan time = 3 s). fMRI data were processed using functional connectivity toolbox CONN.

Results: No statistically significant differences in correlation strengths between control group and group of patients were detected as a result of DMN analysis (see Fig.1). Seed-based correlation ROI analysis in control group revealed statistically significant ($p < 0.05$) links between DMN regions and the following structural cerebellum parts: lower and upper semilunar lobes and flocculus. In mTBI group these correlations are not revealed ($p = 0.39$).

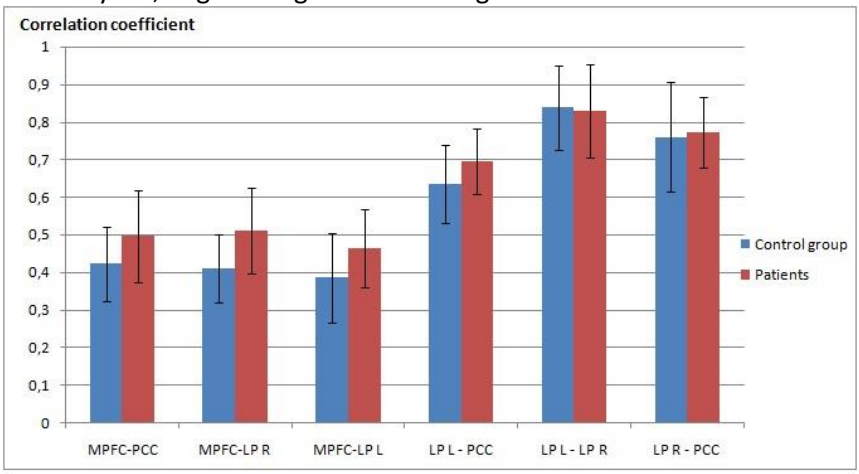

Fig.1. Result of intergroup analysis of correlation strengths between DMN regions.

Conclusion: The revealed changes in DMN neuronal connection and cerebellar regions in acute stage of mTBI patients can be an initial step of damages leading to cognitive deficit which can be developed in future in long-term period of injury.

This study is supported by the Russian Fund Basic Research (RFBR) grant 18-315-00165.

MICROSTRUCTURE AND METABOLISM ANALYSIS IN CHILDREN WITH SEVERE TBI

M.V. Ublinskiy[1,2], P.E. Menshchikov[1,3], A.V. Manzhurtsev[1,2], N.A. Semenova[1,2,3], T.A. Akhadov[1,2]

[1]Clinical and Research Institute of Emergency Pediatric Surgery and Trauma, Radiology, Moscow, Russia.
[2]Institute of Biochemical Physics N.M. Emanuel RAS, Moscow, Russia
[3]Semenov Institute of Chemical Physics RAS, Moscow, Russia
Presenting author: M.V. Ublinskiy, maxublinsk@mail.ru

Objection: Aim of this study was to explore the dynamics of microstructure and brain metabolism parameters in children with severe traumatic brain injury (sTBI) and hypoxic-ischemic brain injury (HIBI).

Methods: 8 patients (mean age = 12.5) with sTBI comprised group 1. 4 children (mean age = 13.6) with HIBI caused by drowning in fresh water. MR studies of patients from both groups were carried out twice: first - during the first seven days after injury (period 1); second - a month after injury (period 2). All studies were performed at Phillips Achieva 3.0T MRI scanner. DT MR images were acquired with diffusion gradients applied in 32 non-collinear directions. 1H-MRS voxel (TR/TE =1500 ms/ 40 ms, NSA = 128) was localized in left and right thalamus (for groups 1 and 2) and in brain stem (for group 2).

Results: ^{1}H MRS analysis in thalamus revealed significant decrease in dynamics of NAA/Cho value in group 1 (41% decrease) and absence in dynamics of this index in group 2. Significant increases in dynamics of ADC and FA values were found in corpus callosum in group 1. In group 2 we detected increase in dynamics of ADC value and NAA/Cho ratio in brain stem.

Conclusion: The significant decrease of NAA/Cho dynamics in thalamus in group 1 may indicate an active NAA intake in synthesis of oligodendrocytes to restore myelin sheath, for which Cho compounds are required (see Fig.1). Dynamics of spectroscopy and DTI parameters in brain stem correlates with the restoration of CNS functions in patients after drowning.

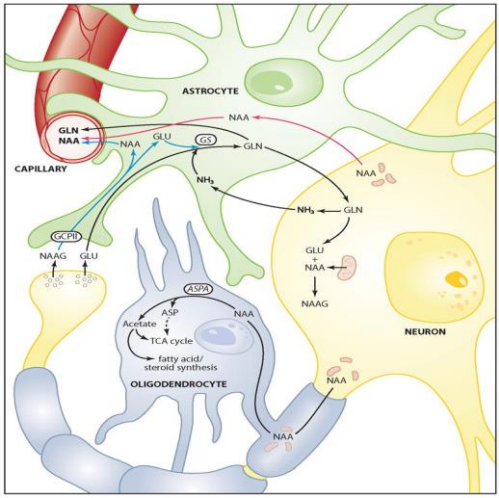

Fig.1. NAA Metabolism

This study is supported by the Russian Fund Basic Research (RFBR) grant 18-315-00165.

CEREBRAL MICROSTRUCTURE DISORDERS IN THE ACUTE PHASE OF MILD TRAUMATIC BRAIN INJURY

O.R. Vasiukova[1], A.V. Manzhurtsev[2,3] , P.E. Menshchikov[4,3,2], M.V. Ublinskiy[3,2], T.A. Akhadov[3], N.A. Semenova[2,4,3]

[1] *National Research Nuclear University MEPhI (Moscow Engineering Physics Institute), Moscow, Russia*

[2]*N.M. Emanuel Institute of Biochemical Physics of the Russian Academy of Sciences, Moscow, Russia*

[3]*Clinical and Research Institute of Emergency Pediatric Surgery and Trauma, Moscow, Russia*

[4]*N.N. Semenov Institute of Chemical Physics of the Russian Academy of Sciences, Moscow, Russia*

olechkavas57@gmail.com

Introduction. Standard visualization methods (CT and MRI) are not sensitive to a mild traumatic brain injury (mTBI). Mild TBI causes changes on microstructural level, that could be revealed by means of Diffusion Tensor Imaging (DTI) [1]. The aim of this study is to reveal the impact of acute mTBI on diffusion parameters in corpus callosum (CC), corticospinal tract (CST), and in thalamus in children.

Materials and methods. Subjects: 11 healthy subjects and 11 patients with mTBI (up to 41+19 hours since the injury), mean age 16+2. Philips Achieva dStream 3.0T and 32-channel SENSE head coil were used. The standard TBI MRI protocol revealed no pathological changes in brain tissue of any subject.

DTI was performed in 32 directions. Diffusion data was processed in Fibertrak package in Philips Intellispace Portal (Philips the Netherlands). To acquire FA and ADC values the tracts of CC, left and right thalamus and CST in both brain hemispheres were defined by selecting the regions of interest (ROI). The thalamus ROI was selected in three orthogonal planes, CC – in saggital plane, CST – in axial plane. For left and right thalamus apart from FA and ADC the AD and RD values were found using Fibertrak in Philips Extended Workstation.

Statistical analysis was performed in STATISTICA 12 (Statsoft). The nonparametric Mann-Whitney criterion was used to reveal the sig-

nificance of group differences, p-value < 0.05 was considered significant.

Results. Statistically significant increase in FA and decrease in RD in mTBI was revealed for the tracts of the right thalamus (fig. 1 (a,b)); decrease in ADC found for the tracts of the left thalamus (fig. 1 (c)).

No significant changes in FA and ADC for the tracts of other cerebral structures analyzed are found. No difference in AD in thalamus of normal and pathology groups is revealed either.

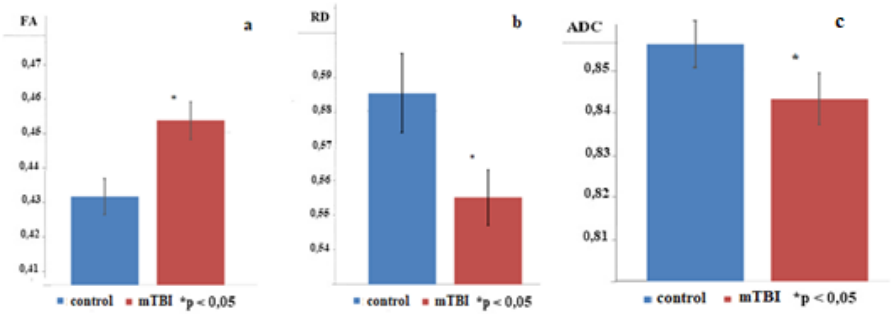

Fig.1. Median (+range) of FA (a) and RD (b) for tracts of the right thalamus, of ADC for tracts of the left thalamus (p<0,05)

Discussion. The results of this study signify the presence of microstructural damage in thalamus. The changes in diffusion parameters arise from the cytotoxic swelling, that happens because of alterations in metabolic processes caused by the traumatic impact [2].

[1] Rabinowitz A. R., Levin H. S. Cognitive sequelae of traumatic brain injury. PsychiatrClinNorthAm. 2014;37(1):1–11.

[3] Veeramuthu V., Narayanan V., Kuo T. L., Delano-Wood L., Chinna K., Bondi M. W., Waran V., Ganesan D., Ramli N. Diffusion Tensor Imaging Parameters in Mild Traumatic Brain Injury and Its Correlation with Early Neuropsychological Impairment: A Longitudinal Study. J Neurotrauma. 2015;32(19):1497-1509

THE RATING FACTORS IN THE PROGRESSION OF ACUTE PANCREATITIS

Vlasov A.P.[1],Trofimov V.A.[1], Anaskin S.G.[2], Malakhova O.S.[1], Morozova M.M.[1], Muratova T.A.[1], Vasiliev V.V.[1], Vlasova T.I.[1], I.D. Korniletskiy[2]

[1]National Research Ogarev Mordovia State University, Saransk, Russia
[2]National Research Nuclear University MEPhI, Moskow, Russia
Presenting author e-mail address: vap.61@yandex.ru

Acute pancreatitis is one of the most frequent surgical diseases. More than 10% of urgentny pathology of abdominal organs fall to its share. Frequency of acute pancreatitis around the world makes from 4,9 to 73,4 cases on 100 000 people. At the same time the lethality at acute pancreatitis remains high (10–20%) that is explained by lack of specific diagnostic and therapeutic methods [1]. It is shown that at acute pancreatitis both cellular, and humoral factors of system of a complement, system of a hemostasis and kallikrein-kinin system are activated, causing release of nitrogen oxide (NOS). NOS in turn strengthens peroxide oxidation of membrane lipids of various cells, increases permeability of a microcirculator bed, causes ischemia of bodies, stimulates apoptosis of cells of an endothelium [2]. According to a genetic research it is shown that at destruction of NOS3 the factors associated with gland damage in particular become more active activity of intrapancreatic trypsin increases. It is shown that the nitrogen oxide induced by endothelial NO synthase renders protective effect through activation, most likely, of endothelial cells that promotes the best intrapancreatic blood-groove [3]. The considerable disturbances of microcirculation leading to a hypoxia of fabrics and a perversion of fabric metabolism are one of the reasons of progressing of a disease and development of multiorgan insufficiency [4].

Research objective. To define a role of disturbances of microcirculation and the processes defining a structurally functional condition of a microcirculator bed in progressing of acute pancreatitis.

We`ve done a clinical study of 150 patients with acute pancreatitis, whom are divided into 3 groups: group I (n = 50) - patients with mild

pancreatitis; II group (n = 50) - patients with moderate pancreatitis; III group (n = 50) -patients with severe pancreatitis, both sexes and in age 21-55 years. Healthy individuals were examined like control (n = 20). The studied patients were cared by standardized complex therapy according to clinical recommendations. The paper presents data on the evaluation of the state of microcirculation using the technique of Doppler flowmetry, lipid peroxidation by the content of malonic dialdehyde in blood plasma in reaction with 2-thiobarbituric acid, diene conjugates by spectrophotometric method, activity of phospholipase A2 by the titration method, genetic diagnosis. It was proved that there is a significant violation of microcirculation in the early stages of acute pancreatitis, which is more pronounced in severe form of the disease. It was also revealed that these abnormalities are accompanied by C774T polymorphism of the NOS3 genes, which is involved in the pathogenesis of endothelial dysfunction, on which the microcirculation condition largely de-pends. It is shown that in the pathogenesis of the latter in patients with acute pancreatitis, the excessive activity of oxidative processes and phospholipases, which take part in the formation of destabilization phenomena of cell membranes, including from the side of endothelial cells, is important.

[1] Acute pancreatitis//Abdominal surgery. National leaders: the short edition / under the editorship of I. I. Zatevakhin, A. I. Kiriyenko, V. A. Kubyshkin. M.: GEOTAR-media, 2016. Page 716-734.
[2] Rakhimov B. M., Galkin I. V., Simatov A. M, Kolesnikov V. V., Sherstnev I. A., Snopov S.A., Matviyenko V. A Treatment acute heavy//plenum Materials правл. associations of gepatopankreatobiliarny surgeons of the CIS countries. Samara, 2015. Page 120 – 121.
[3] Ye-Chen Feng, Min Wang, Feng Zhu, Ren-Yi Qin. Study on acute recent stage pancreatitis. World. J. Gastroenterol. 2014. Nov. 21. Vol.20(43). P.16138–16145.
[4] Timerbulatov M. V., Senderovich E. I., Ziganshin T. M., Rakhimov R. R. Multistage approach in treatment of necrotic pancreatitis//Questions of transfer of experience and development of new technologies in low-invasive surgery: materials of the XIX Congress of Society of endoscopic surgeons of Russia (ROEH) (Moscow, on February 16-18, 2016). M, 2016. Page 105-106.

DEVELOPMENT OF A SYSTEM OF SUPPORTING THE ADOPTION OF MEDICAL DECISIONS FOR THE DIAGNOSTICS OF THE DEFORMATIONS OF THE GASTROINTESTINAL TRACT

E. Vorobyeva, V. Nikitaev, V. Selchuk, A. Pronichev, E. Polyakov

National Research Nuclear University MEPhI (Moscow Engineering Physics Institute), Kashirskoe shosse 31, 115409, Moscow, Russia.
E. Vorobyeva e-mail: vorobusha12@mail.ru

Histology - the science of the patterns of development, structure and function of human tissues. The accuracy of oncological diagnosis, the success of treatment, the prognosis is largely determined by the histological diagnosis (HD). Modern HD is based on the analysis of images of histological preparations, their morphological quantitative and qualitative evaluation using micro- and macroscopy.

The purpose of this work is to study the problems of the development of information-measuring systems (IMS) of HD and propose approaches to their solution.

The main problems of creation IMS of HD:

1. The weak formalizability of HD objects at the crucial stage - microanalysis - is due to the complex spatial-brightness organization of images of histological preparations.
2. The complexity and uniqueness of the structure of histological images determine the lack of solution to the present time of the tasks of their quantitative description relating to the problems of perception of visual images, artificial intelligence.
3. There is a low information content of classical morphological and color measurement methods at the stage of histological macroanalysis, in which morphological measurements are reduced to measurements of the size of a tumor using a ruler. There are problems of formalization of macroscopic tumors.

Suggested approaches to solving the construction of information-measuring systems (IMS) of HD:

1. Forming a strategy for building clinical diagnostic systems based on artificial intelligence methods (expert systems, knowledge bases, pattern recognition).
2. Realization of intelligent IMS as a decision support system by a doctor with a probabilistic assessment of diseases.

The core of the clinical diagnostic system is the expert systems used at its crucial stage - the analysis of a micro-preparations, during which the recognition of tumors is carried out [1].

[1] V. Nikitaev Expert Systems in Information Measuring Complexes of Oncological Diagnoses, Measurement Techniques, vol. 58, №. 6. pp. 719-723, (2015).

COMBINATION OF CRYOGENIC DIAGNOSTICS AND TREATMENT OF ONCOLOGICAL DISEASES

Vorontsov V. A.

NRNU MEPhI, Moscow, RF
+7 495 56 99 ext 9042 VAVorontsov@mephi.ru

The cryogenic surgery is known, but works on cryogenic oncological diagnostics it was revealed not. Therefore this direction of researches can be of particular interest. The main ideas are in watching a living cell, its external data the size in color. a form and, perhaps, a smell and also behind her behavior, body height, its speed, division process, its features and so on.

It is known that sick cells react to fall of temperature more weakly, than healthy ones. Besides we consider diagnostics on cytologic but not at the histologic level, leaving cells alive. It gives the chance to use dynamics of their body height and development as indexes and symptoms of a disease or their health.

Let's consider gradual cooling of cells and change of their properties and behavior under the influence of this cooling. In the beginning the speed of manifolding of these cells will change and healthy cells will have it more slowly, than at sick ones. On the difference of these speeds it is possible to try to distinguish sick cells from healthy ones. Then at increase in cooling cryo diagnostics gradually turns into cryotherapy and a cryosurgery. But also at these stages of cooling it is possible to distinguish sick cells from healthy ones.

So process of gradual freezing of the site of fabric having a tumor and behavior healthy and sick cells of fabric was considered. It is shown that the difference of a look and behavior of cells can form an oncodiagnostics basis at different stages of freezing of fabric. Besides process of freezing of fabric can turn gradually into cryotherapy and a cryosurgery and diagnostics will turn into treatment of a tumor.

The differences and common features of cryosurgery and cryotherapy are discussed and methods of oncology cryodiagnostics are shown.

3rd International Symposium on
"Physics, Engineering and Technologies for Biomedicine"

SPECIFIC ABSORPTION RATE OF ORIENTED ASSEMBLES OF ELONGARED CLUSTERS OF MAGNETIC NANOPARTICLES

Gubanova E.M.[1], Epshtein N.B.[1], Belyaeva G.A.[1] Usov N.A.[1]

[1]*MEPhI, Moscow*
Tel.: 8 (910) 5467732, e-mail: elizaveta.gubanova.1995@mail.ru

Assemblies of magnetic nanoparticles are widely used in biomedicine, in particular, in magnetic hyperthermia for local heating of biological media in an alternating magnetic field [1]. It is known [2] that due to the influence of a strong magneto- dipole interaction in a dense assembly of nanoparticles, the specific absorption rate (SAR) of the assembly depends not only on the properties of magnetic nanoparticles, but also on the shape of the sample in which the particles are distributed.

In this report, using computer simulation the SAR of dilute oriented assemblies of ellipsoidal clusters is calculated depending on the cluster aspect ratio. The calculations were performed for clusters consisting of magnetic nanoparticles $MnFe_2O_4$ with a diameter D = 50 nm, saturation magnetization M_s = 350 emu/cm^3 and uniaxial anisotropy constant $K = 5.5\times10^4$ erg/cm^3.

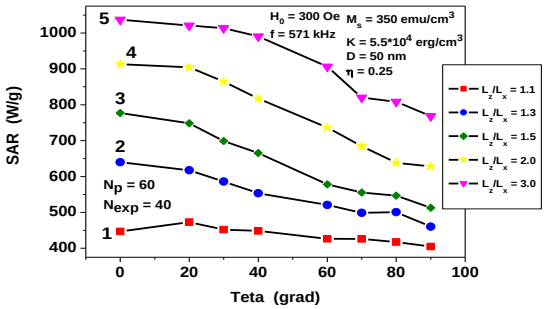

Fig.1. The dependence of SAR on the direction of the alternating magnetic field with respect to the common axis of the oriented assembly of ellipsoidal clusters

with different aspect ratios: 1) $L_z/L_x = 1.1$, 2) $L_z/L_x = 1.3$, 3) $L_z/L_x = 1.5$, 4) $L_z/L_x = 2.0$, 5) $L_z/L_x = 3.0$.

The cluster filling density is fixed at $\eta = 0.25$, the aspect ratios of the clusters lie within the range $L_z/L_x = 1.1 - 3.0$. As Fig. 1 shows, for an oriented assembly of elongated clusters SAR substantially depends on the direction of the alternating magnetic field with respect to the orientation axis of the clusters. For the alternating magnetic field frequency $f = 571$ kHz and the field amplitude $H_0 = 300$ Oe the SAR of cluster assembly increases by 20-25% when the field is rotated from perpendicular to parallel direction. It reaches maximum, SAR = 1040 W/g, for the clusters with the greatest elongation, $L_z/L_x = 3.0$ (see curve 5 in Fig. 1).

References

1. E.A. Périgo, G. Hemery, O. Sandre, D. Ortega, E. Garaio, F. Plazaola, and F.J. Teran. Fundamentals and advances in magnetic hyperthermia. Appl. Phys. Rev. Vol. 2, P. 041302 (2015).

2. S.A. Gudoshnikov, B.Ya. Liubimov, A.V. Popova, and N.A. Usov. The influence of a demagnetizing field on hysteresis losses in a dense assembly of superparamagnetic nanoparticles. J, Magn, Magn. Mater. Vol. 324, P. 3690 (2012).

Подписано в печать .10.2018
Формат 60×84 1/16 Заказ № Тираж экз. Печ. л.

Нацональный исследовательский ядерный университет « МИФИ»
Типография НИЯУ МИФИ
115409, Москва, Каширское ш., 31